SCEC SOUTHERN CALIFORNIA EARTHQUAKE CENTER

UNIVERSITY OF SOUTHERN CALIFORNIA

CALIFORNIA INSTITUTE OF TECHNOLOGY

LAMONT-DOHERTY EARTH OBSERVATORY OF COLUMBIA UNIVERSITY

UCLA

U.C. SAN DIEGO, SCRIPPS INSTITUTION OF OCEANOGRAPHY

UNIVERSITY OF CALIFORNIA SANTA BARBARA

UNITED STATES GEOLOGICAL SURVEY

1998 Annual Meeting

October 17-20, 1998

Riviera Resort and Racquet Club
Palm Springs, California

Los Angeles, CA 90089-0742 • Telephone: (213) 740-5843 • Facsimile: (213) 740-0011
E-mail: scecinfo@usc.edu • Internet: http://www.usc.edu/go/scec/

Table of Contents

1998 SCEC ANNUAL MEETING AGENDA

Saturday, October 17

9:00 - 4:30	Education and Outreach Workshop and Working Group Meeting
9:00	Continental Breakfast
9:30 - 10:00	Introduction and Description of CERC proposal (Jill Andrews)
10:00 - 10:45	Knowledge transfer (Jill Andrews) *Current activities *Plans for the future *Partnerships
10:45 - 11:45	Post-secondary Programs (Mark Benthien) *Intern program review *Year round program development *SCEC chapters concept *Cascading Mentoring System
11:45 - 12:45	**Lunch**
12:45- 2:30	Modules (Sara Tekula, Jill Andrews) *Why modules? *Demonstration of Regional Seismicity and Discussion *GPS module Demonstration and Discussion *Teacher Training Materials for Modules *Future modules: PEER, ECHO-Elsie, etc. *Virtual field trips: San Andreas Fault, Mammoth Lakes
2:30 - 4:40	Web pages (Mark Benthien) *Tour & Review of the SCEC Web site *(Tentative) Demo of Future Ideas for Web Construction *Structured feedback on SCEC Web pages
4:40 - 4:30	Wrap up (Jill Andrews)

Other Saturday Activities

1:00 - 5:00 pm	SCIGN Coordinating Board Meeting
6:30 - 9:00 pm	SCEC Advisory Council Meeting with SCEC Steering Committee
9:00 pm	SCEC Advisory Council Executive Session
	SCEC Steering Committee

Sunday, October 18

8:30 - 3:00	SCIGN Advisory Council Meeting
9:00	Informal Field Trip led by Jim Brune to Precarious Rocks Near Banning
9:00 - noon	3-D Mapping Group Meeting (Clayton)
1-3	GEM Meeting (Rundle)
1-3	Santa Clara Basin Project Meeting (Abrahamson)
3:00	SCEC Plenary Session I Introduction by Henyey Remarks by Whitcomb and Unger/Filson State of Science by Jackson "Community Based Outreach: the Long Run" by Jill Andrews Group A (Master Model) talk by Ross Stein Group B (Strong Motion Prediction) talk by Steve Day
6:00	**Icebreaker and Dinner**
7:15	**Poster Session (Posters remain available during working group meetings until Tuesday @ 10 a.m.)**

Monday, October 19

8:00	Session II: Plenary Session Group C Talk (Earthquake Geology) by Kerry Sieh (45) Group D (Subsurface Imaging and Tectonics and Seismicity and Source Parameters) Talk by Rob Clayton (45)
9:30	Working Group A Meeting (Jackson)
10:45	Working Group B Meeting (Day)
Noon	**Lunch**
1:30	Session III: Plenary Session Group E (Crustal Deformation) Talk by Ken Hudnut Group G (Earthquake Source Physics) Talk by Leon Knopoff
3:00	Working Group C Meeting (Sieh)
4:30	Working Group D/F Meeting (Clayton)

Dinner at 6:00 p.m. with presentations by Jill Andrews to follow

7:15 Working Group E Meeting (Hudnut)

8:30 Working Group G Meeting (Knopoff)

Tuesday, October 20

8:30 to 10 Summaries from Working Group Chairs

End of SCEC Meeting

10:00 a.m. SCEC Advisory Council Meets

10:00 a.m. Joint SCEC/PEER Meeting on Ground Motions (Tom Heaton)

1998 SCEC ANNUAL MEETING PARTICIPANTS

Mark Abinante	UCLA
Norm Abrahamson	Pacific Gas and Electric
Duncan Agnew	UC-San Diego
Greg Anderson	UC-San Diego
John Anderson	Nevada-Reno
Jill Andrews	USC
Rasool Anooshehpoor	Nevada-Reno
Ralph Archuleta	UC-Santa Barbara
Donald Argus	JPL
Ramon Arrowsmith	Arizona State
Luciana Astiz	UCSD
Shirley Baher	UCLA
Eli Baker	Maxwell Technologies
John Baldwin	William Lettis and Assoc.
Leslie Ballenger	Chapman
Gerald Bawden	USGS-Menlo Park
Jeffrey Behr	USC
Eric Bender	Orange Coast College
Mark Benthien	USC
Yehuda Ben-Zion	USC
Mike Bevis	Hawaii
Jacobo Bielak	Carnegie-Mellon
Tom Bjorklund	Houston
Ann Blythe	USC
Yehuda Bock	UC-San Diego
Fabian Bonilla	UC-Santa Barbara
David Bowman	USC
Jim Brune	Nevada-Reno
Sara Carena	Princeton
Ji Chen	Caltech
Rob Clayton	Caltech
Lloyd Cluff	PG&E
David Coblentz	Oregon
Alain Cochard	Harvard
C.B. Crouse	Dames and Moore
Jim Davis	CDMG
Paul Davis	UC-Los Angeles
Tim Dawson	San Diego State
Steve Day	San Diego State
Jishu Deng	Caltech
Safaa Dergham	Columbia/SCEC Summer Intern

Jim Dieterich	USGS-Menlo Park
Francesca DiLuccio	ING-Rome
James Dolan	USC
Andrea Donnellan	JPL
Don D'Onofrio	National Geodetic Survey
Herb Dragert	Geological Survey of Canada
Doug Dreger	UC-Berkeley
Wen-Xuan Du	Lamont
Jennifer Eakins	UC-San Diego
Leo Eisner	Caltech
Diane Evans	JPL
Larry Fenske	Caltrans
Ned Field	USC
John Filson	USGS-Reston
Mike Forrest	Rio Hondo College
Geoffrey Fox	Syracuse
Bill Foxall	LLNL
Jeff Freymueller	Alaska
Gary Fuis	USGS-Menlo Park
John Galetzka	USC
Eldon Gath	Earth Consultants Int.
Kathy Gerst	UC-Los Angeles
Maggi Glasscoe	UC-Davis
Nikki Godfrey	USC
Jim Goltz	Caltech
Lisa Grant	UC-Irvine
Robert Graves	Woodward-Clyde
Leland Green	UC-Santa Barbara/SCEC Summer Intern
Susanna Gross	Colorado
Dawei Guo	UC-Los Angeles
Larry Gurrola	UC-Santa Barbara
Katrin Hafner	Caltech
Brad Hager	MIT
Tom Hanks	USGS-Menlo Park
Jeanne Hardebeck	Caltech
Ruth Harris	USGS-Menlo Park
Ross Hartleb	USC
Michael Hasting	China Lake Naval Air Station
Egill Hauksson	Caltech
Elizabeth Hearn	Oregon
Tom Heaton	Caltech
Moritz Heimpel	UC-Los Angeles

Don Helmberger	Caltech
Ed Hensley	SCEC Outreach
Sally Henyey	USC
Tom Henyey	USC
Alan Hoffman	Consultant
Phil Hogan	Dames and Moore
Heidi Houston	UC-Los Angeles
Susan Hough	USGS-Pasadena
Ken Hudnut	USGS-Pasadena
Gene Humphreys	Oregon
Ken Hurst	JPL
DeAnn Icenogle	UC-Los Angeles
Kojiro Irikura	Kyoto
Dave Jackson	UC-Los Angeles
Paul Jamason	UC-San Diego
Eleanore Jewel	UC-Santa Barbara
Peg Johnson	USGS-Pasadena
Hadley Johnson	UC-San Diego
Wayne Johnson	Los Angeles Unified School District
Lucy Jones	USGS-Pasadena
Tom Jordan	MIT
Yan Kagan	UC-Los Angeles
Marc Kamerling	UC-Santa Barbara
Teruyuki Kato	Tokyo
Ed Keller	UC-Santa Barbara
Louise Kellogg	UC-Davis
Lowell Kessel	UC-Santa Barbara/SCEC Summer Intern
Nancy King	USGS-Pasadena
Robert King	MIT
Bill Klein	Boston College
Leon Knopoff	UC-Los Angeles
Monica Kohler	UC-Los Angeles
Robert Langridge	Oregon
Barry Last	Rialto High School
Daniel Lavallee	UC-Santa Barbara
Matthew Lee	UC-Los Angeles
Mark Legg	ACTA Inc.
Jennifer Lewis	San Diego State
Yong-Gang Li	USC
Grant Lindley	UC-Santa Barbara
Scott Lindvall	William Lettis Assoc.
Peng-Cheng Liu	UC-Santa Barbara

Yun-Feng Liu	USC
Bruce Luyendyk	UC-Santa Barbara
Harold Magistrale	San Diego State
Mehrdad Mahdyiar	Vortex Rock Consultants
Chris Marone	MIT
John Marquis	Caltech
Aaron Martin	UC-Santa Barbara
Geoff Martin	USC
Sally McGill	Cal State-San Bernardino
Seth McGinnis	Colorado
John McRaney	USC
Myra Medina	UC-San Diego
Andrew Meigs	Oregon State
Dennis Mileti	Colorado
Bernard Minster	UC-San Diego
Jackie Moccand	USC/SCEC Summer Intern
Jack Moehle	PEER
Lalliana Mualchin	Caltrans
Karl Mueller	Colorado
Robert Nadeau	UC-Berkeley
Sue Nava	Utah
Julie Nazareth	Caltech
Xiao-Xi Ni	UC-Los Angeles
Craig Nicholson	UC-Santa Barbara
Robert Nigbor	Agbabian Associates
Rosanne Nikolaidis	UC-San Diego
David Oglesby	UC-Santa Barbara
David Okaya	USC
Kim Olsen	UC-Santa Barbara
Nate Onderdonk	UC-Santa Barbara
John Orcutt	UC-San Diego
Meridith Osterfeld	K-12 Alliance
Susan Owen	USC
Lewis Owen	UC-Riverside
Jay Parker	JPL
Tracy Pattalena	Pasadena City College/SCEC Summer Intern
Zhi-Gang Peng	USC
Mark Petersen	CDMG
Arben Pitarka	Woodward-Clyde
Jascha Polet	Caltech
Dan Ponti	USGS-Menlo Park
Jack Popejoy	KFWB Radio/Los Angeles

Will Prescott	USGS-Menlo Park
Charles Real	CDMG
Judy Reagon	Burke Middle School/LAUSD
Jim Rice	Harvard
Keith Richards-Dinger	UC-San Diego
Meredith Robertson	USC
Cliff Roblee	Caltrans
Tom Rockwell	San Diego State
Mousumi Roy	New Mexico
Charlie Rubin	Central Washington
Justin Rubinstein	UC-Los Angeles/SCEC Summer Intern
John Rundle	Colorado
Chandan Saikia	Woodward-Clyde
Charlie Sammis	USC
Javier Santillan	UC-Santa Barbara/SCEC Summer Intern
Lee Sapaden	California Disaster Response
Lisa Sarma	Columbia/SCEC Summer Intern
Brian Savage	Caltech
Jim Savage	USGS-Menlo Park
John Scheid	JPL
Craig Scrivner	CDMG/SMIP
Nano Seeber	Lamont
Paul Segall	Stanford
Bruce Shaw	Lamont
John Shaw	Harvard
Peter Shearer	UC-San Diego
Kaye Shedlock	USGS-Denver
Zheng-Kang Shen	UC-Los Angeles
Kerry Sieh	Caltech
Gerry Simila	CalState-Northridge
Bob Smith	Utah
Mark Smith	JPL
Stewart Smith	Washington
Paul Somerville	Woodward-Clyde
Jamie Steidl	UC-Santa Barbara
Ross Stein	USGS-Menlo Park
Tim Stern	Victoria University
Jeff Stevens	Maxwell Labs
Elizabeth Stone	Arizona State
Michael Suess	Harvard
Mike Sullivan	Dana Hills High School

Lynn Sykes	Lamont
Sara Tekula	USC
Leon Teng	USC
Hong-Kie Thio	Woodward-Clyde
Tim Tierney	UC-Santa Barbara
Molly Trecker	UC-Santa Barbara
Jerry Treiman	CDMG
Susan Tubessing	EERI
Allan Tucker	USC
Terry Tullis	Brown
Alexei Tumarkin	UC-Santa Barbara
David Ulin	Los Angeles Weekly
John Unger	USGS-Reston
David Valentine	UC-Santa Barbara
Shannon VanWyk	USC
Danielle Vanderhorst	UC-Santa Barbara
Jan Vermilye	Lamont
John Vidale	UCLA
Paul Vincent	Colorado
Mladen Vucetic	UCLA
Dave Wald	USGS-Pasadena
Lisa Wald	USGS-Pasadena
Chris Walls	Earth Consultants International
Steve Ward	UC-Santa Cruz
Mike Watkins	JPL
Karen Watson	UC-San Diego
Alex Weaver	Colorado
Kris Weaver	USC
Frank Webb	JPL
Shelly Werner	USC
George Westrom	FSEA
Jim Whitcomb	NSF
Clark Wilson	NASA
Paula Wilson	Utah
Jay Wilson	FEMA
Frances Winslow	San Jose OES
Cory Wisnia	SCORE
Frank Wyatt	UC-San Diego
Bob Yeats	Oregon State
Bill Young	SCIGN
Doug Yule	Caltech
Yuehua Zeng	Nevada-Reno
Lupei Zhu	USC

SCEC ORGANIZATION - 1998

Management

Center Director:	Thomas L. Henyey University of Southern California
Science Director:	David D. Jackson University of California, Los Angeles
Director for Administration:	John K. McRaney University of Southern California
Director for Outreach	Jill H. Andrews University of Southern California
Outreach Specialists:	Mark Benthien and Sara Tekula University of Southern California

Board of Directors

Chair:	David Jackson University of California, Los Angeles
Vice-Chair:	Bernard Minster University of California, San Diego
Members:	John Anderson University of Nevada, Reno
	Ralph Archuleta University of California, Santa Barbara
	Robert Clayton California Institute of Technology
	Lucile M. Jones United States Geological Survey
	James F. Dolan University of Southern California
	Thomas Rockwell San Diego State University
	Leonardo Seeber Columbia University
Ex-officio:	Thomas Henyey University of Southern California

Research Group Leaders

A: Master Model:	David D. Jackson University of California, Los Angeles
B: Strong Motion Prediction:	Steve Day San Diego State University
C: Earthquake Geology:	Kerry Sieh California Institute of Technology
D/F: Subsurface Imaging and Tectonics and Seismicity and Source Parameters:	Robert Clayton California Institute of Technology
E: Crustal Deformation:	Kenneth Hudnut United States Geological Survey
G: Earthquake Source Physics:	Leon Knopoff University of California, Los Angeles

Steering Committee Members (ex-officio)

Director Emeritus	Keiiti Aki University of Southern California
State of California Representative	James Davis California State Geologist
SCIGN Board Chairman	Frank Webb Jet Propulsion Laboratory

Southern California Earthquake Center

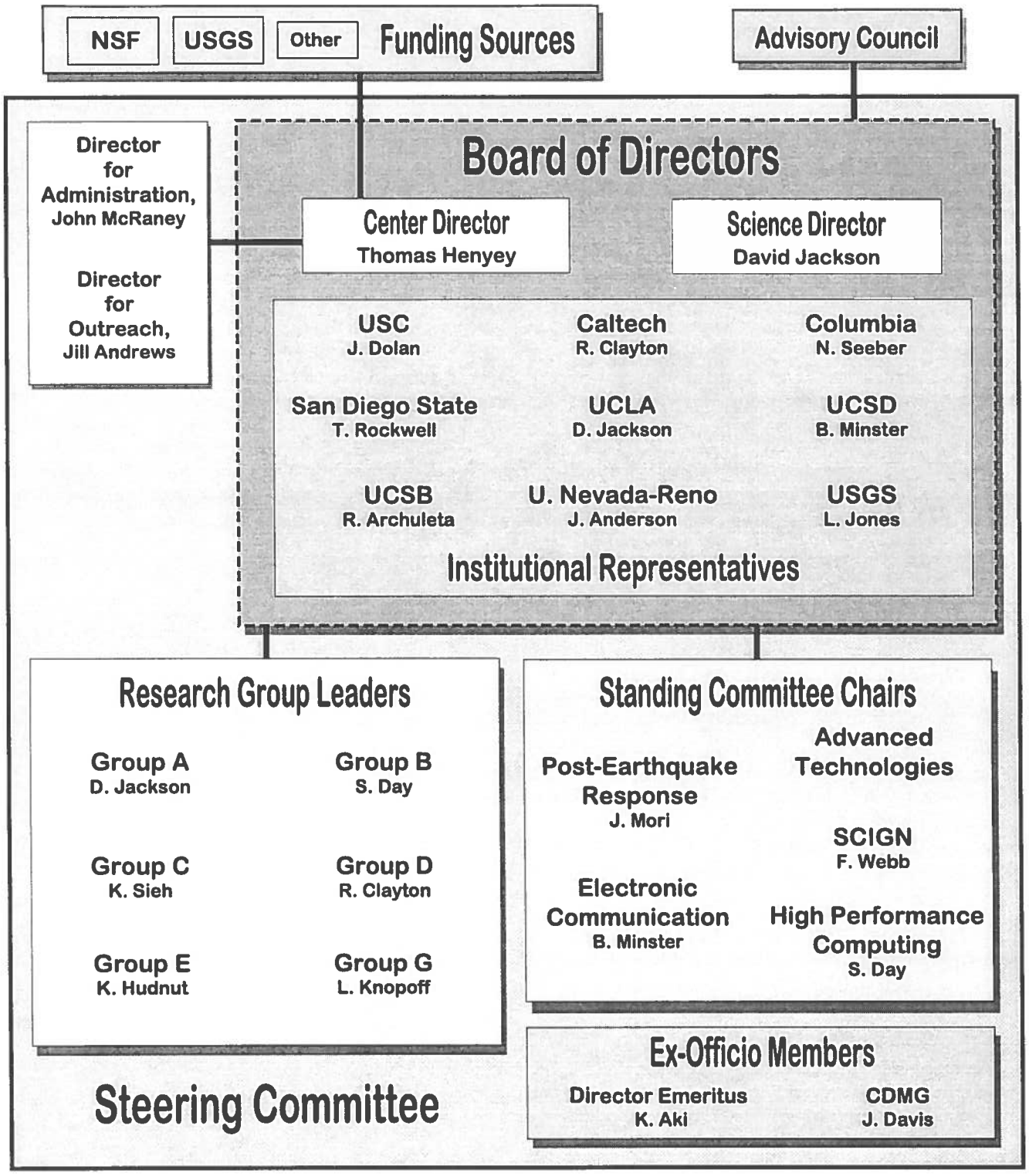

1998 SCEC ADVISORY COUNCIL

Robert SMITH (Chair), University of Utah, Department of Geology and Geophysics, Salt Lake City, UT 84112-1183

Lloyd S. CLUFF, Pacific Gas and Electric Co., Geosciences Department, P.O. Box 770000, Mail Code N4C, San Francisco, CA 94177

C. B. CROUSE, Dames and Moore, 2025 First Avenue, Suite 500, Seattle, WA 98121

George DAVIS, Department of Geosciences, University of Arizona, Tucson, AZ 85721

James DIETERICH, United States Geological Survey, 345 Middlefield Road, MS 977, Menlo Park, CA 94025

Thomas JORDAN, Massachusetts Institute of Technology, Department of Earth, Atmospheric and Planetary Sciences, Cambridge, MA 02139

Shirley MATTINGLY, 1965 Vistazo West, Tiburon, CA 94920

Dennis MILETI, University of Colorado, Natural Hazards Research and Applications Information Center, Institute of Behavioral Science #6, Campus Box 482, Boulder, CO 80309-0482

Jack MOEHLE, Pacific Earthquake Engineering Center, University of California, 1301 South 46th Street, Richmond, CA 94804-4698

Barbara ROMANOWICZ, University of California, Berkeley, Department of Geology and Geophysics, Berkeley, CA 94720

John RUNDLE, University of Colorado, Department of Geology, CIRES, Boulder, CO 80309

Kaye SHEDLOCK, United States Geological Survey, Denver Federal Center, MS 966, Denver, CO 80225

Cheryl TATEISHI, California Governor's Office of Emergency Services, 74 North Pasadena Avenue, West Annex, 8th Floor, Pasadena, CA 91103

Susan TUBBESING, EERI, 499 14th St., Suite 320, Oakland, CA 94612-1902

Southern California Earthquake Center
Senior Research Investigators (1998)

Principal Investigator and Center Director:	**Thomas L. Henyey** Department of Earth Sciences University of Southern California Los Angeles, California 90089
Co-Principal Investigator and Science Director:	**David D. Jackson** Department of Earth and Space Sciences University of California Los Angeles, California 90024

Principal Institutions	**Scientists**
University of Southern California Department of Earth Sciences Los Angeles, California 90089	Keiiti Aki Yehuda Ben-Zion James F. Dolan Edward Field Yong-Gang Li David Okaya Charles G. Sammis Ta-liang Teng
University of Southern California Department of Civil Engineering Los Angeles, California 90089	Geoffrey R. Martin
California Institute of Technology Seismological Laboratory Pasadena, California 91125	Robert Clayton Michael Gurnis Egill Hauksson Thomas Heaton Donald Helmberger Hiroo Kanamori Kerry Sieh Joann Stock
Columbia University Lamont-Doherty Earth Observatory Palisades, New York 10964	John Armbruster Leonardo Seeber Bruce Shaw Lynn Sykes
University of California Department of Earth and Space Sciences Los Angeles, California 90024	Mark Abinante Paul Davis Monica Kohler Zheng-kang Shen Li-Yu Sung John Vidale
University of California Institute of Geophysics and Planetary Physics Los Angeles, California 90024	Yan Kagan Leon Knopoff

University of California Department of Civil Engineering Los Angeles, California 90024	Mladen Vucetic
University of California Scripps Institution of Oceanography LaJolla, California 92093	Duncan Agnew Yehuda Bock Hadley Johnson Bernard Minster Peter Shearer Frank Vernon Nadya Williams Frank Wyatt
University of California Department of Geological Sciences Santa Barbara, California 93106	Ralph Archuleta Marc Kamerling Edward Keller Bruce Luyendyk Craig Nicholson Kim Olsen Peter Rodgers Jamie Steidl Alexei Tumarkin
University of Nevada Department of Geological Sciences Reno, Nevada 89557	John Anderson James Brune Raj Siddharthan Feng Su Steven Wesnousky Yue-hua Zeng
San Diego State University Department of Geological Sciences San Diego, California 92182	Steven Day Harold Magistrale Thomas Rockwell
United States Geological Survey	Gary Fuis Tom Hanks Ruth Harris Susan Hough Ken Hudnut Lucy Jones Nancy King James Mori Ross Stein David Wald Lisa Wald

Member Institutions	**Scientists**
Arizona State University Tempe, Arizona	Ramon Arrowsmith
University of California Davis, California	Louise Kellogg

University of California Irvine, California	Lisa Grant
University of California Department of Earth Sciences Riverside, California 90024	Stephen Park
University of California Earth Sciences Board of Studies Santa Cruz, California 95064	Steven Ward
California Division of Mines and Geology	James Davis Mark Petersen Michael Reichle
California State University Department of Geology San Bernardino, California 92407	Sally McGill
Carnegie Mellon University Pittsburgh, Pennsylvania	Jacobo Bielak
Central Washington University Department of Geology Ellensburg, Washington 98926	Charles Rubin
University of Colorado Department of Geological Sciences Boulder, CO 80309	Karl Mueller John Rundle
Harvard University Department of Earth and Planetary Sciences Cambridge, Massachusetts 02138	James Rice John Shaw
Jet Propulsion Laboratory Pasadena, California	Danan Dong Andrea Donnellan Michael Watkins Frank Webb
Lawrence Livermore National Lab Livermore, California	Bill Foxall
Massachusetts Institute of Technology Department of Earth, Atmospheric, and Planetary Sciences Cambridge, Massachusetts 02139	Brad Hager Tom Herring Robert King Robert Reilinger
University of Oregon Department of Geological Sciences Eugene, Oregon 97403	Gene Humphreys Ray Weldon

Oregon State University Department of Geosciences Corvallis, Oregon 97331	Robert Yeats
Woods Hole Oceanographic Institute Department of Geology and Geophysics Woods Hole, Massachusetts 02543	Jian Lin

Industry Participants

Earth Consultants International Orange, California	Eldon Gath
Maxwell Labs La Jolla, California	Jeffry Stevens
Willis Lettis and Associates Walnut Creek	John Baldwin Christopher Hitchcock William R. Lettis Keith Kelson Scott Lindvall
Pacific Gas and Electric San Francisco, California	Norman Abrahamson
Vortex Rock Consultants Diamond Bar, California	Mehrdad Mahdyiar
Woodward-Clyde Associates Pasadena, California	Robert Graves Arben Pitarka Chandon Saikia Paul Somerville

International Participants

CICISE/Ensenada, Mexico	Juan Madrid
Institut de Physique du Globe Paris, France	Geoffrey King

1998 SCEC Highlights

David D. Jackson
SCEC Science Director
University of California, Los Angeles

1. Path and Site Effects on Strong Ground Shaking

We have addressed the difficult and important problem of the local variability of strong ground shaking with several studies. In the (still) soon to be released "Phase III" report we assess the degree to which variability in strong ground motion can be explained by near surface shear velocity or mapped surface geology. Ned Field is leading this effort, with strong contributions from Norm Abrahamson, John Anderson, Yajie Lee, Mehrdad Mahdyiar, Kim Olsen, Steve Park, Jamie Steidl, and many investigators throughout California.

We found that in general high frequency shaking (over 1 Hz) is less predictable than lower frequency shaking. We also find evidence for significant contributions from intrinsic attenuation (1/Q), even for frequencies below 1 Hz. Near surface geology is significantly correlated with anomalous strong shaking, and subdivisions of Quaternary soil by age or grain size have distinguishable median amplification factors. However, the variability of ground motion within the subdivisions is still large, typically a factor of two. Similarly, near surface shear velocity is significantly correlated with shaking anomalies, but correcting for it leaves large residuals. The latter result is based on extrapolated shear velocity measurements from as far away as 5 km, as there are still few strong-motion sites at which the shear velocity has been measured directly. However, the variability in measured shaking amplitude is large even for individual stations observing multiple earthquakes, especially at high frequencies. Remaining variability apparently comes from complexity of the source, directivity effects, hanging-wall and near-fault effects, surface waves generated at basin margins, and other effects not included in most models of ground motion attenuation. While many of these effects can be treated well for past earthquakes, their predictability in future earthquakes is doubtful.

We found three dimensional wave propagation effects in sedimentary basins to be quite important. Surrogate one-dimensional models accounting for basin depth predict ground-motion anomalies that are significantly correlated with observed values, but they underestimate the anomalies predicted from true 3-D calculations. Figure 1 (from Kim Olsen) shows a comparison between the amplification factors for peak velocity using separate 1-D calculations at each site (top figure), and the averages of complete 3-D calculations at 0.3 Hz for nine hypothetical earthquakes. Including basin depth as a factor in strong-motion attenuation models reduces the residual anomalies by a modest but statistically significant amount.

2. Three-Dimensional Seismic Velocity Model

Several different 3D seismic velocity models of southern California have been developed for the specific purposes of strong ground motion simulations, tectonic studies, tomographic imaging, and earthquake location. Under the leadership of H Magistrale, R Graves and R Clayton, SCEC has developed a single standard 3D velocity model capable of supporting all these research needs.

Version 1 of the model fits a range of geological and geophysical observations. It consists of the major populated basins (Los Angeles basin, Ventura basin, San Gabriel Valley, San Fernando Valley, and San Bernardino Valley) embedded in a crust with velocity smoothly varying with depth, over a depth varying Moho. The model is parameterized as a set of objects and rules that are used to generate any 3D mesh of seismic velocity and density values (at length scales appropriate for different uses). The detailed basin portion of the model has over 70 defined surfaces that generally represent lithological interfaces. This parameterization is

convenient to store and update as new information (e.g., oil well sonic logs) and verification results become available.

Version 1 of the model will be tested by a variety of waveform modeling, tomographic studies, and new data releases that will provide constraints to be incorporated into Version 2. The model is available on the SCEC Data Center at http://www.scecdc.scec.org.

3. Geodetic Strain Model

Version 1 of the SCEC Crustal Deformation Velocity Map, released in 1996, was used extensively in studies of the mechanism of tectonic motions, postseismic deformation following earthquakes, and the effects of deformation on stress accumulation and earthquake potential. Shen et al. (1996), Souter et al. (1997), and Walls et al. (1998) all employed these data in constructing models for ongoing crustal deformation and its relationship to earthquakes. Savage and Svarc (1997), Bock et al (1997), Donnellan et al. (1998) and Savage et al (1998) used this model in studies of postseismic deformation. Version 1 was based on a combination of trilateration data acquired between 1970 and 1992 and survey-mode GPS data from 1986 to 1996.

The SCEC Crustal Deformation Working Group recently released its Crustal Deformation Velocity Map v2.0 (Figure 2; available online at http://www.scecdc.scec.org/group_e/release.v2). We included nearly all of the EDM, VLBI, and SCEC archived GPS data acquired for southern California between 1970 and 1997. The map and accompanying table include 363 stations for which the uncertainty in horizontal velocity is less than 5 mm/yr. For stations close to the Landers epicenter, we have provided estimates of both the pre- and post-Landers velocities.

The most important differences between Release 2.0 and Release 1.0 (October 1996) are the direct use of the VLBI data and the addition of GPS data from continuous observations since 1992, post-Landers surveys of the epicentral region, a 1992 survey of about 60 stations in and around the Los Angeles basin, and a 1997 re-survey of about 60 stations in the southern San Andreas system. These additions have added 76 stations to the map and have reduced 2/3 of the station velocity uncertainties to about 1 mm/yr.

4. Stress Evolution and Earthquake Triggering

SCEC has long emphasized stress accumulation as a promising criterion to recognize faults or regions most likely to experience earthquakes. A major SCEC contribution in this field has been to produce the important ingredients of stress evolution models for southern California: earthquake catalogs, fault maps, and deformation data.

Thanks to Ruth Harris, Joan Gomberg, and numerous authors, 13 papers resulting from a 1997 SCEC conference on this subject will soon be published in a special edition of JGR. This year SCEC sponsored another such conference, hosted by Ross Stein, who wrote a more detailed summary in the SCEC Quarterly Newsletter. Examples of sequences of quakes, each encouraged by Coulomb stress increments from previous events in the sequence, continue to accumulate. In addition, global and regional studies of complete catalogs show that main shock and aftershock occurrence are both favored in regions where shear stress has been increased by previous events. Attention has focused on the relative effectiveness of shear stress and normal stress. The studies of complete catalogs, and targeted studies of quakes on mature strike slip faults, generally show little influence of normal stress. On the other hand, some studies of other faults imply that a reduction of normal stress may act to increase seismicity. One problem that has complicated stress evolution calculations is the "nodal plane ambiguity:" two orthogonal planes, each giving identical displacements for point sources, respond differently to Coulomb stress.

Hardebeck and Hauksson have made progress in providing statistical tests that are tolerant of this ambiguity; Kagan has used tensor invariants to circumvent the ambiguity; Venkataraman, Mori and Kanamori have shown that broad band seismic data can resolve the fault plane ambiguity for earthquakes as small as magnitude 5.

SCEC's primary interest in stress evolution results from its possible predictive power. Several investigators have combined stress increment calculations with Dieterich's "rate-state" friction models to calculate theoretically the influence of Coulomb stress increments on individual fault segments. A result of the recent conference is ongoing discussions on ways that the predictive power of stress evolution calculations can be quantified and tested using data from future earthquakes.

5. Earthquake Sources in the Metropolitan Los Angeles Region

Several SCEC investigators have continued their work on source characterization in the greater Los Angeles region in 1998. Rubin, Lindvall and Rockwell published their paleoseismic work at the Loma Alta site, across a strand of the Sierra Madre fault in Altadena [Rubin et al., 1998]. They interpret radiometric- and soils-age estimates of two colluvial wedges to indicate that this fault at the base of the San Gabriel mountains has sustained two slippages totaling about 10.5 meters in the past 15,000 years. Such large slip events would be consistent with earthquake magnitudes above 7. This result supports the hypothesis that large earthquakes on the large, composite fault systems in the region relieve most of the north-south strain. But the implied recurrence times are several times longer than those proposed by *Dolan et al.* [1997]. The recent Nature paper by Walls, Rockwell and others (1998) may help resolve this disparity, since they propose that much of the slip rate formerly placed on the range-front fault is shunted off onto strike-slip faults south of the mountain front

The 1994 Northridge earthquake raised everyone's consciousness about blind thrust faults. Dolan et al.(Science, 1995) presented evidence that several blind thrusts could cause damage in the populous parts of southern California. SCEC has made it a high priority to understand blind thrusts well enough to resolve some of the uncertainties about their relative hazard. SCEC sponsored work by Mueller and others showed that the Compton-Los Alamitos thrust ramp has been inactive for 300,000 years, implying that the associated shallow thrust ramp below the Los Angeles basin is not as threatening as perceived in 1995. Nevertheless, the shortening across the Los Angeles basin, estimated at 7 to 9 mm per year >from geodetic data, still implies that strain is accumulating, and a complete understanding is not yet a reality. Walls et al. (Nature, 1998) have constructed a model (Figure 3) that integrates GPS data with geological slip rate estimates. An important conclusion is that the seismic moment rate, and hence the hazard, is smaller from blind thrusts and larger from strike slip faults than our 1995 study showed. Below latitude 34.7, geological slip rates and those inferred from GPS data are in very close agreement. Above that latitude, rates inferred from geology are substantially lower than those implied by GPS. Possible explanations are that the geological slip rates are underestimated, that additional faults contribute to the geodetic slip rates, or that random data errors account for the difference. Direct measurements of the strain distribution from more of the fixed GPS sites of the SCIGN array should help substantially to resolve this question.

Oskin and Sieh have just submitted their manuscript on the active folds and fold scarps of the central Los Angeles area. Their geomorphic, geochronologic and stratigraphic evidence indicate that these structures accommodate about 1 mm/yr of north-south contraction across the Elysian Park anticline. They contend that this is evidence of an active reverse fault, which extends 20 km from Hollywood to Whittier, beneath the central LA region. Other work published in the past year includes a study of the Hollywood fault (Dolan et al., 1997), which was made possible by SCEC's collaboration with the Metropolitan Transit Authority.

A few years ago, SCEC geologists Grant, Gath and Mueller began working on the raised marine terraces in the hills behind Newport Beach and Laguna Beach in coastal Orange County. These terraces suggested the possibility of large earthquakes generated by a blind thrust fault beneath coastal Orange County. The shape of the anticlinal uplift and U-Th ages have yielded an uplift rate of about 0.25 mm/yr and determination that the causative fault is a blind thrust that dips seaward from beneath the coastal communities of central Orange County. Recent discovery of an emerged late (?) Holocene terrace in upper Newport Bay may lead to establishment of the timing of the most recent large seismic event produced by this structure.

6. Theoretical Studies of Seismicity on Fault Networks

Knopoff, Ben Zion, Heimpel, Li, Abinante, and others have studied the evolution of seismicity on a complex network of faults, and the evolution of the faults themselves. The treatment of earthquakes in these problems is quasistatic. We also have been evaluating the importance of rough fault geometry on the properties of their seismicity.

Ben-Zion and his colleagues have studied fault evolution in an elastic-brittle seismogenic layer viscoelastically coupled to a substrate. The form of the fault system that develops is strongly dependent on the healing rates after fractures. If the healing rate is rapid, a network of disordered faults is obtained, while if the rate is slow, the fault systems are more regular.

Heimpel has considered an elastic-plastic seismogenic zone, with a simple through-going fault with two strike-slip segments parallel to the regional stress field, connected by a transverse segment at two "big bends", modeled on the San Andreas Fault (SAF) in Southern California. As slip evolves on the model SAF over long times, secondary zones of high slip begin to develop and extend and grow from one big bend that is similar to a Landers fault complex, and its image at the other bend (see Figure 4). If earthquakes are introduced into the above model, the transverse segment ruptures infrequently in comparison with the strike-slip sections. Now the fault structure off the main fault becomes more complex; in addition to the above features, the models exhibit orthogonal, complementary left-lateral features. The fault system is much more heterogeneous.

Li and Ben-Zion have found that stress correlation lengths fluctuate with time on a spatially heterogeneous fault. The correlation lengths are small after a large event and increase in the early times after a large event. After some time, the correlations saturate until the next big event; there are some fluctuations in the latter episode.

Abinante has studied the energy-to-moment ratio for dynamic fractures on a heterogeneous fault. The energy is given by the integral of stress drop times slip over the rupture surface. Its approximation by the product of average stress drop, average slip, and area is particularly inappropriate for an asperity model of fracture since large slips may take place in low stress-drop regions. The ratio of strain energy to seismic moment can differ by as much as a factor of 3 from expectations for a classical barrier model of fracture.

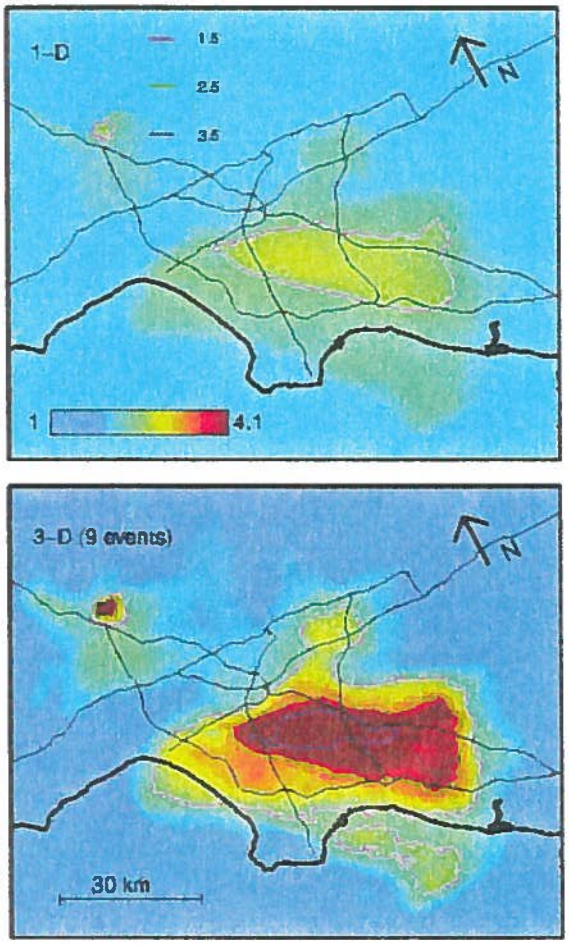

Figure 1. Maps of 0.3 Hz peak horizontal ground velocity corrections to a simple 1-D model, using two separate methods. The upper plot shows the result of a simple 1-D correction to a uniform model, in which ground motion is estimated using a separate 1-D model for each site. The lower plot shows the results of averaging full 3-D finite difference calculations for nine hypothetical scenario earthquakes.

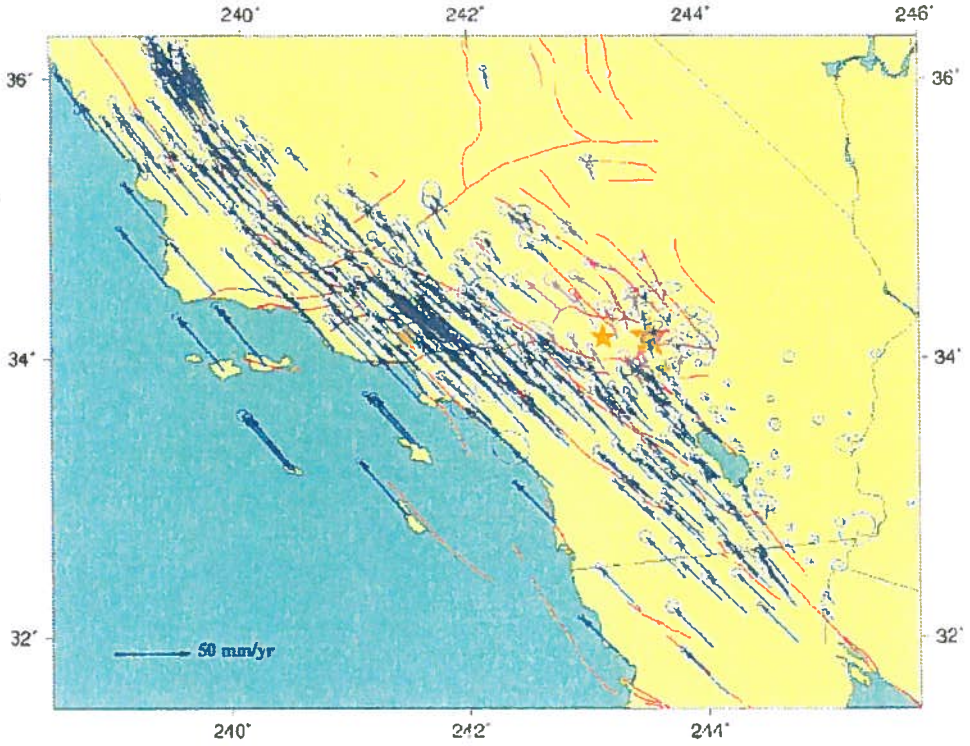

Figure 2. Horizontal crustal deformation velocity determined from Global Positioning System, Very Long Baseline Interferometry, and Electronic Distance Meter data in southern California. Velocity is relative to a group of GPS and VLBI stations on the stable North American Plate. 95% confidence error ellipses are shown for 363 sites.

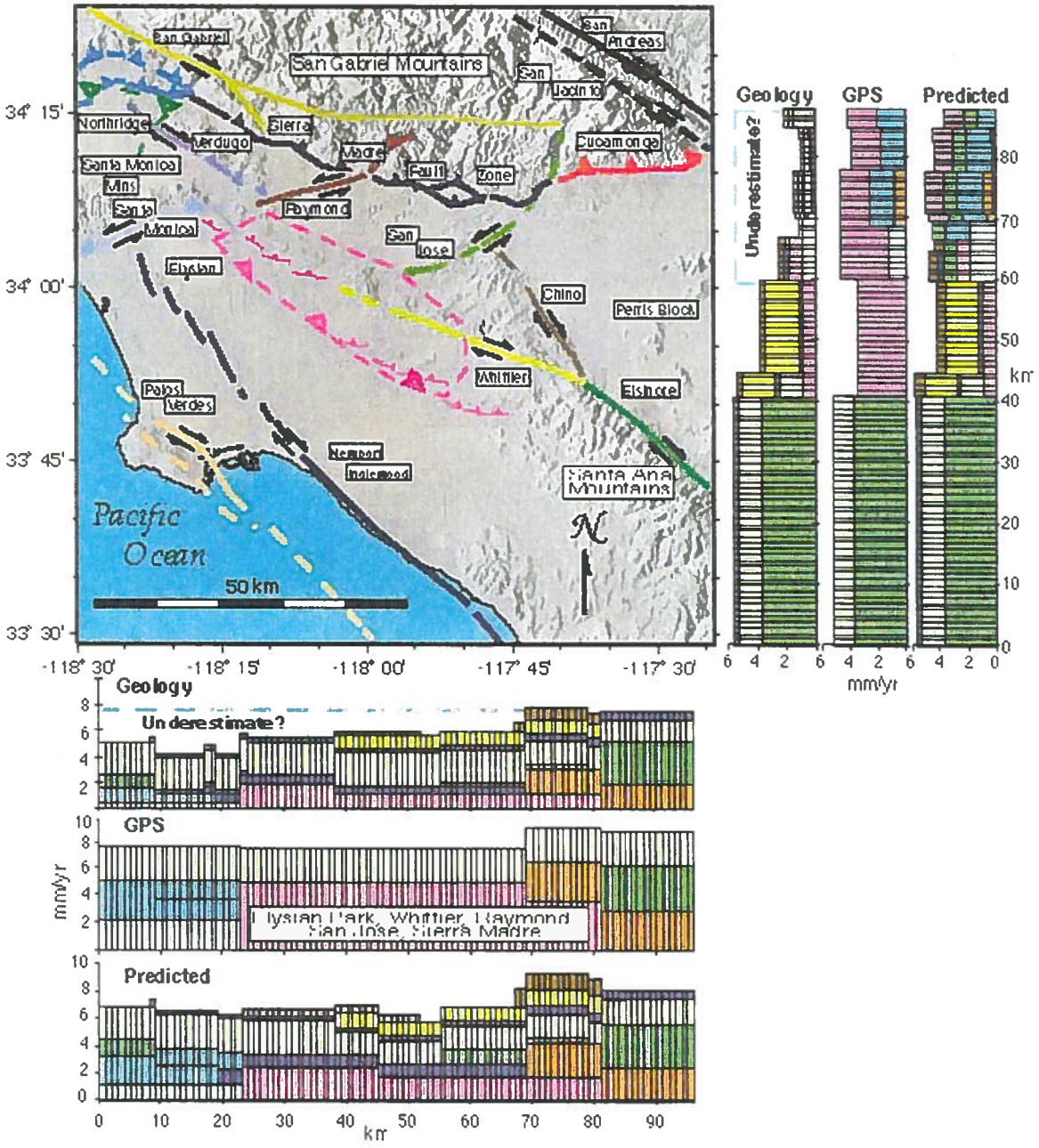

Figure 3. Map of fault-slip distribution in southern California as estimated from geological observations and GPS data. Also shown is the slip rate estimated from a model using both data sets. The side bar and bottom bar show the projection of fault slip rate into the north and east directions, respectively, relative to a reference point at the southwest. Faults are color coded, so that the contribution from each fault may be seen in the side and bottom bars.

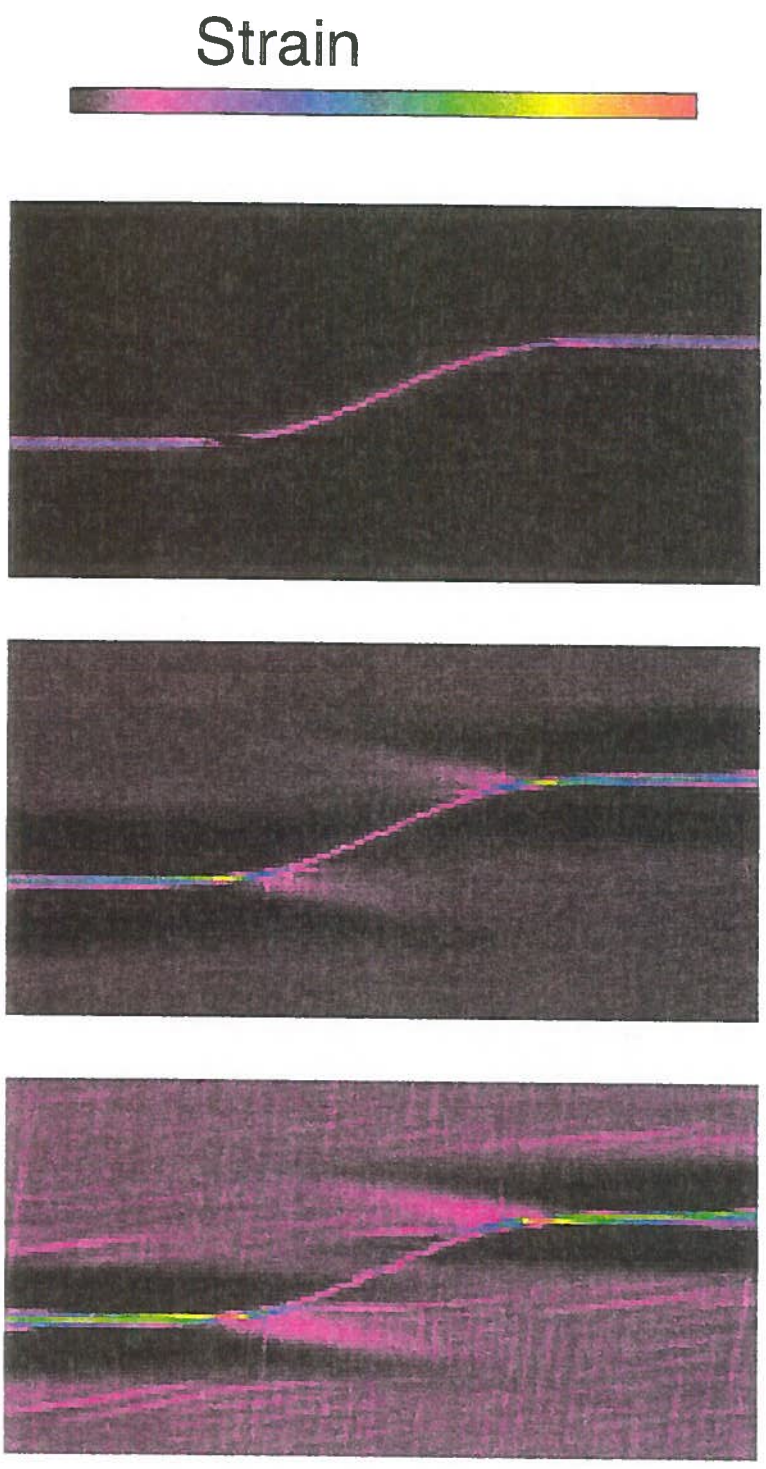

Development of strain at three times in an elastic-plastic model of a "San Andreas Fault". After some time, Landers type faults begin to develop from the big bends, to compensate for reduced strain on the transverse section. Strain is greatest on the strike-slip sections.

Southern California Earthquake Center Outreach Report: Public Awareness, Education and Knowledge Transfer Programs and Fiscal Year 1998 Activities

By Jill Andrews, Director for Outreach
With Mark Benthien and Sara Tekula, Outreach Specialists

Background In February 1998, the SCEC Board of Directors discussed ways to continue the education and outreach efforts in an efficient manner that would provide outreach products with the most impact and sustainability, and still fulfill our commitments in education and knowledge transfer to our funders. Tom Henyey and Jill Andrews recommended to the Board that for SCEC's final years (1998-2001), outreach projects should be already well-established, have short-term (4 years or less) results or products, and the potential for a lasting impact. The Board unanimously approved an outreach work plan for FY 1998 that combined education and knowledge transfer into an integrated program that represents and serves all SCEC institutions. We merged the missions, strategic goals, and objectives of the education and knowledge transfer programs under a single director for outreach (Andrews), thereby cutting some costs and reducing some overlap, while still keeping all important elements of the two programs intact.

In the spring of 1998, SCEC principal investigators and the Outreach team wrote a preproposal to the National Science Foundation (**NSF**) Science and Technology Centers open competition for renewal as the California Earthquake Research Center (**CERC**) commencing in the year 2002. The SCEC Outreach team conducted a July 1998 workshop to gain feedback from SCEC end users and potential CERC end users to write the full proposal, which was submitted September 3, 1998. A report on the results of the workshop is available from SCEC Outreach.

Outreach Team Our team is an effective broker of information between the academic community and practitioners, between earth scientists and engineers, between technical professionals and public officials, and between scientists and educators. The Center is known for its effective partnerships with local, state, and national government entities, academic institutions, industry, and the media. Our outreach efforts have evolved from concepts on paper to a multi-dimensional enterprise that provides notoriety to the Center while engaging all sectors of the community at large.

SCEC's Outreach staff is a results-oriented team that manages an array of activities consisting of workshops, publications, web sites, education modules, partnerships in industry and education, and database development and management. We organize the growing knowledge bases of academic scientists, engineers, and social scientists and make sure that their work is applied to reducing earthquake-related risks. We are committed to the notion that SCEC's outreach programs should complement -- not eclipse -- the science. Sara Tekula, a recent graduate of the psychology Department at USC, has joined the SCEC as an Outreach Specialist for Education. Mark Benthien enters his third year with SCEC, continuing his outstanding work on the SCEC Web site, running our workshops, overseeing the LARSE II permitting process, and directing the SCEC Summer Interns program. With Ed Hensley's (Hensley Communications) excellent skills in newsletter writing, editing and production, and with occasional help from John McRaney, Tom Henyey, Dave Jackson and the rest of the SCEC office staff, the outreach program is flourishing.

Mission and Goals The SCEC Outreach mission is *to promote earthquake loss reduction and lifelong learning by engaging the public at large in activities that focus on earthquake-related education, research-based technology development and transfer, and systemic reform.* We have divided our efforts into three programmatic categories: *Public Awareness, Education, and Knowledge Transfer* (see Figure, *A Mutually Influencing Network to Promote Earthquake Education and Outreach*).

Our public awareness programs target civic groups and professional organizations, media reporters and writers, and the general public.

- The SCEC Web site (www.scec.org) has undergone a major renovation during the last year. As with most Web sites, changes will occur frequently to keep information up to date and visual appeal interesting. Several sections of the site have been expanded to include much more information. To benefit university researchers, students and practicing professionals, we will expand our Web-based activities. Please visit the Web site and tour the Outreach pages.
- With the Multidisciplinary Center for Earthquake Engineering (**MCEER**) and ~50 other earthquake information providers, we continue our contribution to the Earthquake Information Providers' (**EqIP**) Web site (www.eqnet.org). Jill Andrews now chairs the EqIP Steering Committee and Ed Hensley provides maintenance and support with NSF funds.
- We plan to form an assessment team to periodically review the outreach programs of all SCEC affiliates. The team will identify SCEC*hub* participants who share a common vision to minimize duplication; tabulate and document their existing resources, strengths, and weaknesses; and produce a report comparing study results to a consensus *ideal*. To reduce unnecessary competition we will continue to establish agreements to resolve duplicate programs and share each others' products.
- An essential SCEC asset and marketing tool is the SCEC Quarterly Newsletter (**SQN**). More than 4,400 copies are mailed out each year and an electronic version is mounted on the SCEC Web site. SQN features research and activities sponsored by the Center, abstracts from the latest scientific and technical articles written by SCEC scientists, researchers, and staff, and news and articles from other organizations emphasizing research on earthquake phenomena. Readers include representatives of the U.S. government, California state, county, and city agencies; business and industry leaders interested in earthquake hazard mitigation; academic institutions, including pre-college teachers and students; the media; and the general public. To view on-line, go to: http://www.scec.org/news/newsletter/index.html.
- We distribute other print and electronic public awareness materials such as seismic hazard reports, general awareness publications, abstracts of SCEC author publications, and media advisories for researchers, educators, practicing professionals, building and safety and insurance industries, government officials and the general public. Before submitting a research paper for publication, SCEC scientists visit the SCEC Web site at http://www.scec.org/research/papers.html to receive a SCEC Contribution Number and NSF/USGS grant numbers. Authors use an on-line form to mount information and receive their numbers. This process is required by NSF and is also a requirement for SCEC funding. The result is a database of SCEC research papers, now available interactively online on the same page.

- We encourage earthquake loss reduction through acknowledgment and support of the California State Seismic Safety Commission's Loss Reduction Plan and the National Mitigation Strategy. Many SCEC projects fall under the geosciences and education and information elements contained in the California Earthquake Loss Reduction Plan. The State Seismic Safety Commission endorses our actions and has committed to support our research and educational outreach programs that help achieve the plan's objectives.
- As part of our commitment to an outreach effort funded by the USC Neighborhood Outreach Grant program, we completed a local Neighborhood Earthquake Watch program earlier this year. This project included presentations on urban earthquake hazards, a preparedness survey, Spanish translation of the (currently under development)*LA Underground* publication, and provision for installation of automatic gas shut off valves and a neighborhood earthquake safety fair. A community guidebook has been developed and is in final preparation and review. The booklet, entitled *An Earthquake Community Preparedness Plan Handbook,* offers instructions on:
    - Creating a community-preparedness plan: where to start
    - How to partner with earthquake-related educational organizations (like SCEC)
    - Elements of a community plan (meetings, educational activities, fund raisers, guest speakers program, preparedness fair, follow-up
    - How to run an earthquake fair
    - How to share the experience with other communities
    - Information on intergenerational issues within a community
- We provide speakers for public presentations (Center scientists and engineers as well as educators and outreach professionals) and experts who lead field trips and conduct workshops on local seismicity. Professional organizations, civic groups, museums, and schools have all been served by our speakers. A sample list of community outreach activities provided by SCEC-affiliated researchers during the last year can be found on the SCEC Web site at http://www.scec.org/outreach/community2.html.
- We sustain established relationships with local media organizations (print, radio and television) to educate and inform the public about earthquake-related issues. One of the most exciting projects this year was the *Care and Prepare* earthquake awareness and preparedness campaign with Los Angeles-based television station KTLA Channel 5 during the month of April. KTLA printed excerpts from *Putting Down Roots in Earthquake Country* in both English and Spanish, and aired three half-hour specials (two for adults and one for children) during California's earthquake preparedness month. A video tape of the specials and morning news show interviews with SCEC representatives will be on continuous display at the Outreach poster during the SCEC Annual Meeting in Palm Springs.
- We are planning to create Web-based materials that can be used by reporters and writers following damaging events. In partnership with IRIS's Outreach staff, we are launching plans to create these materials as part of a joint *Teachable Moment Initiative*. We may pre-identify a seismic event based on known global distribution of seismicity; select a target date; prepare educational materials in advance; then release media advisories on the event and its environmental impact and probable effects if the event had been located in an urban area.

- With the State of California Office of Emergency Services, we are laying plans to launch *Earthquake Studies and the Civic Scientist*, a series of mini-workshops to educate earth scientists, earthquake engineers and Public Information Officers on how to better communicate with reporters, writers, and the public. This initiative was conceived last fiscal year and we are seeking funding for the project. Joint plans will be discussed in a mid-October 1998 meeting with OES officials.

Our education programs target students and educators, museums, building industry professionals, insurers, urban planners and code officials, public policy makers, and emergency planners and responders.

- Education activities at the undergraduate and graduate level promote career development of earth science students, with special attention to minorities and women. We are continuing with our career-oriented programs for undergraduates by supporting earth science undergraduate student research projects through the SCEC Summer Intern Initiative. All interns present papers or posters at SCEC's Annual Meeting and have the opportunity to attend regular seminars conducted at Caltech as part of that institution's Summer Undergraduate Research Fellowship (SURF) program. Eight undergraduate scholars were chosen for SCEC's Summer Internship Program for 1998, the fifth year of this successful program. SCEC Internships allow undergraduate students to earn valuable experience through conducting a research project with a SCEC scientist. Please see http://www.scec.org/outreach/undergrad/98interns.html for the list of project titles, students, their personal goals, and research mentors; and a description of the 1998 Interns Colloquium.
- We are using the Internet to facilitate communication among researchers and students. For example, we have added to the on-line database of SCEC participants a new student demographics reference resource to aid tracking capability of all graduate students, post-doctorals, and interns. The database enables users to simply click a button on the database to view principal investigators' and others' outreach projects descriptions, research project descriptions, group affiliations, publications links, and speakers by categories.
- SCEC institutions recruit highly qualified students in all disciplines. Nationwide, the percentage of females pursuing advanced natural science degrees is typically well below 30%; those studying earth science is but a fraction of that. SCEC investigators have managed to keep their female graduate population at an admirable 26% (see Summary Chart below). SCEC P.I.s have not previously attracted as many underrepresented minority graduate students; however, the summer undergraduate internship program has consistently achieved very high marks in attracting both women and minorities—an important goal of the program. In 1998 half the eight interns were female and most ethnic groups were represented. To increase these numbers, we will work with SCEC institutions' minority-serving programs to attract underrepresented minority and women students by contacting institutional student advisors and initiating poster and flier campaigns that target colleges with large underrepresented populations and have excellent science, math, and engineering curricula. We will recruit them as undergraduate (transfer), graduate, and post-graduate students within SCEC universities. California's community college system, for example, has significant African American and Hispanic populations and is the state's primary *feeder* to its universities. We will do a feasibility study to consider establishment of a liaison program with these and other minority-serving schools. We will encourage SCEC scientists and students to visit these institutions and make presentations to science faculty and students on SCEC programs, internships and opportunities for graduate work.

M.S. AND PH.D. DEGREES COMPLETED, 1994-97 UNDER DIRECTORSHIP OF CERC PERSONNEL

DEGREE: 39 M.S. TIME TO DEGREE: 3.07 YEARS (AVERAGE)	
GENDER	14 FEMALE
RACE/NATIONALITY	1 ASIAN (US) 2 HISPANIC (US) 11 WHITE (1 HOLLAND; 1 UK; 9 US)
GENDER	25 MALE
RACE/NATIONALITY	4 ASIAN (1 INDIA; 2 JAPAN; 1 PRC) 21 WHITE (1 HOLLAND; 20 US)
DEGREE: 75 PH.D. TIME TO DEGREE: 5.85 YEARS (AVERAGE)	
GENDER	16 FEMALE
RACE/NATIONALITY	3 ASIAN (1 INDIA; 2 PRC) 13 WHITE (1 ISRAEL; 1 RUSSIA; 11 US)
GENDER	59 MALE
RACE/NATIONALITY	17 ASIAN (1 HOLLAND; 1 INDIA; 1 JAPAN; 12 PRC; 1 TAIWAN; 1 US) 2 HISPANIC (1 ARGENTINA; 1 US) 40 WHITE (1 FRENCH; 3 GERMAN; 1 HOLLAND; 1 ISRAEL; 2 NEW ZEALAND; 1 ROMANIA; 1 SERBIA; 1 SWEDEN; 1 SWITZERLAND; 2 UK; 26 US)

- To increase diversity in our graduate programs, we are designing a cooperative agreement with the Incorporated Research Institutions in Seismology (**IRIS**). We will work with IRIS to create a program in association with college science and engineering professors who are not affiliated with SCEC to help us identify and attract top tier undergraduate students.
- Our collaborators in the K-16 sector stand ready to establish mentoring programs for teachers and students. A cascading network in the exploration phase with our partner schools involves scientist-to-teacher-to-student instruction, with SCEC as a scientific resource for the community. We also have fostered a mentoring network to connect SCEC researchers with teachers through workshops, field trips, supervision of special projects, and provision of financial assistance. Through SCIGN and TriNet facilities siting programs, contact with teachers and students will grow to include all portions of the state and beyond its boundaries.
- SCEC's former Education director formed high school partnerships. Early in the spring of 1998, we conducted a survey of our three partnership schools (Palos Verdes, La Cañada, Rialto, and other schools that host detection equipment sites for our various research projects).Responses regarding the following categories were gathered. We are currently assessing SCEC's capabilities in light of these suggestions. Please see http://www.scec.org/outreach/education.html to view information on our partnership agreements and to view the feedback we are considering.
- We support attention to and alignment with the national science education standards and California state education standards (especially in our K-12 programs and materials). We distribute throughout the nation our original educational products (i.e., our earth science education modules) that highlight SCEC scientific research. We have formed working agreements with professional educators from groups such as the K-12 Alliance, California Science Implementation Network (**CSIN**), Los Angeles Educational Partnership (**LAEP**), and Los Angeles County Office of Education (**LACOE**), which serve California state teachers and students in the K-12 sector.

  The relationships developed since Sara Tekula joined SCEC in February have proven to be mutually beneficial. We contribute to science curriculum development and enhancement, for example, through Tekula's participation in LACOE's South East Educational Technology Consortium (**SEETC**), which covers a student population of about 200,000 and makes up 13% of Los

Angeles County's total student body. SEETC is also a Community of Excellence (**CoE**) focusing on science. (See http://www.scec.org/outreach/eduscec.html for more information on the LACOE and SEETC projects.) Tekula, in collaboration with curriculum developers and teachers, is helping design a *storyline* for an earth science unit in a middle school classroom. A historical approach will be taken, telling the story of science instead of an outline of factoids. Instead of memorization methods and multiple-guess testing styles, students will learn to think like the scientists who first tested the theory of plate tectonics. Instead of matching proper definitions in a testing situation, students will be asked to re-tell the story of how the theory was born. To encourage communication outside the bi-weekly meetings, LACOE secured a virtual room on the TAPPED IN on-line professional development Web site. A SEETC CoE Room hosts the group for on-line meetings, posted documents to be shared, to tour Web sites and provide a place to leave ongoing work for group members to review. The first meeting occurred on September 3rd. When the DESC On-line modules have been modified for the middle school level, the same teachers that were trained on the modules will have a familiar teaching tool from which to pull activities, lessons, interactive real-time maps, GPS and seismic data, and information about local faults. The middle school modules will mirror the storyline framework developed with SEETC.

- With help from these and other dedicated educators in the community, we have continued the process of creating the on-line education modules for K-12 students. This project has been dubbed the Development of Earth Science Curricula On line (**DESC On-line**). We have assembled a group of scientists and educators to measure the impact and implementation of current products. With an advisory group drawn from this group of professionals, we conducted a formal scientific and education standards review of the modules, with a commitment to bringing the products on line by the end of the calendar year. See http://www.scec.org/outreach/edudesc.html for more information.
- Our community-based activities include field trips to local faults, museum lectures and exhibits, civic group presentations, and participation at annual conventions and conferences. We help improve exhibits and patron programs with the California Science Centers. SCEC has already influenced the development of an earthquake exhibit at the California Science Center (CSC) in Exposition Park, and based on its success, they have requested our assistance with compiling earthquake data and graphics for a new *Technopolis* display. We have recently agreed to furnish speakers for CSC's museum-based children's programs, the grand opening of the *Powers of Nature* exhibit that features earthquakes, and to recruit our scientists to lead museum patrons to local trips to active faults. In January 1999, we will lead a group of Denver Museum of Natural History patrons to a series of local faults and conduct a tour of the Caltech-USGS seismic network and seismological laboratory displays in Pasadena.
- We are pursuing collaborative efforts with the Los Angeles Educational Partnership (**LAEP**) to develop teacher training workshops and enhance our on-line materials. SCEC will link to LAEP Web sites (and vice versa). Together we plan to develop virtual tours since they have already mounted this type of Internet learning tool on the Web and can provide assistance. LAEP is an independent non-profit public education fund working to improve public education for the children of Los Angeles. Since 1984, LAEP has invested more than $35 million in the efforts of educators and community members to develop, test and implement new strategies for strengthening classrooms, schools and communities. Its work ranges from

supporting the innovative efforts of individual teachers to the development of comprehensive designs for the schools of the future.

- We have initiated contact with the Los Angeles Physics Teachers Alliance (LAPTAG) program to support undergraduate Geophysics Curriculum enhancement; and with the Future Scientists and Engineers of America (FSEA) project to support after school technology clubs in K-12 schools.

Our Knowledge Transfer programs target technical professionals, geotechnical and structural engineers, engineering geologists and seismologists, and scientists and engineers in academia and government.

- We have formed partnerships to facilitate societally-based systemic reform (e.g., better building practices, code upgrades, introduction of legislative initiatives) through interactive workshops, symposia, and continuing education programs for the community of scientists and technical professionals working in related fields.
- With the State of California Office of Emergency Services, we participate in the Post-Earthquake Technical Clearinghouse working group following damaging earthquakes in California. In the event of a damaging urban earthquake in California, we will simultaneously station SCEC staff at computer sites at Caltech and the OES Clearinghouse, who will serve to coordinate communication via the Internet, telephone, and in person among scientists, engineers and response and recovery groups. Information will also be packaged to accommodate the needs of writers and reporters.
- We produced a proceedings volume and convened a working committee to address the outcomes of the *Earthquakes and Urban Infrastructure* workshop held in late January 1998, in partnership with the Los Alamos National Laboratory's Urban Security group. To address end users' needs and gather input, we held a second workshop collocated with the Western States Seismic Policy Council's Annual Meeting in September 1998. We are collaborating with the Los Alamos National Laboratory Urban Security Team and others to provide a set of science- and technology-based computational tools analogous to the computer game *Sim City*. Our tools will include real-time feedback for disaster planning, training, and management in time of crisis and long-term recovery.
- We are continuing with our sponsorship of the Los Angeles City / SCEC / SEAOSC Ground Motion Joint Task Force monthly workshops. Now that a dialogue has been established among structural engineers, civil engineers, geotechnical engineers, building officials, planners, and earth scientists, this task force is providing recommendations regarding earthquake ground motion hazards to the Los Angeles City Department of Building and Safety for determining public policy related to design of new buildings and seismic retrofit of existing structures. FEMA is underwriting production and printing of two public awareness booklets aimed at owners and occupants of the two types of vulnerable buildings. The booklets have been written by leaders from the task force and are currently under review.
- We have begun the process of planning a joint workshop with the County of Los Angeles and Association of Engineering Geologists to discuss consensus views on a common database of parameters on Los Angeles Region Active Folds and Faults.
- Currently in the planning stages is a joint SCEC and Pacific Earthquake Engineering Research Center (PEER) Workshop to compile a referenced Ground Motions and Time Histories Library.
- We are planning a series of workshops to address the needs of the Los Angeles County Urban Search and Rescue (US&R) teams. The first in the series will be conducted in mid-January 1999 to commemorate the 1994 Northridge event. We are working with US&R chief for County of Los Angeles Larry Collins to recruit

speakers for the January workshop. Topics of interest that will be covered are hazardous local faults and probable damage to buildings and infrastructure; prediction capabilities; early warning capabilities; engineering issues; and using new technologies to enhance response and recovery.

- We co-sponsored with the Western States Seismic Policy Council and the Council of State Governments WEST a Summit on Earthquake Insurance in Sacramento in June. The summit provided a platform for Exposition, Clarification, and Commentary by all constituents regarding issues and variables involved in earthquake insurance. A book with abstracts and papers by presenters and panelists with general proceedings has been published and is now available through WSSPC.
- SCEC will continue to organize workshops for insurers to address topics such as an update on the California Earthquake Authority; outcomes of the WSSPC Insurance Summit; and how to use new hazard maps and other mapping products (HAZUS, DMG, EPEDAT, ZOD depictions with an overview of recent studies and research results in simple language). One goal is to receive insurers' and risk assessment professionals' input on usefulness of these and other tools; and solicit their opinions regarding usefulness of existing products.
- Another alliance SCEC Outreach has formed is with the California Universities for Research in Earthquake Engineering (CUREe). We have designed the *CUREe/SCEC Lectures*, a seminar for earthquake engineering and earth science students and professionals that address the joint concerns and issues relating to state-of-the-art practice in both disciplines. The first workshop will be held November 5, 1998.
- A September 1998 FEMA grant through the State of California's Office of Emergency Services will support a three-year study by CUREe called *Earthquake Hazard Mitigation of Woodframe Construction*. SCEC's Outreach director has been appointed as Associate Manager for Outreach for the project. SCEC Outreach was featured at the September 28, 1998 press conference to announce commencement of the project at Caltech. Over the next three years, Andrews will oversee four outreach projects plus media production beginning winter 1999, including:
  - House retrofitting
  - retrofit of multi-story residences
  - wood engineering seminars; and
  - construction quality.
  - We also expect to update, in collaboration with local cities and counties, existing short course curricula and materials using results from the research.

Electronic-based Outreach projects include:

- A SCEC science seminar to be hosted by UCSB to acquaint SCEC scientists with the digital library systems statewide and discuss how SCEC's own archives and databases might be integrated.

International Projects

SCEC's Outreach program is a participant and cosponsor in the planning and convening of the Fourth International Conference on Corporate Earthquake Programs, to be held in Shizuoka, Japan, in November 11-13. SCEC's Outreach projects, including most of its community-based programs, will be featured through Andrews' participation in 2 panel discussions and one formal presentation.

Past activities include:
1995: SCEC was represented in several presentations and 2 small workshops by the Knowledge Transfer director and several SCEC scientists at 11th Course, Active Faulting Studies for Seismic Hazard Assessment, in Ericé, Sicily. There were 150 representatives from 75 countries in attendance.

1997: SCEC Knowledge Transfer convened a one-day workshop at the Int'l Association for the Study of Physics of the Earth's Interior (IASPEI) in Thessaloniki, Greece, August, 1997. *Educating the Public About Earthquake Hazards and Risk* was co-convened by representatives from China and Greece.

Future activities will include:
1999: SCEC Outreach will co-convene an Outreach Session at the IUGG meeting in Birmingham, England.

Projects to Launch through Funds to be Raised

We hope to raise funds this year to host a First Annual Non-Technical Summit in partnership with local engineering firms. *The Real Meaning of Seismic Risk,* an idea formed during discussions at a CLA / SEAOSC / SCEC Joint Task Force meeting, will be a summit panel consisting of well-informed experts with differing or opposing views on urban seismic risk issues. The summit would feature a lively, compelling exchange among earth scientists, earthquake engineers, building officials, public policymakers, architects, insurers, developers and the media. Five or six topics could be addressed by the panel: possibilities include a critique of methods used to interpret the earthquake threat; vulnerability of tall buildings and other structures located near faults; whether the *life safety* design code is the best practice given what we now know from Northridge; cost-benefit analyses of various retrofitting techniques and strengthened codes for new construction; perceived socio-economic impacts of earthquakes and secondary hazards in California vs. other natural hazards outside the State; etc. A product of the summit would be a SCEC report for the public, with audio and video tapes of the proceedings.

SCEC Annual Meeting Abstracts
1998 Summer Undergraduate Interns

Paleoseismic Studies of the San Andreas Fault in the San Bernardino Area

Safaa Dergham
Columbia University

A trench across the San Bernardino segment of the San Andreas Fault in San Bernardino, California, revealed vertical offsets that provide strong evidence for two surface ruptures in the past 800 years. The average recurrence interval between the two events is about 160 years. Seven radiocarbon dates of detrital charcoal are in correct stratigraphic order and indicate an average sedimentation rate of 5.3 mm/year. In addition, these dates constrain the ages of the individual faulting events. The oldest event occurred shortly after A.D. 1235-1410 and the youngest event occurred between A.D. 1439 and A.D.1643. There was no evidence for younger ruptures at the Plunge Creek site that could correspond to the A.D. 1812 and the A.D. 1700 events at Pitman Canyon and Wrightwood. A second trench will be open on another young alluvial fan at this site to further investigate the occurrence of recent earthquakes in this area.

Development of an Interface for 3D Visualization of SCEC Earthquake Data on the World Wide Web

Leland R. Green
University of California at Santa Barbara

The distribution of earthquakes in space is fundamentally a 3 dimensional problem. In order to properly understand and interpret the properties of an earthquake, researchers must be able to visualize an earthquake and its relationship with past seismic events in 3-D. I have developed an interface that allows viewers of the SCEC web page to access earthquake hypocenter data, display and control the viewing perspective of this data, and produce time based animation of the database. The interface was developed using Java based tools. This will allow the interface to be displayed on any web browser (e.g. Netscape, Microsoft Internet Explorer) that has the ability to display Java applets. In the past, visualization of earthquake data in 3-D required a program compatible with your operating system (e.g. Xmap8, a UNIX based system developed by Dr. Jonathon Lees of Yale). Now SCEC will be able to provide the public, scientists, students and educators with the ability to better understand the 3-D aspects of an earthquake regardless of the system from which they access the information. Also, the object oriented nature of the Java programming language will allow the interface to be expanded to include any type of subsurface data present in the SCEC earthquake database or other geologic databases.

Folding and Faulting along the San Andreas Fault, Palmdale, California: Implications for Simple Shear mechanics and Education of the Public

Lowell Kessel and Arthur Sylvester
University of California, Santa Barbara

Palmdale, California, along the Antelope Valley freeway (state route 14), is the location of one of the best exposures of the San Andreas fault zone and its related structures. The fault zone consists of several faults that parallel the San Andreas fault (SAF), striking 114^0, and commonly spans a width of several kilometers. The north-south road cut is aligned nearly perpendicular to the strike of the fault and can be considered to be a large "trench." The road cut is about 27m high and about 700m long and exposes complexly folded and faulted middle

Pliocene lacustrine sandstone and gypsiferous shale (Anaverde Formation). Large and small-scale east-west trending folds oriented approximately 10^0-15^0 to the SAF are cut by numerous faults with differing orientations. The fault zone segment, located within the road cut, is a strike-slip regime in which the entire roadcut is "sandwiched" between two strike slip faults, the SAF and the Little Rock fault. Many fault segments are parallel to the SAF with an average strike of 113^0. East-west trending faults contained within the road cut and oriented approximately 20^0-30^0 to the SAF are Riedel shears or thrust faults.

Geomorphology of Landslides along Oak Ridge and South Mountain, Southern California, with Exploration of Possible Dating Techniques for Landslide Scarps

Jacqueline Moccand
University of Southern California

The aim of this project was to examine the geomorphology of the massive landslides that are prevalent on the northern slopes of Oak Ridge and South Mountain, Southern California. Complimentary to this was the investigation of different rock dating techniques currently available, including the relatively new methods of using cosmogenic isotopes to date rock exposures. Had it been possible to access the steep scarp slopes of these massive, (1000 ft in some cases) landslides, an approximation of the time of surface rupture would have been obtained from analysis of the mineral olivine using the method of 3-He geochronology. An age for the exposed rock surface would have been obtained thereby giving a window for the time of sliding. However this was not possible, and only relative ages of the mass movement events could be obtained. Cross sections of 4 of the major landslides were made using topographic maps of the area, as well as studying aerial photographs, and a qualitative age was given to each slope failure event based on the gradients of the slopes. If precise quantitative ages had been obtained for the landslides, this study could be extended by looking at historic seismicity in the area, and trying to see if the two types of events are linked in any conclusive way.

What prompted this investigation is the hazard these types of catastrophic movements can present to human life and property, and the need to better understand these movements and their frequency in order to help mitigate against potential future danger.

Velocity Structure of the Near-Surface San Fernando Valley from Tomographic Inversion of Active Source Data

Tracy H. Pattelena
Pasadena City College
David Okaya and Nicola Godfrey
University of Southern California

In 1994 the Northridge earthquake (MW = 6.7) struck the Los Angeles area causing significant damage to the San Fernando Valley of southern California. Using existing active-source reflection data collected by Chevron prior to the Northridge earthquake, we obtain both compressional wave (VP) and shear wave (VS) velocity information for the upper 500 m of crust. We do this by analyzing the data for three different north-south trending seismic lines. To analyze the VP velocities we pick the refraction phases for VP and apply the tomographic velocity inversion method of Hole (1992) to calculate the first-arrival times. We further compare our VP models to well VP sonic log data available for the area. To analyze the VS velocities we pick the refraction phases for VS after applying bandpass filtering to 12 Hz and apply the tomographic velocity inversion method of Hole to calculate the first-arrival times. We conclude with calculating Poisson's ratio (sigma) based on the determined VP to VS ratio to compute the VP-to-VS conversion factor applicable for the San Fernando Valley (SFV).

Our VP models show velocities dipping south into the SFV as do the seismic profiles obtained for all three lines. VP velocity models for all three lines show an overall near-surface velocity range beginning at 1.3 km/s along the base of the San Gabriel Mountains (SGM) decreasing to roughly 1.0 km/s southward into the valley with an overall average velocity convergence to 2.6 km/s at depths of approximately 500 m. Our VS model shows near-surface velocities beginning at 0.3 km/s just beneath the foothills of the SGM and remaining constant southward into the SFV. At depths of roughly 200 to 300 m, there is a convergence to 1.2 km/s beneath the SGM which decreases to between 0.8 and 0.9 km/s into the valley. Based on these findings, we calculate s to be 0.4 for near-surface areas beneath the SGM and at depths greater than 200 m once into the SFV and 0.2 for near-surface depths of less than 200 m in the SFV.

Analysis of Azimuthal Variation in Amplitude Factors in Sherman Oaks and Santa Monica During the Northridge Earthquake Aftershock Sequence

Justin Rubinstein
University of California, Los Angeles

The Northridge earthquake caused unexpectedly high amounts of damage in Santa Monica and Sherman Oaks, two regions far removed from the rupture. My project was to investigate the cause of the anomalous high damage in both locations. Working with data from the Northridge Earthquake Aftershock Recording (NEAR) Experiment, a dependence of high amplitude areas upon source location was investigated. Analysis of data from the twenty-nine seismic stations placed in Santa Monica indicates that there is lens structure at depth which creates the enhanced damaged in the mid Santa Monica region. Using contour plots of amplitudes of the 29 stations in Santa Monica for each event indicated a movement of a "hot zone" where the amplitudes were much higher than the surrounding regions. Tracing rays through a moveable lens from the hypocenter of an event to the surface allows one to pinpoint the location of lens. The finite nature of the lens indicates that the high damage in Santa Monica was dependent upon the location of the main shock. As evidenced from aftershocks in this data set, an earthquake of similar size in a slightly different location would most likely not reproduce this damage pattern. Sherman Oaks produced two regions of concentrated amplification, but no systematic azimuthal pattern as seen in Santa Monica was detected.

Understanding Ground Motion Variations at the Van Norman Dam Complex Site

Javier D. Santillan
University of California, Santa Barbara

During the 1994 Northridge event, seismic stations at the Van Norman Dam Complex recorded peak accelerations that significantly varied over short distances. In an effort to gain further understanding of this behavior, this project focused on comparing weak ground motion a six different sites around the dam. The first station was an existing SCEC borehole at the Jensen Generator Building. The other stations were placed at the Jensen Administration Lawn, Sylmar Converter Station West and East, the Los Angeles Dam, and the Rinaldi Station. Over the course of two months, a few weak motion events yielded enough data to begin a comparison of the array stations to data recorded at the borehole station during the previous seven months. The weak motion data recorded during this project have shown ground motion variation similar to those observed during the Northridge earthquake.

Characterizing the Damping of Multi-Story Buildings Through the Forced Excitation of a Nine-Story Building

Lisa Sarma
Columbia University
Thomas Heaton and J. Favel
California Institute of Technology

Seismic waves were generated through forced vibration of the nine-story Millikan Library building located on the campus of the California Institute of Technology in Pasadena, California, in February of 1998, at the building's east-west natural frequency of 1.135 Hz. The wave velocities produced by these vibrations were recorded at distances of 1 to 6 kilometers away from the building. The accelerations of each floor of the building in both the north-south and the east-west directions were also recorded. A mathematical model was developed, which predicts the radiation pattern from the rocking and shearing of a rigid disk on the surface of a homogenous half-space. The inputs to the model were the shearing force and the rocking moment that the structure transfers to the ground as a result of its motion.

The acceleration data was used to calculate the forces and the moments from the building. The experimental data was plotted as a function of its distance to the building and shows the exponential decrease in wave velocity with the increase of distance.

Further work will be done, ultimately comparing the experimental data to the model data and assessing the accuracy of the model. The forces and moments will be input into the model and a plot of the radiation pattern produced. Since February of 1998, seismometers have been placed in 68 different locations throughout the San Gabriel Valley between 1 and 7 kilometers away from Millikan Library. Data from the Southern California permanent broadband instrument network was also collected, and the signal from the building can be seen as far away as Barrett (~230 km South East of the building). At each point where data was collected, the energy predicted by the model will be compared to the energy received at that point. The ratio between the radiated kinetic energy and the input kinetic energy is instrumental in calculating the damping of the building due to energy radiation.

Energy to Moment Ratio as a Function of Geometry

Mark S. Abinante
University of California, Los Angeles

Large variations exist in the relation between moment, energy release, and average stress drop in earthquakes. Given two earthquakes of similar moment-magnitude, one may be found to have an average stress drop of a few bars while the other may have an average stress drop of thirty bars or more. Earthquake magnitudes calculated from energy release may differ from those calculated by moment by over an order of magnitude. How can such wide variations be accounted for? We investigate the degree to which geometrical differences may be responsible for such large variations in energy-to-moment and energy-to-stress-drop ratios. We use an anti-plane dynamic crack model to compare earthquakes on homogeneous fault segments with earthquakes dominated by a single strong asperity. These two types of earthquake processes may be taken as extreme end members of possible fault geometries.

We find that for a given moment release, the seismic energy, or work done, is much higher in asperity-type earthquakes than in earthquakes on homogeneous fault segments. One the other hand, the average stress drop is actually lower in the asperity-type earthquakes. Depending on the narrowness of the asperity zone, these geometrical considerations may be sufficient to explain the variations in energy-to-moment ratios observed in nature.

Strain-Rate Changes After the Landers Earthquake

Duncan Carr Agnew and Frank K. Wyatt
University of California, San Diego

Postseismic strain variations following the 28 June 1992, M 7.4, Landers earthquake were recorded by the high-resolution long-base instruments at Pinyon Flat Observatory (PFO), 66 km from the epicenter. All the PFO long-base strainmeters showed a rapid expansion, decaying away in the week after the earthquake. Over the next 6 years our best data come from the one fully-anchored long-base laser strainmeter and show a change in strain with the same sense as the coseismic offset (expansion) lasting about 6 months after the event and amounting to 15% of the strain change at the time of the earthquake. This change was followed by a reversal of strain rate, lasting for the next two years, and the eventual return to the pre earthquake rate of strain change -- a rate (0.03 microstrain/year) in accord with long-running geodetic measurements. A similar pattern is evident, though less clearly, on the best-anchored long-base tiltmeter at the observatory. Groundwater changes, monitored in 4 wells on site, show responses to precipitation, but behave differently from the strain changes.

A New Statistical Test for Static Stress Triggering: Application to the 1987 Superstition Hills Earthquake Sequence

Greg Anderson and Hadley Johnson
University of California, San Diego

Over the past several years, a number of investigators have argued that static stress changes produced by large earthquakes influence the spatial and temporal distributions of subsequent regional seismicity, with earthquakes clustering preferentially in regions of increased Coulomb stress. More recently, some have developed quantitative methods to test for the existence of such static stress triggering, but no firm consensus has yet been reached as to the significance of these effects. We have developed a new test for static stress triggering in

which we compute the change in Coulomb stress for a set of events spanning the occurrence of a large earthquake. We compare the distributions of these stress changes for events before and after the mainshock, to decide if we can reject the hypothesis that the distributions are the same. Such rejection would support the idea of stress triggering. We have applied this test to the 24 November 1987 Elmore Ranch/Superstition Hills earthquake sequence and find no evidence for static stress triggering if we look at all events in our data set. However, if the events after the mainshock are restricted to those that experienced stress change magnitudes of at least 0.01 to 0.03 MPa (0.1 to 0.3 bar) or that occurred from 1.5 to 3 years after the mainshocks, we do find evidence for static stress triggering.

Probabilistic Seismic Hazard Analysis Without the Ergodic Assumption

John G. Anderson and James N. Brune
University of Nevada, Reno

The standard model used for probabilistic seismic hazard analysis makes an ergodic assumption in the attenuation relation. Specifically, this assumption is that the spatial distribution of ground motion amplitudes in a single earthquake correctly matches the temporal distribution of ground motion at a single site over many earthquakes. To the extent that path and site response play a major role in controlling ground motions, this assumption cannot be correct. If path and site factors play a major roll, as is generally believed, a major fraction of the uncertainty is epistemic (due to lack of knowledge of the role they play). The distinction is crucial for a probabilistic seismic hazard analysis which treats aleatory (random) and epistemic uncertainty differently. We propose that the distinction between aleatory and epistemic uncertainty in the attenuation relationships depends on an absolute standard rather than a model-dependent standard. The aleatory uncertainty should only include uncertainty that arises from temporal dependence in the Earth's behavior, such as variability in the source processes in same rupture zone from one earthquake to the next. In contrast, epistemic uncertainty treats the repeatable, but presently unknown, behavior caused by path and site response. The optimum distribution of uncertainty between aleatory uncertainty and epistemic uncertainty must be determined from data, not assumed. Evidence from the distribution of precarious rocks near the San Andreas fault suggests that the ergodic assumption causes the aleatory uncertainty to be overestimated and the epistemic uncertainty to be underestimated. If these results generalize to sites where seismicity is not dominated by a single fault, and where exposure times are longer than earthquake return times, the economic consequences of designing sensitive structures for low probability ground motions assuming ergodic vs. non-ergodic distributions are potentially huge.

Southern California Earthquake Center
Outreach Program

By Jill Andrews, Director for Outreach

Mission and Goals The SCEC Outreach mission is *to promote earthquake loss reduction and lifelong learning by engaging the public at large in activities that focus on earthquake-related education, research-based technology development and transfer, and systemic reform.* We have divided our efforts into three programmatic categories: *Public Awareness, Education, and Knowledge Transfer* (see *A Mutually Influencing Network to Promote Earthquake Education and Outreach*).

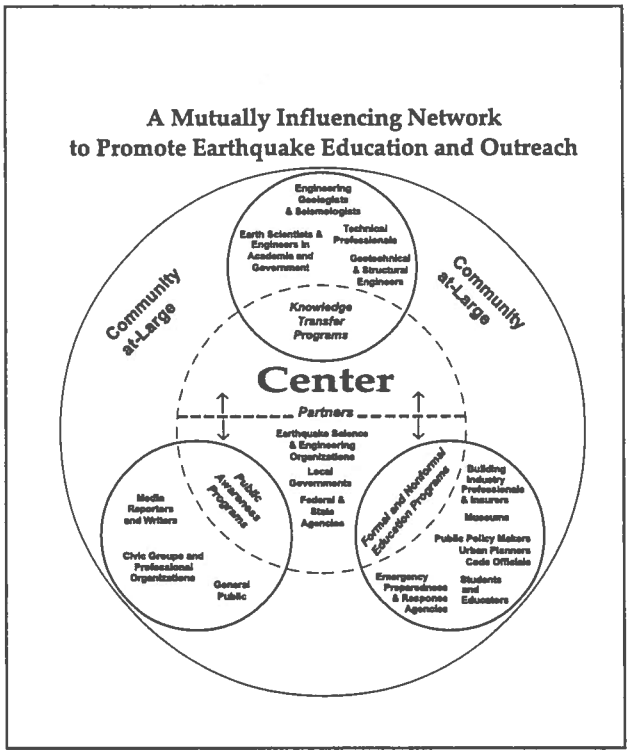

Outreach Team Our team is an effective broker of information between the academic community and practitioners, between earth scientists and engineers, between technical professionals and public officials, and between scientists and educators. The Center is known for its effective partnerships with local, state, and national government entities, academic institutions, industry, and the media. Our outreach efforts have evolved from concepts on paper to a multi-dimensional enterprise that provides notoriety to the Center while engaging all sectors of the community at large.

SCEC's Outreach staff is a results-oriented team that manages an array of activities consisting of workshops, publications, web sites, education modules, partnerships in industry and education, and database development and management. We organize the growing knowledge bases of academic scientists, engineers, and social scientists and make sure that their work is applied to reducing earthquake-related risks. We are committed to the notion that SCEC's outreach programs should complement -- not eclipse -- the science. Sara Tekula, a recent graduate of the psychology Department at USC, has joined the SCEC as an Outreach Specialist for Education. Mark Benthien enters his third year with SCEC, continuing his outstanding work on the SCEC Web site, running our workshops, overseeing the LARSE II permitting process, and directing the SCEC Summer Interns program. With Ed Hensley's (Hensley Communications) excellent skills in newsletter writing, editing and production, and with occasional help from John McRaney, Tom Henyey, Dave Jackson and the rest of the SCEC office staff, the outreach program is flourishing.

Field Test Results for Quasi-Static Toppling Acceleration of Precariously Balanced Rocks

Abdolrasool Anooshehpoor and James N. Brune
University of Nevada, Reno

Field measurements of the quasi-static toppling accelerations of precariously balanced rocks can be used to constrain the peak ground accelerations experienced during earthquakes in those locations. The quasi-static acceleration is determined by the ratio of the toppling force (a horizontal force through the center of mass) and the estimated mass of the rock. Measurements of the toppling accelerations of a number of the precariously balanced rocks near Victorville and Jacumba in southern California indicate that ground accelerations less than 0.2 g will topple some rocks. Toppling horizontal ground accelerations for eight precarious rocks identified near Victorville are about 0.11-0.19 g; toppling accelerations for three rocks tested near Jacumba are about 0.07-0.16 g; the measured quasi-static toppling acceleration of a large boulder near Banning, California, is less than 0.1 g. Field tests on several rocks located on the footwall of the Pleasant Valley normal fault in northern Nevada give toppling accelerations of about 0.11-0.22 g. In the Yucca Mountain Area, Nevada, the quasi-static toppling accelerations of several precariously balanced rocks range from 0.14 to 0.3 g. Numerical and laboratory modeling indicates the approximate dynamic toppling accelerations for a time history with the same shape as the El Centro seismogram are about 20% higher than the quasi-static toppling accelerations.

There are numerous granite outcrops of the type that produce precarious rocks distributed at a range of distances perpendicular to the Mojave section of the San Andreas fault near Palmdale and in the San Gabriel Mountains. We are in the process of determining the quasi-static toppling acceleration for selected rocks in this region. We will have some field test results by the time of the meeting.

Quasi-Static Slip-Rate Shielding by Locked and Creeping Zones as an Explanation for Small Repeating Earthquakes at Parkfield

Abdolrasool Anooshehpoor and James N. Brune
University of Nevada, Reno

Seismicity at Parkfield, California, is characterized by quasi-periodic repeating sequences of small earthquakes that are essentially identical in waveform, size and location. Nadeau and Johnson (1998) interpreted these as repeated slip on a given asperity driven by a steady slip rate of 2.3 cm/yr, and concluded that the stress drops needed to be extremely high, of the order of 20 kilobars. We propose another explanation for these small repeating events, namely that an inner asperity is surrounded by a larger creeping zone, which in turn is surrounded by a still larger locked zone. This geometry produces a local slip velocity much less than the overall creep velocity observed on a still larger scale (slip velocity shielding). We have constructed a foam rubber model to illustrate the phenomenon. We create the creeping zone by a circular semi-annulus of smooth plastic with the small inner circle representing a small asperity - the source of the small repeating earthquakes. The foam block outside the annulus represents a larger locked zone. This geometry creates a quasi-periodic sequence of small, similar-size events on the inner asperity, punctuated by large events which rupture the whole block (including the creeping zone and the small inner asperity). The time sequences of small events look very similar to the cumulative moment plots of Nadeau and Johnson. The actual stress drops are of the same order as for the large events. However, if it had been assumed that the slip rate for the small events was the same as the overall slip rate for the system, the inferred stress drops would have been more than an order of magnitude larger, and larger than are ever been observed directly in the foam rubber model. Thus the results of the model correspond directly to the observations of Nadeau and Johnson, and suggest that the model may be appropriate to explain their observations, without requiring super-strong asperities.

Below is a sequence that would be interpreted as 20 small repeating events. The larger events nucleated outside the creeping zone.

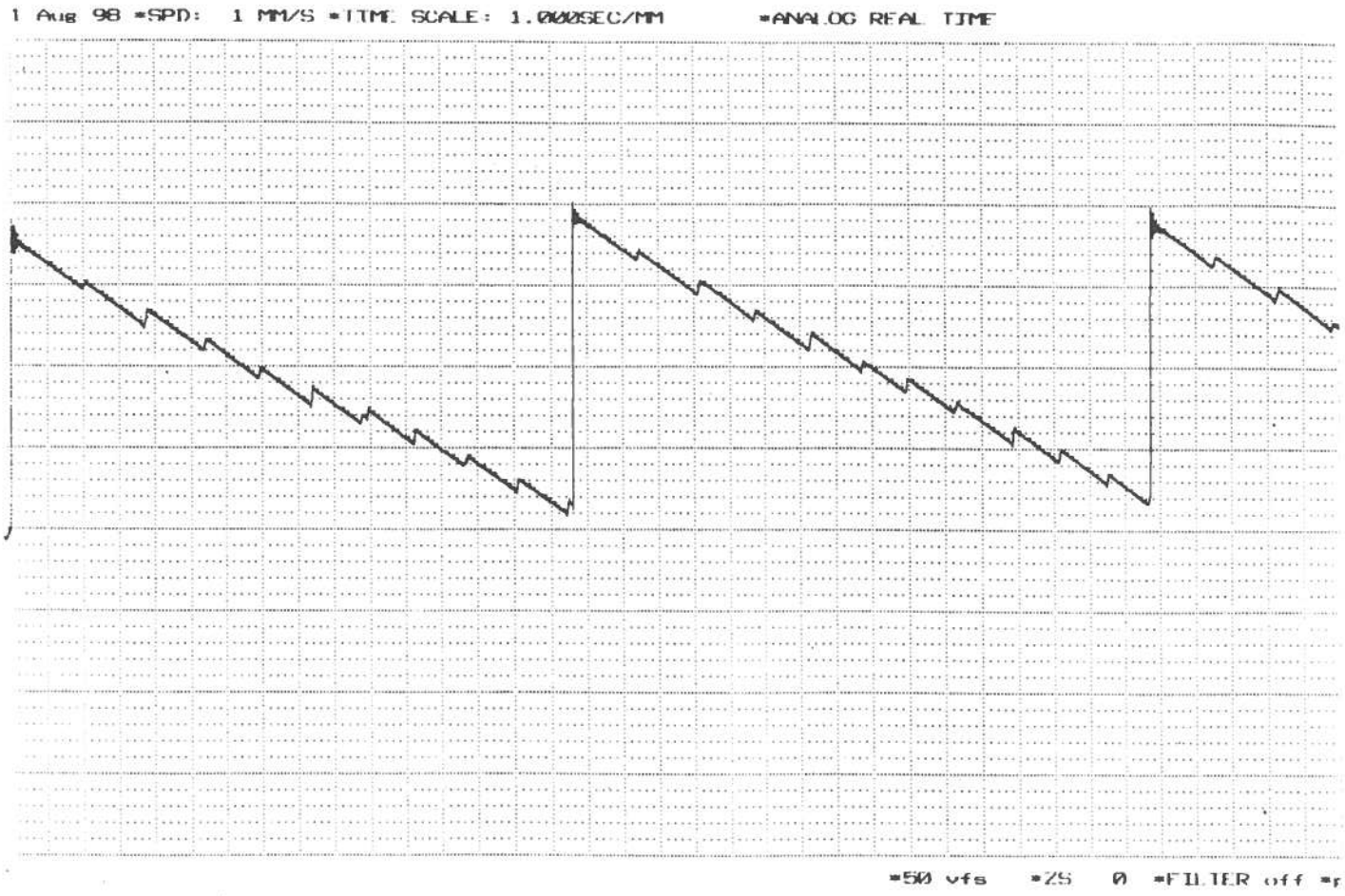

Figure for abstract by Anooshehpoor and Brune

Metropolitan Los Angeles Shortening Belt from Geodesy

Donald Argus, Mike Heflin, Andreas Donnellan, Frank Webb, Danan Dong,
Ken Hurst, Greg Lyzenga, and Mike Watkins
Jet Propulsion Lab

SCIGN and other geodetic data are resolving the distribution of the N-S shortening SSW of the big bend in the San Andreas fault and NW of islands off the California coast. The data suggest the following:

1. N-S shortening is fastest across an ESE striking belt crossing northern metropolitan Los Angeles The belt is 5 to 20 km wide and is contracting at 5 mm/year. In the east the belt is south of the front of the San Gabriel mountains and north of UCLA and USC The belt extends westward to the northern San Fernando valley, where it includes the ruptures of the 1971 M=6.6 San Fernando and 1994 M=6.7 Northridge earthquakes. In the west the belt consists of the Ventura basin.

2. The San Gabriel mountains are acting as an elastic microplate. Over the interseismic period the mountains are building up elastic strain due to locking of the San Andreas fault. Over many earthquake cycles all of this strain is recovered, so that over the geologic period the mountains are rigid.

3. Aside from the elastic strain building up due to locking of the San Andreas fault, E-W extension across metropolitan Los Angeles is minor. Crustal thickening is the main process accommodating the N-S shortening.

Experiments with L1-norm Relocations for the 1994 Northridge Sequence

Luciana Astiz and Peter M. Shearer
University of California, San Diego

The January 17, 1994 Northridge earthquake (M_w=6.7) occurred on a buried thrust fault in the San Fernando Valley northwest of the Los Angeles metropolitan area. We relocate 15,005 events occurring from 1981 to 1997 in an area 40 km x 40 km surrounding this event (most events are aftershocks). First, we relocate all events using existing P (378,447) and S (47,534) picks from 148 stations of the Southern California Seismic Network (SCSN) located within 100 km of the events. We apply a L1-norm, grid-search algorithm that uses station terms to account for three-dimensional velocity structure outside the aftershock region. This simple procedure reduces the scatter in the epicentral locations, as compared to those in the SCSN catalog. Estimated relative location errors have median horizontal (herr) and vertical (zerr) values of 217 and 370 m, respectively. "Quality A" aftershocks define a 40 to 50 degree north dipping plane with most of the events between 5 and 15 km depth, and a few events extending to 23 km depth. Next, we use over 400,000 seismograms recorded by the SCSN which are available through the SCEC Data Center to perform waveform cross-correlation with the 100 nearest neighbors to each event. The waveforms are low-pass filtered at 10 Hz and resampled to a 100-Hz sample rate prior to the cross-correlation. Event pairs sufficiently similar provide well-defined peaks in their cross-correlation functions from which we obtain differential P and S arrival times. From these differential times and the existing picks we solve for an adjusted set of arrival times that are more consistent and more complete than the original picks. The events are then relocated using the adjusted set of picks; we plan to present these improved locations at the SCEC workshop. Because the Northridge aftershock sequence spans a large area, a single set of station terms cannot provide optimal results for all of the events. Future plans include implementation of spatially varying station terms to better account for three-dimensional velocity structure. In addition, we are investigating whether velocity profiles of nearby stations can be determined so that we may obtain better absolute event depths. Precise relocations of Northridge aftershocks may provide a better understanding of the tectonics of this area and help assess the seismic potential of adjacent fault structures.

A Structural Analysis: Southeast Section of the Wrightwood Pull-Apart, San Andreas Fault

P. Niklas Bacher[1], Kūrt D. Solon[2], Robert M. Langridge, and Ray J. Weldon II
University of Oregon
Thomas E. Fumal
United States Geological Survey, Menlo Park
[1] now at Duke University; [2] now at Syracuse University

A series of secondary structures were mapped and structure contoured and stratigraphic units were isopached from the southeast part of the Wrightwood paleoseismic site on the southern San Andreas Fault (SAF), California. The Wrightwood structural depression has formed between the main trace of the SAF and a nearly parallel secondary zone, possibly as a pull-apart. This 150 meter wide basin offers an unrivaled sequence of interbedded clastic and peat deposits. A total of 30 trenches (with 80 radiocarbon dates) have been dug at Wrightwood. We will focus on the structural geology found in three of the trenches (T21-23) at the southeast end of the site. These trenches were logged photographically and mosaiced in the lab. Units were correlated from wall to wall and between trenches and connecting slots. We recognize a thrust fault and related ramp anticlines and synclines, and normal faults, which were mapped and structure contoured to develop a 3-dimensional representation of the deformation. Episodic deformation is documented by isopaching syntectonic sedimentary layers. Structurally, the orientation and vergence of the normal faults support a pull-apart model for the site. Compressional structures appear to be caused by gravitational sliding into the basin. We suggest that the structures are oblique en echelon extensional ruptures on the SAF with sub-orthogonal compressive features driven by gravity into the resulting depression. All of these structures appear to be associated with paleoearthquakes, whose timing can be inferred from the isopached syntectonic sediments. These data are more consistent and compelling than other paleoseismic indicators, like upward termination of ruptures.

Topography, Gravity, and Lg and Pg Propagation in Southern California

Eli Baker
Maxwell Laboratories

We are investigating the relationship between various statistics of topography, gravity, and crustal thickness and the efficiency of Lg and Pg propagation, with the goal of better understanding the effects of structure on the propagation of these crustally guided phases. This detailed quantification of observable effects will be fundamental to more meaningful numerical simulation at high frequency.

We have compiled a unique data set consisting of changes in Lg and Pg amplitudes over 10 to 60 km long paths between southern California seismic network stations along with values of geophysical parameters integrated along the paths. Site amplification corrections permit separate measurements for each phase and permit the attribution of amplitude changes to propagation effects. The short path lengths permit observations on the scale over which these regional phase amplitudes change.

Cluster analysis, based only on parameter values measured along the paths (i.e. not on the amplitude changes), separates the paths into tectonically reasonable groupings without relying on a priori knowledge of tectonic boundaries. Both Lg and Pg propagation efficiencies are significantly different for different groups of paths. These results suggest that crustal types with distinct effects on propagation can be characterized by geophysical parameter values.

We rely heavily on analysis of variance (ANOVA) in investigating the relationships between amplitude changes and the parameter values. It allows us to investigate relationships between the parameters and propagation without assuming they are linear, which observations indicate can be inappropriate. It also provides a rigorous means of testing hypotheses regarding such relationships. Multivariate ANOVA also allows us to

investigate the interaction effects of combinations of parameters on Lg and Pg propagation.

Application of ANOVA to 1-2 and 2-4 Hz rms amplitude measurements has verified the statistical significance of relationships between several of the geophysical parameters and Lg and Pg propagation. It also indicates differences between the effects on Lg and Pg propagation and between the effects on a single phase at different frequencies.

Late Quaternary Fold Deformation Along the Northridge Hills Fault, San Fernando Valley, Southern California

John N. Baldwin, Keith I. Kelson, and Carrie E. Randolph
William Lettis & Associates

Geologic investigation of the Northridge Hills fault (NHF), in the northern San Fernando Valley, helps assess the timing and style of near-surface Quaternary deformation in the epicentral area of the 1994 Northridge earthquake. The NHF, a 15-km-long, north-dipping reverse fault, exhibits geomorphic evidence of late Quaternary surface deformation, including topographic scarps across late Quaternary fluvial terraces and aligned alluvial-fan apices on the footwall block. We excavated one 40-m-long trench, dug six test pits, and drilled nine soil borings along a NE-SW transect across a 2-m-high scarp developed in probable Holocene terrace deposits adjacent to Aliso Canyon Wash. Data from closely spaced boreholes confirm a continuous clayey gravel identified in the trench and test pits. Combined these subsurface data define a monoclinal fold with 6 ± 1 m of vertical separation. The borehole data also suggest that an unconformity developed on the Plio-Pleistocene Saugus Fm is warped into a south-facing monocline that has 15 ± 2 m of vertical separation across the NHF. The absence of distinct scarp-derived colluvium and secondary brittle fracturing or faulting suggests that the monocline is related to either moderate-magnitude earthquakes on a blind NHF, or to secondary deformation induced by earthquakes on other faults. Based on evidence of surface uplift near the trench site during or following the 1994 earthquake, this deformation may be a result of: (1) secondary slip on the NHF related to movement on the underlying Northridge blind reverse fault; or (2) a combination of secondary slip related to the Northridge blind fault and primary slip on the NHF. A seismic survey to be conducted across the escarpment by Cal-State Long Beach in late October 1998 will help constrain the geometry of the monocline interpreted from trench, test pits and borehole data.

Subsidence Inferred by InSAR Near Proposed SCIGN Sites South of Los Angeles

Gerald Bawden[1], Gilles Peltzer[2], Kenneth Hudnut[3], Ross Stein[1], Wayne Thatcher[1], and Shannon Van Wyk[3]
[1]United States Geological Survey, Menlo Park
[2]Jet Propulsion Laboratory
[3]United States Geological Survey, Pasadena

Anthropogenic deformation, such as the pumping and withdrawal of fluid from both petroleum reservoirs and hydrologic aquifers, is widespread throughout the Los Angeles and Ventura basins. Observed vertical motion associated with the fluid extraction in the Los Angeles basin is 1-4 mm/yr, with related horizontal displacements of possibly up to 1 mm/yr in some portions of the basin. Distinguishing the deformation caused by human activity from that due to tectonic processes is vital to understanding the sources of the active tectonic deformation. The principal objective of the Southern California Integrated GPS Network [SCIGN] is to measure the displacement field associated with a mosaic of faults now thought to underlie the greater Los Angeles region. However, without a quantitative measure of the anthropogenic deformation throughout the region, it will be difficult to properly assess the magnitude of human-induced signal vs. tectonic signal at any given SCIGN site. To overcome this anticipated problem, we

are combining InSAR [interferometric synthetic aperture radar] images of the Los Angeles basin with gas, oil, and water extraction records, water level and ground compaction records, and extant geodetic leveling. Preliminary analysis of the data shows four regions of rapid subsidence that will likely induce non-tectonic deformation on the SCIGN network. The areas of concern are Pomona, Redondo Beach, Long Beach, and Santa Fe Springs, with subsidence rates of up to 16 mm/yr. Continued data analysis will refine the rates and spatial extent of the deformation. The sources of non-tectonic deformation will also be modeled using poroelasticity and compaction theory to develop methods to separate tectonic from human-induced sources of ground displacement.

Scripps Orbit and Permanent Array Center Operations Summary

Y. Bock, J. Dean, P. de Jonge, P. Fang, P. Jamason, R. Nikolaides, C. Roelle, M. Scharber, M. van Domselaar, and S. Williams
University of California, San Diego

The Scripps Orbit and Permanent Array Center (SOPAC) is committed to collecting, archiving, analyzing, and publishing high-quality continuous GPS (Global Positioning System) data in a timely manner to support the GPS research community. This poster summarizes SOPAC's analysis, archiving, and GPS site responsibilities to the SCIGN (Southern California Integrated GPS Network) and other permanent GPS arrays.

Archiving operations at SOPAC include the download and quality control of data from over 350 GPS sites. Total archive capacity is over 8 terabytes, and an online capacity of more than 800 gigabytes allows public access to all GPS and meteorological data. Monthly transfers >from SOPAC for 1998 have averaged greater than 85,000 files. Analysis activities include the use of the global GPS network to generate time series for studying the crustal deformation cycle. Data from this network are used to calculate precise satellite orbits and earth orientation parameters (EOP's). Then, while tightly constraining these orbits and EOP's, regional network site coordinates are estimated. SOPAC is also involved in integrating GPS measurements with Interferometric Synthetic Aperture Radar (InSAR) data for enhanced spatial measurement of crustal deformation. Finally, SOPAC is currently responsible for the direct download and maintenance of 17 SCIGN sites (expanding to 50), installation of meteorological packages throughout the network, and the development of new GPS site download software (Ashtech Communication and Networking; Extended GPS Array Download Software) for a more reliable downloading system.

Nonlinear Effects on Sand Deposits: Field Data Observations and Synthetic Modeling

Fabian Bonilla, Daniel Lavallee, and Ralph Archuleta
University of California, Santa Barbara

We model laboratory tests on sands by applying extended Masing rules for hysteresis that follow general hyperbolic stress-strain relationships. First, we find that the extended Masing rules better describe the hysteresis of soils. Second, the shape factor, usually assumed to be two, can be different than two. Third, the strain rate time history is necessary to fit the observed data and represents the anelastic attenuation of the medium. We developed a functional form for the extended Masing rules and incorporated it into a finite difference code to propagate vertically incident SH-waves in a layered medium. The simulations show amplitude reduction as well as the shift of the fundamental frequency to lower frequencies as observed on vertical arrays. In addition, the synthetic accelerograms show the development of high frequency peaks later in the signals as observed in acceleration records; these peaks seem to be related to the contribution of the strain rate, and cusps in the stress-strain space. Finally, with this model we study the nonlinear evolution for the 1987 Superstition Hills event recorded at the Wildlife Refuge and the 1993 Kushiro earthquake recorded at Kushiro Port.

Using Aftershocks to Monitor Changes in the Correlation Length of the Stress Field Before and After Large Earthquakes

David D. Bowman and Charles G. Sammis
University of Southern California

Many researchers have proposed that statistical physics can be used to understand spatial and temporal patterns of regional seismicity. One approach has been to model the earthquake process as a critical phenomenon. This approach has found support in recent theoretical demonstrations that rupture in heterogeneous media is a critical phenomena, and in observations of accelerating seismicity before large events and paleoseismic observations of temporal clustering of great earthquakes. In the critical point model, these effects can be understood in terms of a growing correlation length of the regional stress field before a large earthquake. Early in the earthquake cycle, the correlation length of the stress field is short and earthquakes tend to be small, reflecting a stress field which is very rough on the regional scale. As the earthquake cycle progresses towards a great earthquake, events smooth the stress field at longer length scales by redistributing stress to neighboring regions, causing earthquakes to become larger. At the same time, the stress field is being "roughened" at short wavelengths through aftershocks. One implication of this model is that, as the correlation length of the stress field grows, there should be an observable growth in the number and area of aftershocks. This effect has been observed by Keilis-Borok et al (1980) and is an element of the M8 algorithm. We have extended this idea to explore how the observed number and energy in aftershocks sequences evolves with time before and after the Kern County and Landers earthquakes in southern California. In agreement with the critical-point model and with previous studies, we find that aftershock sequences tend to be more energetic before large events and less so afterward.

Examples of Precarious Rocks and Semi-Precarious Rocks in the San Gabriel Mountains and the Mojave Desert: Potential Constraints on Input for Calculations of Los Angeles Basin Ground Motions from Large San Andreas Fault Earthquakes and Large San Gabriel Frontal Fault Earthquakes

James N. Brune
University of Nevada, Reno

Olsen et al.(1995) and Graves(1998) have published ground motion models for the Los Angeles Basin resulting from large San Andreas fault earthquakes. There are large differences between the predictions of the two models. The models include predictions of ground velocities near the San Andreas fault in the San Gabriel Mountains and the Mojave Desert at distances of 15 km, where there are a number of semi-precarious rocks which can be tested for toppling accelerations. Since there are no instrumental recordings of such large San Andreas fault earthquakes the semi-precarious rocks may be the only quantitative way to test the various models. A similar situation will exist for ground motion calculations from large San Gabriel Mountains frontal thrust fault earthquakes. Thus it is important to determine the constraints on ground motion provided by precarious rocks in this region. Examples of rocks discovered to date will be presented, along with preliminary conclusions regarding possible constraints on ground motion and discrimination between ground motion models.

The Norwalk Fault System: Evidence from the Coyote Hills

P. Burrato[1], Robert S. Yeats[2], Eldon M. Gath[2], and Gary J. Huftile[3]
[1]Istituto Nazionale di Geofisica, Rome, [2]Earth Consultants International
[3]Queensland University of Technology, Brisbane, Australia

The Norwalk fault system is a set of north-dipping blind reverse faults that control the west-trending Montebello, Santa Fe Springs, West Coyote, and East Coyote folds. Seismic data show a blind reverse fault beneath Santa Fe Springs that projects downward to the 1987 Whittier

Narrows mainshock. Coseismic uplift and the mainshock fault-plane solution support this interpretation. To the east, the Coyote folds are offset en Èchelon from Santa Fe Springs, suggesting segmentation of the Norwalk fault itself. West Coyote and East Coyote-Hualde are expressed in tectonic topography. Major Puente Hills drainage, with a drainage divide west of and parallel to the Chino fault, is offset right-laterally across the Whittier fault and is in part antecedent to uplift of the Coyote folds, indicating that right slip on the Whittier fault and uplift of the hills proceeded concurrently. Quaternary deposits exposed in the Coyote Hills include the marine San Pedro Formation and the nonmarine Coyote Hills and La Habra formations; appearance of Puente clasts in the La Habra Formation and possibly in the upper Coyote Hills Formation dates the uplift of the Puente Hills.

W-trending folds of the Norwalk fault system are juxtaposed against the NW-trending Anaheim nose and LA trough. The Santa Fe Springs anticline is adjacent to the Anaheim nose, but farther east, the West Coyote and East Coyote-Hualde anticlines are separated from the LA trough by flat-lying Pliocene-Pleistocene strata unconformably overlying the Anaheim nose. The Norwalk fault and related folds are related not to the LA trough but to the NW decrease in slip rate from the Elsinore to the Whittier fault and are in large part limited to the region south of the Puente Hills, where the Whittier fault is in a restraining bend.

3D Imaging of the Northridge Earthquake Source Fault

Sara Carena
Princeton University

As part of a largest study pursuing the use of earthquake data in structural model building, we examined the 3D geometry of the source fault of the 1994 Northridge Earthquake, as outlined by aftershocks, using Gocad. Gocad is a powerful tool for 3D model building from data as well as viewing and manipulating spatial and property information. It allowed us to get a clear 3D view of the aftershocks distribution and to interpolate it to generate fault surfaces. We used about 10,000 aftershocks (SCEC database). Before loading them into Gocad, the aftershocks hypocenters were clustered using a code by Jones and Stewart (1997). We also imported a set of focal mechanisms by Seeber (SCEC database), to be displayed together with the aftershocks. The surfaces were generated from the clustered aftershock set. The Northridge Earthquake source fault shows a well marked slip-parallel step near its SE margin, and this same feature can be recognized from the nodal planes. The fault strike changes by 10 degrees from the SE section to the NW section. The two sections are joined by a segment striking 95 degrees. The average dip is 40 degrees, but it tends to become steeper above a depth of 8 km. This could be an effect due to a poorly resolved complex geometry at shallow depths. In fact some of the aftershock clusters here can well belong to smaller faults connected to the main one. Other faults can be outlined in the area, though for some of them there are not enough data available to determine a reliable geometry. However, the main fault is bounded to the NW by a surface dipping 45 degrees to the North. West of the main fault there is a smaller one, possibly strike-slip, dipping 70 degrees to the NE. Finally we projected the slip model by Wald (1996) onto the fault surface. The rupture appears to initiate at the step, and then it propagates to the NW section.

Dynamics of the Intraplate Stress Field in the Western U.S.

David D. Coblentz and Gene D. Humphreys
University of Oregon

We seek to understand the dynamics of the intraplate stress field in the Western U.S. with the aim of providing constraints for kinematic deformational models of the San Andreas Fault Zone (SAFZ). For example, it is postulated that the tectonics along the SAFZ can be explained in terms of compressive stresses due to the "collapse" of the elevated topography in conjunction with shear stresses due to transform processes. An evaluation of the plausibility

of such a scenario depends on an understanding of regional stress field. Because the regional stress field is governed by far-field forces, we approach the problem with a study of the North American plate dynamics.

The North American intraplate stress field is the product of a rich variety of tectonic processes, which are (for the most part) relatively well-constrained. To a first-order, these forces fall into four categories: potential energy variations, drag, distributed shear, and plate boundaries. We evaluate the relative importance of these forces through an elastic finite element analysis. Constraint for the modeling is provided by abundant information about the present state of stress in the North American plate.

Within the limitations of our modeling assumptions we draw the following conclusions about the state of stress in the vicinity of the SAFZ. The nature of the stress field is primarily controlled by ridge push and topographic forces modulated by drag (including that due to a lithospheric root) and forces acting along plate boundaries near the San Andreas. We note that it is possible to match most of the features in the observed stress field with a simple dynamic model without appealing to poorly constrained sources of stress. We also present the results of a analysis which isolates those boundary forces which exert the greatest influence on the observed intraplate stress field in the Western U.S. and, in particular, along the SAFZ.

Propagating Slip Pulse Between Dissimilar Materials

Alain Cochard
Harvard University

Following Andrews and Ben-Zion (JGR, 1997) and Ben-Zion and Andrews (BSSA, 1998) [hereafter referred to as ABZ], we study numerically the propagation of ruptures on a frictional fault, without rate or slip weakening, that separates 2 materials with different shear and dilational wave velocities. Faults may separate materials of different lithologies, and gouge zones of mature faults have properties different from those of the surrounding, intact, rock. Like in ABZ, we use a 2D plane strain geometry, choose a uniform initial normal and shear stress, the latter less than the frictional strength, and artificially nucleate the rupture by imposing some stress-drop inside a localized space-time region. We use the spectral formulation of a boundary integral equation method, as extended to dissimilar materials by Breitenfeld and Geubelle (Int. J. Fracture, 1998, in press). As reported by ABZ, who used a finite difference method, we find that the numerical solutions often depend on grid resolution, making the results difficult to interpret. Nevertheless, it is possible to solve this in some cases by introducing a length scale dc (that can be made arbitrarily small, given suitable grid refinement, and hence irrelevant to the results) in arate/state constitutive law with no steady state velocity dependence, i.e., choosing $a = b > 0$. ABZ found that self-healing slip pulses can propagate in a single direction in a self-sustained way, even when the initial shear stress is less than the initial normal stress times the friction coefficient, provided that the material contrast is large enough. Further, they found that the slip pulse velocity is a little less than the slower shear wave speed. In the very limited range of parameters explored so far (including those of ABZ), we have found pulses, but not (yet) self-sustained pulses, rather decaying pulses. Further, the pulses that we observe have velocities larger than the slower shear wave speed, the larger the material contrast, the larger those velocities are. Furthermore, in each case, the pulse does not split into a swarm of smaller pulses as had been reported (and questioned) by ABZ.

Economic Values of Using Geohazards Mapping Information in Mitigating Effects of Future Earthquakes in Southern California

James F. Davis
California Division of Mines and Geology
Richard L. Bernknopf and Amy E. Craven
Stanford Center for Earthscience Information Research

The estimation of the economic values of using geologic hazards information in mitigation of future earthquake effects is feasible employing an analytical GIS-based model. Dollar values will be compared for the net loss avoidance outcomes of employing the information in contrasting public policy frameworks, e.g., mandatory or discretionary information use. The conditional probability of earthquake-triggered secondary hazards will be estimated using a statistical model that includes the quantification of hazard susceptibility (0-1 range) based on scientific principles and judgment, and the probability of damage based on a sample of a variety of levels of shaking. With this stochastic modeling approach, expected losses can be estimated on a spatial basis. Comparisons can be made for loss avoidance scenarios that include policy frameworks in which mitigation is required for new construction based on hazards information and those that do not. There are three frameworks to be evaluated: (1) a market based model, (2) a local government requirement, and (3) a statewide standard, e.g., the Seismic Mapping Act in California. A conceptual comparison of various policy frameworks is applied to a study area in southern California for which extensive digital geologic and hazards information is available. The economic cost and value of incrementally reducing the uncertainty of hazard identification by refining geologic detail is examined. In addition, the advantages and disadvantages of public vs private sector (developer) acquisition of information are evaluated. Scenario outcomes are expressed in loss avoidance (benefit of framework scenario) = net damage without mitigation minus net damage with mitigation minus cost of mitigation policy.

Timing of the Past Two earthquakes Near Frazier Mountain, Midway Between Pallet Creek and the Carrizo Plain, Southern California

Timothy E. Dawson and Thomas K. Rockwell
San Diego State University
Scott C. Lindvall
William Lettis and Associates

We report preliminary results of paleoseismic investigations near Frazier Mountain, located about halfway between Pallet Creek and the Carrizo Plain. At the site, a minor right step in the San Andreas fault has formed a closed depression, which has been further enhanced by a small alluvial fan that blocks the drainage outflow. The main strand of the fault bisects the sag, with other strands bounding the northern margin of the sag. This central strand is expressed at the surface by a 30-cm-high scarp, as a vegetation lineament, and a pronounced ground water barrier. We believe that the central scarp formed during the 1857 Fort Tejon earthquake.

An exploratory trench was excavated north of the central scarp, exposing a ~2.5 meter section of well-stratified, distal fan and pond deposits, interrupted by two discontinuous, weakly developed buried A horizons. Two fault strands cut up section to the same paleosurface, located approximately 1.3 meters below the present day surface. We interpret the faults to have formed in an event prior to the 1857 earthquake.

Nearly 50 samples were collected for radiocarbon dating of which 8 were submitted for AMS and conventional dating. Six of the samples from units above, below, and within the event horizon share similar dates, with calendar ages between 1400-1650 AD (2 sigma). One of the samples was recovered from an in situ burn layer, and another was a fragile, charcoalized twig: we contend that reworking of older detrital charcoal is unlikely and that these dates accurately portray the age of the event horizon.

Based on the radiocarbon dates obtained, the penultimate event at the Frazier Mountain site may correlate with a similar aged event at the Bidart site in the Carrizo Plain to the north, as well as event V at the Pallet Creek site to the south. These new data support the idea that the San Andreas fault may have failed in prior 1857 type earthquakes. Alternatively, the event observed at Frazier Mountain may be independent of earthquakes observed at other sites.

Viscoelastic Flow Following the 1992 Landers, Southern California, Earthquake

Jishu Deng, Michael Gurnis, Hiroo Kanamori, and Egill Hauksson
California Institute of Technology

Postseismic deformation following the Mw 7.3 Landers, California earthquake of 1992 has been observed by both Global Positioning System (GPS) and Interferometric Synthetic Aperture Radar (InSAR) measurements (e.g. Massonnet et al. 1996; Savage and Svarc, 1997). The most significant result of the near-field GPS measurements is that the northern part of the fault trace, the Emerson fault, shifted in the fault-normal direction for tens of millimeters. The GPS measurements and InSAR images also constrain strong postseismic rebound in the fault-parallel and vertical directions. Whether this kind of slow rebound is driven by continuous time-dependent afterslip at depth on the fault plane or by viscoelastic flow below seismogenic depths in response to the large coseismic stress concentration is not well understood. Our extensive 3-D modeling shows that the afterslip model can predict the fault-parallel component of the observed displacement field, but has difficulty explaining the fault-normal and vertical components. Only the viscoelastic flow model can explain all three components of the observed displacements. We conclude that the postseismic rebound following the 1992 Landers earthquake is most likely to be driven by viscoelastic flow in the lower crust. The tradeoff between viscosity and the thickness of the weak layer in the lower crust constrained from the horizontal components of the GPS measurements is nearly linear. The best-fitting viscosity increases with the thickness of the weak layer in the lower crust. The viscosity of the weak zone beneath the rupture zone controlling the rebound is ~ 10^{18} Pa.s if the thickness of the layer is ~ 10 km. The InSAR images, however, favor models with higher viscosities and thicker weak zones. The viscoelastic behavior of the lower crust has important implications for seismotectonics and the analysis of earthquake hazard.

Comparison of Waveform Inversions and Arrival Time Techniques to Resolve Earthquake Depths in Southern California

Francesca Di Luccio
Istituto Nazionale di Geofisica, Roma, Italy and United States Geological Survey, Pasadena
Lucile Jones
United States Geological Survey, Pasadena
Lupei Zhu
University of Southern California
Egill Hauksson
California Institute of Technology

The Southern California Seismic Network is being upgraded from an analog short-period network to a broadband digital network as part of the TriNet project. The new broadband data make it possible to apply new techniques that analyze the whole seismograms as opposed to the older techniques that were mostly based on arrival times and first motions. Because both analog and digital data are available for the same events, we seek to address the question if both types of data and techniques provide the same results. In the future as analog stations are turned off we thus will have some idea if significant biases are being introduced into our database.

A set of aftershocks of the 1994 Northridge earthquake, with magnitude greater than 3.5, have been relocated using arrival times with both 3D and 1D velocity models and analyzed with

waveform inversion techniques to examine our ability to resolve hypocentral depths in Southern California. The 1D and 3D velocity models are derived from Northridge sequence arrival times. The set of earthquakes was chosen to have a travel time arrival pick at the station within 10 km epicentral distance. The depths are in agreement within 2 km for all three techniques for earthquakes with hypocentral depths greater than 5 km. For these earthquakes, the distribution of RMS with depth for the arrival time determinations demonstrates that including S-waves picked on horizontal components improves the resolution of depths. For depths lesser than 5-6 km, it is very difficult to model waveforms, because for shallow earthquakes the basin effect becomes significant and consequently modeling depends on the local velocity structure. For these shallow earthquakes, the arrival time RMS distributions appear better resolved when S-wave times are not included. This may be because none of these S waves are within 1.5 focal depths in epicentral distances.

Postseismic Deformation Following the Northridge Earthquake Observed from GPS Measurements

Andrea Donnellan, Greg Lyzenga, Frank Webb, Gilles Peltzer, and Jay Parker
Jet Propulsion Laboratory

Global Positioning System (GPS) observations indicate that significant aseismic deformation occurred in the year following the January 17, 1994, Northridge earthquake. The postseismic observations show the same sense of motion as the coseismic. Compared with the coseismic displacements, the far-field postseismic motions (1-2 fault dimensions away) are proportionally larger than those seen in the near field. The postseismic data are best modeled with two faults: one on the rupture plane and one located in the shallow crust. The upper crustal fault may represent an actual fault or may be indicative of viscous relaxation occurring in the upper crust. The inferred afterslip and/or relaxation moment is approximately $2.9X10^{18}$ Nm or 22% of the mainshock moment release. We analyzed InSAR data covering both the earthquake and 2 years of post-seismic period by removing a co-seismic synthetic phase field based on Wald and Heaton's (1996) inversion results from the observed InSAR map. The residual change includes both mismodelled co-seismic signal, and actual post-seismic deformation. A preliminary comparison between the range change observed at GPS stations by both InSAR and GPS in the 1.5 years following the earthquake shows an excellent agreement between the two data sets. Current developments of this work focus on combining the two sets of data to test and better constrain models of post-seismic processes. Geodetic observations of the January 29, 1994 M 5.1 aftershock of the Northridge earthquake are consistent with seismic solutions showing left-lateral oblique slip on a northeast striking steeply dipping fault. The data surrounding the aftershock do not show precursory or immediate post-seismic motion. This aftershock, and a summation of 65 aftershocks, yield a deformation field similar in style to the geodetically observed deformation field, but the summed deformation from the aftershocks accounts for only 10% of the total geodetically observed deformation.

Coulomb Stress Evolution and Changes in Frequency of Moderate-size Earthquakes Before and After the Landers, California, Earthquake of 1992

Wen-xuan Du and Lynn R. Sykes
Lamont-Doherty Earth Observatory, Columbia University

Changes in frequency of moderate-size earthquakes before and after the Landers earthquake are investigated, and their implications are discussed in the context of Coulomb stress evolution since 1812 in Southern California. We considered two circular regions centered at the epicenter of the June 28, 1992 Landers earthquake with radii of 160 and 100 km. Frequency-magnitude relationships for two 10-year periods before and two 5-year periods around the

Landers event are compared. Only events with magnitude M≥4.0 are included; aftershocks are omitted. For the 160 km radius, the rate of moderate events is markedly greater from 1982 to 1992 than in the earlier decade. For the period 1972-1982 the distribution is well fit with a b-value (slope) of -1. In the later 10-year period just before the Landers earthquake, however, its magnitude distribution is indistinguishable from that of the earlier period for M≤4.8, but it becomes much flatter at larger M. The relationship for the 5-year period just before the Landers event is very similar to that for the 1982-1992 period. For the 5-year period 1993-1998 after the Landers event, the total number of events with M≥4.0 decreases to 10 from 34 in the 5 years before the main shock. Thus, the rate and slope of the magnitude distribution for moderate-size events just before the main event appear to be anomalous compared to those for either the preceding or subsequent periods. For the area with a radius of 100 km, however, the number of events is smaller and the differences are more subtle. Cumulative Coulomb stress changes just before the Landers earthquake are calculated for all of Southern California taking a zero baseline just before the shock of 1812. The region with the radius of 160 km correlates well with the area of positive Cumulative Coulomb stress, which is calculated for strike-slip motion on vertical planes striking 321^0 N at a depth of 8 km, and the values are usually larger than 0.01 MPa.

A Mutually Consistent Seismic-Hazard Source Model for Southern California

Edward H. Field and James F. Dolan
University of Southern California
David D. Jackson
University of California, Los Angeles

Previous attempts to integrate geological, geodetic, and observed seismicity data into a probabilistic-hazard source model predict a rate of magnitude 6-7 earthquakes significantly greater than that observed historically. One explanation put forth was that the apparent earthquake deficit is not real, but an artifact of the upper magnitude limit built into the model. This was controversial, however, because removing the discrepancy required earthquakes larger than are seen in the geological record, and larger than implied from empirical relationships between fault dimension and magnitude. Although several papers have addressed this issue, an alternative, integrated source model without an apparent deficit has not yet appeared. We present a simple geologically-based approach for constructing such a model which agrees well with the historical record and does not invoke any unsubstantiated phenomena. The following factors are found to be influential: the b-value and minimum magnitude applied to Gutenberg-Richter seismicity; the percentage of moment released in characteristic earthquakes; a round-off error in the moment-magnitude definition; bias due to historical catalog incompleteness; careful adherence to the conservation of seismic moment rate; uncertainty in magnitudes estimates obtained from empirical regressions; allowing multi-segment ruptures (cascades); and the time dependence of recurrence rates. The previous apparent deficit is shown to have resulted from a combination of these factors. None alone caused the problem, nor solves it. The relatively simple model presented here is relatively robust with respect to these factors.

Whatever Happened to the SCEC Phase III Report?

Edward H. Field and the Phase III Working Group

About one year ago the SCEC Phase III report was reviewed by a team of nine experts. At that time it consisted of a collection of related studies, combined in an engineering report, aimed at examining sources of uncertainty in probabilistic seismic hazard assessment. The review team agreed the report contained many important findings, but that it needed streamlining. After subsequent delays, it became apparent this would not happen without a full-time editor. One now exists and the report is well on its way to completion.

It has been decided that rather than producing a document primarily aimed at engineers, Phase III will be published as a collection of scientific papers in a special issue of BSSA or GRL. Issues in the earlier version related to the characterization of seismic sources (updating Phase II), and to computing synthetic seismograms, have been removed. The report will now focus exclusively on how, and if, probabilistic seismic hazard assessment (PSHA) can be improved by accounting for site effects. We have made a diligent search for any characteristics that systematically predispose a site to greater (or lower) levels of ground shaking. We have found some significant attributes, such as surface geology and depth to bedrock in sedimentary basins, that indeed correlate with observed amplification factors. Also, we have tested which of several attenuation relations are most consistent with southern California data and with theoretical considerations where data are lacking. We are currently in the process of quantifying the influence of these factors on PSHA. A preliminary conclusion is that, except in some specific circumstances, only modest improvements can be made by accounting for site effects. However, even modest improvements may be significant in terms of implied seismic hazard.

This poster will give an overview of the papers currently slated for the Phase III special issue.

Imaging faults in the Los Angeles Region, Southern California, Using Seismic Data from the Los Angeles Region Seismic Experiment (LARSE)

Gary S. Fuis[1], Janice M. Murphy[1], Trond Ryberg[2], William J. Lutter[3], Cliff Thurber[3], and John J. Shaw[4]
[1]United States Geological Survey, Menlo Park
[2]GeoForschungsZentrum, Potsdam, Germany
[3]University of Wisconsin
[4]Harvard University

Explosion seismic data recorded along a profile from Seal Beach to the Mojave Desert, in Southern California (Line 1 of the Los Angeles Region Seismic Experiment, LARSE), has been processed in several ways to reveal faults and other features in the crust. Refractions and wide-angle reflections have been analyzed using both inverse and forward modeling, and near-vertical-incidence reflections have been analyzed using special CMP methods. Faults imaged with either wide-angle or near-vertical incidence reflections include the upper-crustal Paleogene Vincent thrust fault and an interpreted mid-crustal Holocene(?) thrust-fault zone--a possible "master decollement"--beneath the San Gabriel Mountains and northern Los Angeles basin. Faults imaged as tabular low-velocity zones include the Holocene Duarte fault (the southern branch of the Sierra Madre fault zone) and the San Andreas fault. The Vincent thrust fault is imaged as a concave-upward reflector between two older branches of the San Andreas fault in the San Gabriel Mountains (the Punchbowl and San Gabriel faults), and the interpreted "master decollement" is imaged as a seismic bright zone that projects gently upward from approximately 20-km depth in the vicinity of the San Andreas fault to approximately 13-km depth near the hypocenter of the 1987 M 5.9 Whittier Narrows earthquake. We interpret a ~1.7 km/s maximum velocity reduction in the upper ~500 m of the latter fault zone. The Duarte and San Andreas fault zones are imaged as steeply dipping low-velocity zones, several km wide, extending to at least 5-km depth, with velocity reductions ranging from 0.25 to 0.5 km/s (San Andreas fault zone) to 0.5 to 1 km/s (Duarte fault zone). In the upper 5 km, the Duarte fault zone appears to dip 55 ± 11 degrees northward; and the San Andreas fault appears to dip 80 ±10 degrees northward. Examining offsets or deflections in bright-zone reflections at 20-km depth beneath the San Andreas fault zone, however, indicates an average dip in the upper 20 km of 90 ± 8 degrees for the San Andreas fault zone.

We will present a forward model of LARSE Line 1, a new product which incorporates industry oil-well and seismic-velocity data.

Predicting the Distribution of Modified Mercalli Intensity for Future Earthquakes

Karen Gerst and David D. Jackson
University of California, Los Angeles

Modified Mercalli Intensity (MMI) data are still used widely in earthquake hazard and insurance studies, and in estimating the source parameters of earthquakes that occurred before adequate seismograph networks existed. In this study we provide a model for the probability that the MMI recorded for an earthquake of a given magnitude at a given distance will fall in a given range. This format facilitates computation of expected losses from future earthquakes, allowing for the variability inherent in MMI values. The model was constructed using publicly available data for about two dozen California earthquakes with magnitudes 5.5 and larger. The model is designed to operate in the distance range of 0 to 500 km from an earthquake.

New Decision Support Tools for Emergency Management: TriNet in Southern California

James D. Goltz
California Institute of Technology

This poster will explore the emergency management utility of new real-time seismic information products and how they have been, and will be, implemented in southern California as part of the TriNet project. The immediate aftermath of a damaging earthquake is a time period in which critical decisions must be made, ones which affect not only the quality and timeliness of response but also intermediate and long-term recovery. The minutes, and sometimes hours, following the cessation of shaking have been characterized by partial information and important decisions are often based on limited reconnaissance and guesswork. Following the Northridge earthquake, US scientists and engineers invested considerable effort to develop and test new technologies designed to fill this information gap with rapid information from regional seismic networks. The products of these efforts include: accurate and reliable data on magnitude and location of an earthquake; maps showing the distribution of peak acceleration and shaking intensity; estimates of losses, damage and population impacts; and, the technical capability to provide earthquake early warning. These information products will be available to emergency responders in a period ranging from a few seconds prior to the arrival of strong ground motion to a few minutes after the shaking has ceased.

Investigation of Historic Land Surveys Across the San Andreas Fault between Cholame and the Carrizo Plain ≠ Preliminary Results

Lisa B. Grant[1], J. Ramon Arrowsmith[2], Elizabeth M. Stone[2], and Dallas D. Rhodes[3]
[1]University of California, Irvine
[2]Arizona State University
[3]Georgia Southern University

The objective of this project is to measure displacement from the 1857 earthquake between Cholame and the northern Carrizo Plain by analyzing historic surveys and measuring streams offset along the fault. In 1855-6 James E. Freeman established township and range lines across the San Andreas fault between Rancho Cholame and the northern Carrizo Plain. He divided the township boundaries into 1-mile section lines, established monuments at each section corner and subdivided some townships into 1-mile-square sections. At least 26 section lines were established across the San Andreas fault between Highways 46 and 58 prior to the 1857 earthquake. The distance between monuments constrains the total displacement from the 1857 earthquake and post-1857 strain accumulation. From records of resurveys in San Luis Obispo and Kern Counties, it appears that many original monuments were "lost" after the 1857

earthquake and reset by proportional methods so that they are no longer in their original locations. Several monuments survived the earthquake and were reset in the same place. The distances between ten pairs of monuments spanning the fault were surveyed at least once since 1857 using various types of equipment. Quality of the surveys ranges from poor to good. We field-checked most of the monuments and surveyed one pair with a total station. The post-1857 measurements are 1.6 ≠ 29.6 m longer than the original section lines. Additional work is required to calculate co-seismic displacement, post-seismic strain accumulation and measurement uncertainty.

Holocene Paleoseismology of the San Joaquin Hills Thrust, Orange County, California ≠ Preliminary Results

Lisa B. Grant[1] and Leslie Ballenger[2]
[1]University of California, Irvine
[2]Chapman University

The San Joaquin Hills (SJH) have been rising at a rate of approximately 0.21 - 0.24 m/ka during the late Quaternary (Grant et al., this volume). Geomorphic evidence suggests that the most recent uplift occurred during the Holocene. Stevenson (1954) described a "bench of ancient marsh deposits" around the margins of upper Newport Bay in the northern SJH and proposed that it was created by tectonic uplift of late Holocene-age marshland. We reviewed aerial photos, maps and reports, and surveyed upper Newport Bay on foot and by kayak to map undisturbed remnants of marsh bench for sampling and analysis. There are remnants of marsh bench at the base of cliffs on the west side of upper Newport Bay, immediately above the present shoreline angle. Where exposed, the marsh bench consists of fossiliferous unconsolidated sediments in sharp contact with underlying shale bedrock. The bedrock/sediment contact is approximately 42 cm (average of 36 measurements) above the active shoreline angle. The top of the unconsolidated sediments is approximately 102 cm (average of 24 measurements) above the shoreline, consistent with Stevenson's average measurement of 96 cm "above the present marsh on the western shore". By confirming Stevenson's measurements along the western shore, we conclude that his elevation measurements of the marsh bench (average 157 cm) on the eastern shore (now paved) are reliable. This suggests that the last significant earthquake on the SJH thrust generated >1.6 m maximum uplift, and approximately 1.3 m average uplift along upper Newport Bay. We will collect samples for radiocarbon dating of the marsh bench and search for additional evidence of Holocene uplift along the coastal SJH.

Evidence for an Active Blind Thrust Fault in the Southern Los Angeles Basin, California

Lisa B. Grant[1], Karl J. Mueller[2], Eldon M. Gath[3], Hai Cheng[4], R. Lawrence Edwards[4], Rosalind Munro[5], and George L. Kennedy[6]
[1]University of California, Irvine, [2]University of Colorado, [3]Earth Consultants International, [4]University of Minnesota, [5]Leighton and Associates, [6]San Diego State University,

Movement of a blind thrust fault in the southern Los Angeles basin has uplifted the San Joaquin Hills (SJH) during the late Quaternary and has the potential to generate a M_w6.8 - 7.1 earthquake within this densely populated area. Recognition of this blind thrust extends the known area of active blind thrusts and fault-related folding southward from Los Angeles County into coastal Orange County. Analysis of marine terrace fossils and 230Th dating of solitary corals from these terraces provides a temporal calibration for measuring rates of uplift (0.21 - 0.24 mm/yr) and regional tectonic deformation. Based on structural modeling the SJH thrust dips to the southwest and slips approximately 0.48 mm/yr, suggesting an average recurrence interval of 2650 to 6200 yrs for moderate-sized earthquakes.

Testing a Viscoelastic Model of Aftershock Decay

Susanna Gross
University of Colorado

The physical processes which generate aftershock sequences are not yet fully understood. Stresses transferred from the mainshock correlate with the spatial distribution of aftershocks, and could be the primary trigger of aftershocks. Static stresses last much longer than the aftershock sequence, and so there must be some mechanism which causes the aftershocks to decay. Static stress transfer is not the only possible trigger for aftershocks. Viscoelastic materials flow, producing stress fields that decay in time, and a postseismic adjustment process that can be modeled with a viscoelastic lower crust has been observed for several earthquakes - like the Landers, California 1992 sequence. If viscoelastic processes are responsible for aftershock decay, then aftershocks should decay most rapidly where the stress (or stress rate) from viscoelastic effects is most pronounced. With thousands of well-located Landers aftershocks and a well-modeled stress field, it is possible to explore the viability of viscoelastic stresses as a model of aftershock decay. Viscoelastic stresses and stress rates for a variety of assumed decay times and transition depths can be quantitatively compared with an alternative model based upon rate and state dependent friction. The friction model predicts little change in the spatial distribution of aftershocks during the sequence. Preliminary work showing that viscoelastic models match observed Landers aftershocks less successfully than friction models will be presented.

Modeling Earthquake Process As Three-Dimensional Dynamic Planar Fracture

Dawei Guo and Leon Knopoff
University of California, Los Angeles

We model an earthquake process as a three-dimensional, dynamic, planar shear fracture in an infinite, isotropic elastic medium. The maximum stress criterion is used during the initiation and propagation of fracture on a fault plane with pre-stress and breaking stress distributions. The stress state on the fracture surface is governed by a slip weakening friction law with characteristic slip, $Delta_0$. We use an integral equation representation to solve numerically the three-dimensional wave motion during the dynamic fracture process. We find that $Delta_0$ plays an important role in controlling the fracture velocity. This is to be expected, since this parameter is related to physical properties of energy absorption at the fracture front. Faults with homogeneous breaking stress and homogeneous pre-stress (except for a triggering patch in which the pre-stress is greater than the breaking stress) are used to study the pattern of fracture in the dynamic process. It is found that a large triggering area is required to initiate fracture and maintain propagation, with even moderate characteristic slip, $Delta_0$, (e. g., where $Delta_0$ is only twice the element dimension). Healing starts shortly after initiation and the fractured area forms a expanding ring before final rest of the system. Inhomogeneous breaking stress distributions are also studied in the numerical simulation. They are used to model the geometrical inhomogeneities of the fault plane in nature. The results indicate that complex features in the dynamic process can be produced even with simple shapes of barrier.

Seismic Sources and Rates of Active Tectonics: Santa Barbara Fold Belt, California

Larry D. Gurrola and Edward A. Keller
University of California, Santa Barbara

The southern piedmont of the western Transverse Ranges in Santa Barbara County contains numerous west-striking reverse faults and related folds. A zone of geomorphically well-expressed folds and (sometimes buried) reverse faults on the coastal piedmont form the Santa Barbara Fold Belt (SBFB). Seismic hazard analyses of the fold belt identifies previously unrecognized faults and folds, seismic sources, and rates of active deformation. These include

potentially active segments of the Mission Ridge, the San Pedro and the Channel faults and potentially active folds such as the Mission Ridge monocline, the Goleta Valley, the Montecito, the UCSB-Ellwood, and the Cathedral Oaks anticlines.

The Mission Ridge Fault System (MRFS) is the principal reverse (-oblique slip) fault of the SBFB. Potentially active segments of MRFS consists of, from west to east, the More Ranch, the Mission Ridge, the Arroyo Parida, and the Santa Ana segments. The More Ranch segment is responsible in part for uplifting the 47 +/- 0.5 ka UC Santa Barbara-Isla Vista marine terrace with a vertical uplift rate of 1.2 ± 0.1 m/ka. This terrace is anticlinally folded and exhibits bending moment normal and reverse faults. Marine terraces to the west and east at Ellwood and More Mesa, respectively, are correlated by oxygen isotopic signature to the substage 3a. Therefore, we calculate a vertical rate of uplift of 1.3 ± 0.1 m/ka and a rate of vertical faulting of 0.3 m/ka at Ellwood and a vertical rate of uplift of 1.4 ± 0.1 m/ka at More Mesa. Paleoseismic study of the Loon Point fault determines 2 meters of Holocene (4 ka RCYBP) offset and a vertical faulting rate of approximately 0.1 m/ka. Detailed seismic hazard mapping of uplifted and faulted marine terraces determines rates of active uplift are greater by an order of magnitude than previously recognized and significantly contributes to the state of knowledge of the earthquake hazard of the SBFB.

A Catalog of 20th Century M≥6 Earthquakes in Southern California

Thomas C. Hanks and Ross S. Stein
United States Geological Survey, Menlo Park

Our catalog, published in Stein and Hanks [BSSA, 88, 635-652, 1998], augments and draws upon earlier compilations for southern California, and can be accessed as a clickable map, a table with scalar moments and focal mechanisms, and a detailed appendix with references in http://quake.wr.usgs.gov/study/deformation/. We encourage its use and examination by others. Bounded by $32^0$00'-$36^0$15'N and $114^0$00'-$122^0$00'W, the catalog starts in 1903 following Richter (1958), because instrumental records are available for all earthquakes. Frequency-magnitude relationships and earthquake reporting suggest that the catalog is nearly complete since 1903, and almost certainly complete after 1915. Our catalog b value is 1.0; the rate of M≥6 shocks of 0.42-0.49/yr, and the rate of M≥7.0 shocks is 0.052/yr. The number of M≥6 earthquakes per decade does not depart significantly from a Poisson process during this century. Roughly half of the twentieth century M≥6 earthquakes have struck on the San Andreas system and half on the numerous secondary faults, with most of the seismic moment contributed by the largest earthquakes on the San Andreas. We obtain a southern California moment release rate of 8-12 x 1018 N-m/yr, in distinguishable from the moment release estimated by fault slip, or the moment accumulation inferred from plate motions or geodetic shear strain.

We compare our catalog to the SCEC-1998 and CDMG southern California earthquake catalogs. The CDMG catalog includes 4 events as M≥6.0 that we concluded are M<6.0 and discards 4 earthquakes as M<6 that we believe are M≥6.0. Similarly, the SCEC-1998 catalog includes 6 events as M≥6.0 that we concluded are M<6.0 and discards 5 earthquakes as M<6.0 that we believe are M≥6.0. (The SCEC-1998 catalogue also excludes the 1983 Coalinga and 1985 Kettleman Hills earthquakes on the basis of geographic limitations.) Thus, the number of M≥6.0 earthquakes, in the almost 96 years since 1903 are nearly the same for the three catalogues (40, 40, and 39 for the Stein and Hanks(1998), CDMG, and SCEC-1998 catalogues, respectively), but the ±10% uncertainty is still considerable. This is, we believe, a mostly resolvable, epistemic uncertainty. For only 6 of the 40 earthquakes do M estimates in the three catalogues differ by more than 0.2 units (the 1908 Death Valley, 1915 Volcano Lake, 1922 Parkfield, 1925 Santa Barbara, 1934 Parkfield, and 1942 Salton Sea shocks). These differences, too, should be mostly resolvable. It has now been almost 5 years since the last M≥6.0 earthquake in southern California, close to the third longest interevent time (5.4 years) between such events since 1915.

Role of Fluids in Faulting Inferred from Stress Field Signatures

Jeanne L. Hardebeck and Egill Hauksson
California Institute of Technology

An important open question about lithospheric fault structure is what makes some major seismogenic faults, like the San Andreas, weak. Weak fault zones may contain high-pressure pore fluids, or thin zones of inherently weak materials, or may weaken dynamically. Weakening due to high-pressure fluids should be accompanied by a unique stress field signature. The maximum principal stress should be at high angle to the fault outside the fault zone, and at lower angle inside. We look for evidence of this signature across the San Andreas fault zone in southern California, using stress orientations inferred from earthquake focal mechanisms.

Most segments exhibit the stress field signature of high-pressure fluids. The spatial extent of the stress rotation varies from a few km to over 50 km, implying that high fluid pressures can extend into relatively intact rock. The width appears to scale with the width of interseismic strain accumulation, suggesting that repeated strain-related fracturing and crack sealing has created low-permeability barriers which seal fluids into the network of currently active fractures. The technique presented here can easily be used to look for evidence of high-pressure fluids in any fault zone with well-recorded seismicity. Wide application of this method should help resolve the question of why some major faults are weak.

3D Simulations of Spontaneous Ruptures on En Echelon Strike-Slip Faults

Ruth A Harris[1] and Steven M. Day[2]
[1]United States Geological Survey, Menlo Park
[2]San Diego State University

Although 3D numerical simulations of spontaneous (unforced) earthquake ruptures are becoming more common, most of these simulations still assume that the earthquake occurred on a single fault plane. However, observations show that many earthquakes do not occur on single fault planes. For example, the 1992 Landers, California earthquake was a multi-fault rupture, as shown by geological and seismological data [Sieh et al., Science, 1993].

We have run numerous 3D simulations of a spontaneous rupture encountering a fault stepover in a vertical strike-slip fault, assuming a slip-weakening fracture criterion. We tested wide variations in the strengths and stress-drops as a function of distance along strike, and as a function of depth. Among our observations, are the following: (i) For simple, uniform stress drop configurations, 3D model predictions of whether or not a rupture jumps a stepover are very similar to those previously obtained in 2D by Harris et al., 1991 and Harris and Day, 1993. ii) Simulations in which a rupture jumps across a stepover produce a region of subsidence in the stepover region for dilational stepovers, and a region of uplift in the stepover region for compressional stepovers. This result mimics nature where basins and hills are observed in dilational and compressional stepovers, respectively. iii) When a rupture does jump, rupture of the second fault occurs preferentially at very shallow depth. This finding will be tested in the future as more detailed field observations become available. iv) Repeated earthquakes on faults similar to those at Parkfield, California and at Landers can produce events that jump across a stepover alternating with those that do not, similar to the pattern observed in these two earthquake-prone regions.

Geomorphic Analysis of the Rincon Creek Anticline, Santa Barbara County, California

Ross D. Hartleb
University of Southern California
Edward A. Keller
University of California, Santa Barbara

This research identifies a young, westward propagating, north vergent fold, the Rincon Creek anticline (RCA), near the city of Carpinteria. This 3 km long structure, an elongate topographic ridge, extends from Rincon Creek on the east into the city of Carpinteria on the west. Although at present there is only one forelimb dip and no backlimb dips in the surficial Quaternary alluvial deposits to confirm that this feature is indeed a fold, the data we do have are consistent with this interpretation. Dibblee (1987) mapped the Rincon Creek fault at the base of the north slope of the RCA, although fault exposures are lacking. I believe the Rincon Creek fault is a buried reverse fault expressed at the surface at this location as a fold scarp. The RCA displays a fold morphology with north facing scarp gradients in excess of 35% and maximum relief of 35 m. Relief and gradients of the north facing scarp decrease to the west; south slope gradients are more constant and range from approximately 3 - 10 %. Additionally, an unconformable contact between Pleistocene Casitas Formation and overlying Quaternary gravels is folded. The distributions of dips recorded in the Pleistocene Casitas Formation suggest that there may have been two episodes of folding during Pleistocene time.

Additional geomorphic features, including meander scars, a paleovalley, and wind gaps, are used to reconstruct the erosional and tectonic history of the RCA. It is postulated that Rincon Creek once flowed westward in what is now recognized as a paleovalley, possibly through water gaps of the then young Rincon Creek anticline. Sometime after the initiation of folding a steeper channel flowing south into the Pacific Ocean eroded headward, capturing Rincon Creek and altering its course to the present configuration.

Reference: Dibblee, T.W., 1987: Geologic map of the White Ledge Peak Quadrangle, 1:24,000 scale (H. Ehrenspeck, ed.), Dibblee, Jr. Geological Foundation.

Preliminary Crustal Depth Profiles of Poisson's Ratio for Geological Terranes in Southern California: Contribution to the 2nd Generation SCEC 3-D Velocity Model

Egill Hauksson
California Institute of Technology

Significant regional variations in VP and VP/VS have been imaged, using earthquake arrival time data, across the diverse geological terranes of southern California. These velocity models have been used to determine the average Poisson's ratio for geological terranes as defined by Magistrale et al. (1992). Four classes of terranes are identified. First, the major regional terranes such as the Mojave Desert and Peninsular Ranges show Poisson's ratio of 0.235 to 0.255 over the depth range of 0 to 25 km. Second, the topographically high mountain ranges (the San Bernardino Mountains, San Gabriel Mountains, and Tehachapis) have unique Poisson's ratio signatures (0.24 to 0.27), indicating different crustal compositions. Third, the major basins of southern California show large variations in Poisson's ratio. At shallow depth, in the Ventura basin Santa Barbara Channel, Los Angeles basin, and Coachella Valley, the Poisson's ratio is high (0.27 to 0.31), consistent with sediments and abundant pore fluids. At depth greater than 10 to 15 km beneath the Ventura basin, Santa Barbara Channel, Imperial and Borrego Valleys, the Poisson's ratio remains moderately high (0.27), suggesting mafic lower crustal rocks beneath the basins. Fourth, offshore in the Continental Borderland, the Poisson's ration is high at shallow depth in offshore sedimentary basins, and moderately high at lower crustal depths suggesting a large mafic component in the composition of the lower crust.

Caltech/USGS Element of TriNet: Progress Report for the First Third of the Five Year TriNet Project Period

E. Hauksson, R. Clayton, J. Goltz, K. Hafner, T. Heaton, H. Kanamori, and P. Maechling
California Institute of Technology
L. Jones, D. Given, J. Mori
United States Geological Survey, Pasada

The Caltech/USGS element of TriNet records real-time data from approximately 100 digital seismic dataloggers distributed throughout southern California. Data are transmitted from the remote sites using IP based data communication protocols. Phase 1 of the software development has been completed. The software development at the central site is focused on new real-time data acquisition systems, ORACLE database development, and development of new JAVA based tools for data analysis. Real-time products such as hypocenter, magnitude, and ShakeMap will be provided by the real-time system. We are evaluating a publish-subscribe data distribution model in our real-time data processing system to help us achieve speed, modularity, and scalability in our processing system. Both waveform and derived parametric data will be sent to the ORACLE database as soon as the data are recorded. These data will be available to the users such as researchers, emergency response groups, corporations, and the general public via the web. Research and development includes recursive filtering for rapid magnitude determination, calculation of strong motion centroid, waveform focal mechanisms, and development of ShakeMap methodologies. The TriNet outreach program is focusing on a ShakeMap user feedback workshop and modification of EPEDAT software to accept ShakeMap from TriNet.

Postseismic Deformation Following the 1992 Landers Earthquake: An Evaluation of Earthquake Cycle Models

Elizabeth H. Hearn
University of Oregon

During the 6 months following the 1992 Landers earthquake, postseismic surface displacements consistent with a moment release of about 15% of the coseismic moment were recorded (Shen et al., 1994). These displacements decay with a characteristic time of 5 to 80 days (Savage and Svarc, 1997; Shen et al., 1994; Wyatt et al., 1994) and are superimposed on a longer term postseismic velocity transient (Savage and Svarc, 1997). Models incorporating afterslip, lower crustal relaxation, and poroelasticity have been developed to explain Landers postseismic deformation, but no model has satisfactorily done so. It is important to understand how postseismic deformation and interseismic loading occur, since these loading mechanisms (i.e., earthquake cycle models) govern the patterns of postseismic and interseismic stress accumulation, and provide insight into the structure and rheology of the middle and lower crust.

I have developed a 3D viscoelastic model of postseismic deformation following the Landers earthquake (and the associated Joshua Tree and Big Bear earthquakes) using a tectonics-oriented FE program developed at the University of Oregon (Saucier, 1991). I have modified the program to model biviscous rheology and viscous afterslip.

The decay time, magnitude, and pattern of horizontal surface displacements can be modeled reasonably well assuming either biviscous lower crust or afterslip concentrated below the south half of the rupture. This pattern of afterslip requires that the afterslipping surface weaken rapidly with depth below the seismogenic upper crust. Vertical displacement patterns derived from SAR data (Peltzer, 1998) appear more consistent with viscoelastic lower crust models than with afterslip models. In either case, the rapid phase of postseismic strain represents only a small fraction of the total postseismic response. This suggests that the seismogenic crust is not effectively decoupled from the mantle, and that tractions resulting from mantle flow may contribute significantly to crustal deformation in southern California.

Faulting and Seismicity On and Near a Curved Fault Segment

Moritz Heimpel and Leon Knopoff
University of California, Los Angeles

We use model simulations to investigate the relationship between a main fault that bends, and secondary faulting and seismicity in the bend region. The numerical model is based on exact solutions of elasticity in a three-dimensional half-space. Faulting and earthquakes, governed by the Coulomb-Navier yield criterion in conjunction with a simplified version of the Dieterich-Ruina rate and state dependent constitutive relation, can occur anywhere in the two-dimensional, horizontal model domain.

Results are presented from simulations designed to give insight into the mechanics of earthquakes and faulting in Southern California. In these models, friction is set to be systematically lower on the main fault than in the rest of the model domain. The main fault has a compressional bend and undergoes right-lateral slip due to a uniformly increasing shear stress. A typical result is that seismicity and slip accumulation on the bend segment of the main fault is suppressed with respect to that on straight segments. This is due to higher Coulomb strength on the bend segment. To make up for this deficit in slip, secondary faults form in the bend region. Such secondary faults first form as relatively diffuse accumulations of right-lateral slip, emanating along strike from the straight, main segments into the bend region. In some simulations, conjugate faults with left-lateral slip also form. These model faults bear some resemblance to left-lateral faults in Southern California, such as the White Wolf and Garlock faults.

Determining the Basin Structure by Whole-Waveform Inversion

Don Helmberger and Chen Ji
California Institute of Technology

The analysis of broadband strong ground-shaking as observed in the greater Los Angeles region remains a difficult problem because of the lack of underlying structural information. At present, three 3-D basin velocity models have been proposed: Magistrale Model, which maps geological structure into seismic velocities (Magistrale et al., 1996); Graves Model based mostly on drill-data from the oil industry (Graves, 1996) and Hauksson Model from travel-time tomography(Hauksson and Haase, 1997). However, Wald and Graves'(1998) numerical simulation showed all of them need be refined, especially at shorter periods.

The various broadband seismic networks, such as TERRAscope, TriNet, etc, will be useful for this purpose. As local smaller earthquakes shake these stations, the records of stations inside the basin are very different from those of stations just outside. Such differences are useful measurements to constrain the basin structure. Based on this type of data, we develop a waveform inversion scheme to study the basin structure.

In this work, we model the basin structure as several 2-D layers, the position of the interfaces between the adjacent layers are controlled by some key points. Hence we can obtain different shaped basins by changing the vertical positions of the key points. For the region outside the basin, we use a 1D-layered model. The synthetic seismograms are calculated by a hybrid method combined the generalized ray theory and the finite difference method (Wen and Helmberger, 1996). It is a computationally efficient method since only the propagation response through the basin structure is computed numerically. We use the conjugate gradient method to perturb the basin velocity model until synthetic seismograms fit the travel times and waveforms of basin records.

Monitoring SCIGN Station Data Quality

Thomas A. Herring, Robert W. King, and Simon C. McClusky
Massachusetts Institute of Technology

Effective use of SCIGN to measure co-seismic displacements and time variable motions associated with an earthquake depend on achieving and maintaining reliable receiver performance, stable monumentation, and a local environment conducive to low signal distortion. Since the beginning of 1998, we have analyzed daily the data from 12 stations in the array, estimating position and computing phase residuals as a function of time, azimuth, and elevation, in order to study the "base" and time-variable performance of the stations. These results are available on the web (http://www-gpsg.mit.edu/~tah/cont98.html) in a form that allows the time series to be interactively modified by a web user. Three of the stations (JPL, Mt. Lee, and USC) maintain sub-millimeter (rms) scatters in horizontal position; others show scatters between 1 and 5 mm for reasons that are not yet understood. Three of the stations have shown a sensitivity to rain and snow (thought to be electromagnetic in origin rather ground displacement) that would compromise their use at the time of an earthquake.

Paloeseismic Investigation of the Simi Fault at Arroyo Simi, Simi Valley, Ventura County, California

Christopher Hitchcock[1], Jerome A. Treiman[2], William R. Lettis[1], and Gary D. Simpson[1]
[1]William Lettis & Associates
[2]California Division of Mines and Geology

Results from our paleoseismic investigation at Arroyo Simi within Simi Valley, California, demonstrate Holocene activity and provide data on the sense of slip of the Simi fault. The Simi fault is a left-lateral reverse slip fault of the Simi-Santa Rosa fault system, a series of north-dipping faults that extend from the northeastern end of Simi Valley to the east edge of the Oxnard plain. Within Simi Valley, the Simi fault forms a linear mountain front along the north valley margin. We have defined the location of a major strand of the Simi fault based on detailed mapping, shallow boreholes, and documentation of stream exposures along Arroyo Simi at the northwestern end of Simi Valley. At the base of the southwestern stream bank of Arroyo Simi, Holocene clay and silty clay deposits are exposed in fault contact with sandstone of the Oligocene Sespe Formation. The fault is expressed as a N70^{0}E striking, sub-vertical zone of clay gouge bounded by a vertical bed (?) of cobbles within the Sespe Formation on the north and sub-horizontal laminated clay and silty clay deposits to the south. We interpret the clay deposits exposed on the inferred downthrown fault block to be ponded due to blockage of Arroyo Simi from uplift of bedrock along the fault. Layers within the clay deposits are warped upwards near the fault. This apparent drag folding is consistent with a reverse component of displacement on the fault. However, slickensides on the fault plane show a significant left-lateral component of displacement suggesting that the fault has an overall left-lateral, reverse sense of slip. The timing of the most recent event on the Simi fault is constrained based on calibrated radiocarbon dates between 7666±50 years BP, the age of the faulted clay deposits, and 1205±80 years BP, the age of overlying unfaulted colluvium. Several additional fault strands are located south of the near-vertical fault documented in the Arroyo Simi streambank. These features are expressed as subtle tonal and topographic lineaments within Holocene terrace surfaces and appear, as well, to have bounded a low topographic knob (removed by grading) observed on historic photographs. Recent investigations for proposed development have exposed low-angle (<20^0), north-dipping faults that offset bedrock and overlying soil. These features, along with the near-vertical main strand of the Simi fault, appear to accommodate strain partitioning at a possible compressional stepover within the complex Simi fault zone.

Imaging Attenuation and Source Properties at the Coso Geothermal Field, California

S. E. Hough[1], J. Lees[2], and F. Monastero
[1]United States Geological Survey, Pasadena
[2]Yale University

Source properties of small (magnitude -1 to 1) clustered events from the Coso geothermal region are analyzed using an empirical Green's function (EGF) method. Stress drop values of at least 0.5-1 MPa are inferred for all of the events; in many cases, the corner frequency is outside the usable bandwidth and can only be constrained as being higher than ~3 MPa. P- and S- wave stress drop estimates are identical to within the resolution limits of the data. These results are indistinguishable from numerous EGF results from M2-5 earthquakes, suggesting that similarity in rupture extends to events that are both tiny and induced. Whole-path Q estimates for P and S waves are determined using a multiple-empirical Green's function (MEGF) method (Hough, JGR, 1997) whereby spectra from clusters of colocated events at a given station are inverted for a single attenuation parameter, t*. The t* estimates, which we infer to have uncertainties considerably lower than achievable with conventional methods, are then inverted for three dimensional attenuation structure using a damped least-squares method. Qs/Qp values greater than one are inferred for nearly all source-receiver paths, consistent with restriction of fluids to narrow conduits within the geothermal region. Significant lateral variability in attenuation structure is inferred; a central low-Q anomaly corresponds well to the extent of the high heat flow region.

SCIGN Operation Center at the USGS Pasadena

K. Hudnut, N. King, J. Galetzka, J. Behr, A. Aspiotes, S. Van Wyk, and D. Palmer
United States Geological Survey, Pasadena

We will report on the activities and accomplishments of the Southern California Integrated GPS Network operations center at the USGS Pasadena Field Office. Our SCIGN group will be responsible for downloading and operating 200 of the 250 stations that comprise SCIGN once it is fully installed. We also have the lead role in providing earthquake response information based on SCIGN data.

During the past year, our group has led the site selection and site permitting effort for SCIGN, with help from our SCIGN colleagues at SIO and JPL. At this time, approximately 150 stations have been selected, and of these 70 are now permitted. We will provide summary information about the process and status of this major effort. Also, our group helped to develop several sections of the Statement of Work document for contracting installation of the network, and we are participating in oversight of the installation work.

Our group has also led the development of a new system for downloading data from the array. The new software replaces DASS, an OS/2 platform set of REXX scripts that would not have been capable of readily handling the downloading task before us. The new system was developed jointly with SIO, and includes ASHCAN which runs on NT, and is specific to the Ashtech receivers in the SCIGN array. For the new system we also developed EGADS, which is a set of perl scripts that run on both NT and UNIX platforms. The ASHCAN/EGADS software will be made available for testing and improvements by others outside of the SCIGN project.

In addition, we continue to develop an automated system for processing data from SCIGN and updating results on the web daily. Sub-daily downloading, and sub-daily post-processing with GAMIT/GLOBK will be the next step towards near real-time GPS results from all SCIGN stations. We are also investigating real-time telemetry, real-time kinematic (RTK) GPS modes, and GIS mapping in support of our earthquake response function.

Our group also led the development of a new radome design to protect the GPS antennas while introducing only minimal distortion of the GPS signal. Once the radomes are ready for deployment in Nov. 1998, we will be upgrading existing sites and will also bring the new SCIGN sites up to fully operational status.

P-Wave Amplification in Southern California

D. Icenogle, A. T. Nguyen, and P. Davis
University of California, Los Angeles

The M=6.7 Northridge earthquake on January 17, 1994, caused unexpected excessive damage in Santa Monica and Sherman Oaks, CA. Previous work (Gao et al, 1996) has concluded that a small sub-basin lens structure beneath Santa Monica focused seismic energy into these areas. The goal of this project is to gather evidence supporting the possible presence of other focusing lenses elsewhere in southern California by studying the amplification factors of local seismic stations as determined from small ($M_L \leq 2.5$) earthquakes in the Los Angeles basin and surrounding areas. The earthquakes used were taken from the Southern California Earthquake Center (SCEC) database and were limited to those events for which there was an available fault-plane solution (strike, dip, and rake of the fault plane). This fault-plane solution was then used to calculate the radiation pattern for each event in order to determine the location of the nodal planes. Data from stations with signal-to-noise (S/N) ratios less than 1.5 and from stations at or near the nodal planes were not included. The maximum recorded P-wave amplitude was plotted versus distance from the hypocenter for those stations located farthest away from the nodal planes, and a simple least-squares regression was performed using the equation $A_t=A_o/r^{exp}$ (where A_t is theoretical amplitude, r is hypocentral distance). The theoretical amplitude at each station was calculated based on the resulting Ao and exp values and the SCEC-determined fault-plane solution for that event. The ratio of the observed amplitude to the theoretical amplitude was then calculated at each station. Each station's ratios were then averaged over all the events recorded by that station in order to determine that station's amplification factor. Immediate future work will be to determine the relationship between the pattern of amplification factors and 1) geology and 2) the damage caused by the Northridge earthquake in order to see if weak-motion amplification coincides with strong-motion amplification, and to determine the possible azimuthal dependence of amplification factors on earthquake location.

Long-Period Ground Motion Estimation for the San Francisco Bay Area

Eleanore Jewel, Kim B. Olsen, and Ralph J. Archuleta
University of California, Santa Barbara

We have used finite-difference simulations of finite-fault wave propagation to estimate long-period ground motion amplification in the south San Francisco Bay area, California, for the 1979 M 5.9 Coyote Lake earthquake. The simulations included a 3-D crustal model recently developed by the U.S. Geological Survey and the slip distribution by Liu and Helmberger (1983). Results of the simulations were used to generate a 0-1 Hz peak velocity amplification map for the South Bay as ratios between 3D and 1D horizontal peak velocities from finite-difference simulations, similar to the procedure used for the SCEC phase III project. The largest ratio is 6.6, at a site just east of the southern edge of the bay. The 1D model was taken as the profile at a rock site near the part of the Calaveras fault that ruptured during the earthquake. While the deeper areas of the basins generally show larger amplification, the general direction of propagation of waves from the southeast tends to increase amplification in the "rear" ends of the sedimentary basins (i.e., towards the north-west). After an approximate correction for the contribution from the differences in velocities and densities between the 1D and 3D models the largest amplification was 6. As a validation of the finite-difference simulations we compared the synthetics to data recorded by the Gilroy array and to finite-fault synthetics computed by another numerical method. In order to examine the effects of anelastic attenuation on the ground motion in the San Francisco Bay area we compared 2-hz synthetics from 2-D elastic and viscoelastic simulations of the 1979 Coyote Lake earthquake along a profile perpendicular to the Calaveras fault. The viscoelastic synthetics have durations up to twice the length of those computed in an elastic model.

Short-Baseline GPS Results from PIN1-PIN2: Noise Characteristics and Implications For the Global Reference Frame

Hadley Johnson, Yehuda Bock, and Frank Wyatt
University of California, San Diego

At Pinon Flat Observatory we operate two continuous GPS sites about 50 meters apart (PIN1 and PIN2). Each of these has been in operation since about 1992. The monumentation at each site is a prototype of the standard SCIGN drilled-and-braced mark. We have recently reprocessed the entire data series in "baseline" mode using GAMIT in order to place the tightest possible constraints on the noise characteristics of the GPS system. Processing data in this way avoids complications due to uncertainties in the global reference frame. The resulting time series are remarkable in several ways:

1) the day-to-day scatter (i.e., white noise component) is about 0.15 mm in the horizontal directions

2) the low-frequency noise is best characterized by a sub-mm-amplitude power-law process of spectral index about -1.5 (instead of the several mm-amplitude of 1/f noise present in GPS "position" time series)--it can also be described reasonably well as a random-walk process of amplitude 0.4 mm/sqrt(yr) (this applies to two monuments, so the stability of each is about 0.3 mm/sqrt(yr))

3) offsets due to instrumentation changes are recognizable down to the 0.1 mm level (in two instances simply removing and replacing the same antenna caused 0.3 mm of offset).

Perhaps the most interesting result is the fact that the power spectra are not dominated by 1/f noise as has been found in previous studies of "position" data. This implies that the source of the 1/f noise is the global reference frame itself and is not inherent to GPS. Other evidence corroborates this finding and will be presented.

Worldwide Doublets of Large Shallow Earthquakes

Y. Y. Kagan and D. D. Jackson
University of California, Los Angeles

We investigate all the pairs of $M_w \geq 7.5$ shallow earthquakes in the Harvard catalog which occur at the centroid distance of less than 100 km. We show that most of these pairs have similar focal mechanisms. Since these earthquakes should have a focal area in excess of 100 km, their rupture zones should intersect. For all of these pairs the inter-earthquake time interval is significantly less than the time span needed for plate motion to accumulate the strain released by the first event in a pair; the distribution of the time intervals is a power-law rather than quasi-periodic. This result again implies that the basic assumptions of the earthquake recurrence models contradict observational evidence.

Subsurface Faulting and Folding Onshore and Offshore of Ventura Basin: 3D Map Restoration Across the Oak Ridge Fault

Marc Kamerling, Chris Sorlien, and Craig Nicholson
University of California, Santa Barbara

Late Quaternary deformation of the eastern Santa Barbara Channel and western Ventura basin is examined using seismic reflection data, well logs, paleontology and 3D map restoration techniques. Based on detailed stratigraphy at ODP-893A and extrapolated sedimentation rates, two prominent reflections dated at ~110 ka and ~200 ka are correlatable throughout the central channel. These results are combined with a 1 Ma horizon mapped by Yeats that we have since modified and extended, plus preliminary mapping of a ~1.7 Ma (top Lower Pico) horizon we derived using the Hopps VBSG dataset. The contour maps and correlated cross sections document the pattern of strain partitioning in both space and time, and provide the basis for estimating subsurface geometry, folding, and fault slip rates. The 1 Ma horizon has been

digitized and the surface unfolded and restored to yield the cumulative finite strain. Displacements are calculated by comparing the restored surface to the present state and a fixed reference line. South of Santa Barbara, the increase in amplitude of a fold above the Oak Ridge fault has been 2 mm/yr since 200 ka, the same rate as the vertical motions due to fault slip and folding since 1 Ma. Vertical separations from Oak Ridge fault slip and hanging-wall folding reach a minimum offshore just south of Ventura (1 km for the 1 Ma horizon and 1.4 km for the ~1.7 Ma horizon), while onshore post-1 Ma vertical separations mainly due to faulting reach 4-5 km near Santa Paula. There, the 3D map restoration suggests that the post-1 Ma component of left-slip is either less than half the 3.5 km proposed by Yeats and Taylor, or that it continues offshore. In either case, the component of left-slip may equal or exceed the vertical slip in the offshore region. NE-striking cross faults that may act to segment regional trends are also suggested by sharp bends and terminations of fault and fold limbs.

Mission Ridge, Santa Barbara CA : A Story of Paleochannels, and Earthquakes

E. K. Keller, R. D. Hartleb[1] and L.D. Gurrola
University of California, Santa Barbara
[1]Presently at University of Southern California

Mission Creek in late Pleistocene time flowed south from the Santa Ynez Mountains, through a series of distributary channels of an alluvial fan upon which much of the city of Santa Barbara is now built, discharging into a lagoon (El Estero). These channels are present today as paleochannels in an urbanized environment. The lagoon is filled ,partly with debris from the 1925 (M 6.3) earthquake that nearly destroyed the city. Uplift and lateral propagation of the western end of Mission Ridge (an active monocline) near the fan head resulted in westward deflection of Mission Creek. We believe the lateral propagation to be the result of earthquakes on the Mission Ridge fault. Total deflection of approximately 1 km is delineated by wind gaps which decrease in elevation to the west. Though masked by urbanization, the paleochannels are still expressed in the topography, and along with other drainages on the south flank of Mission Ridge, contribute runoff to the now-filled El Estero in lower Santa Barbara.

Some Strength Weakening Laws are Non-Physical

L. Knopoff and J. A. Landoni
University of California, Los Angeles

We solve analytically the 2-D problem of slip in weakening zones of dynamic fractures on faults characterized by either linear slip- or velocity-weakening properties. The region is uniformly prestressed and has a uniform stress drop; slip is triggered by the application of a sudden shear stress at the point of nucleation. In the slip-weakening case and in some of the velocity-weakening cases as well, the solutions exhibit nonphysical stress waves that either propagate in the perfectly elastic medium with infinite velocities and/or converge toward the source. The nonphysical behavior arises because these strength-weakening laws are not physical. We suggest that caution be exercised before adopting ad hoc strength-weakening relations derived from slow deformation experiments, to describe dynamic behavior at the edges of cracks, without testing to ensure that these relations are causal.

Complex Multi-Pulse Mode of Rupture Propagation

Nadia Lapusta and James R. Rice
Harvard University

Our numerical simulations of dynamic rupture with strong velocity-weakening friction show, in a certain parameter range, complex features of propagation during individual events on a uniform fault. The rupture starts out in a crack-like mode, but the smoothly decaying profile of

slip velocity right after the rupture front peak develops roughening, which grows into well-separated slip velocity pulses. Slip velocity falls and rises several times right after the rupture front, as if a number of pulses are propagating one after another. This behavior, originally thought to be a numerical artifact, actually seems to be well resolved numerically, and to retain its main features under severe refinements of the grid.

We studied this phenomenon in the framework of a 2D scalar elastic model of a faulted crustal plate, slowly loaded via coupling to a steadily moving substrate. We used the classical Dieterich-Ruina logarithmic velocity-weakening rate/state constitutive law, but modified it at very short asperity contact times (high slip rates, V), shorter than those of the conventional laboratory range, in such a way that the steady state strength varies, essentially, as $1/(1+V/V_{weak})$ at high V, like in Zheng and Rice (BSSA, in press). This modification, controlled by parameter Vweak, produces enhanced velocity weakening at high slip speeds. Propagation of echelons of pulses through points of the fault segment is seen in representative events, simulated as a part of earthquake sequences.

Similar multiple pulses of slip velocity have been encountered in other studies as well (Cochard and Madariaga, JGR, 1996; Zheng and Rice, BSSA, in press).

This multi-pulse propagation takes place in a broad transitional regime between the crack-like and truly self-healing modes of rupture propagation, and thus fits the classification of rupture modes given by Zheng and Rice. The wavelength of the pulse sequence scales with the slip weakening distance of the friction law, and is indeed dynamically unstable according to our analysis, following the Rice and Ruina (J. Appl. Mech., 1983) fully inertial studies of stability to spatially periodic disturbance on the boundary between two elastic continua sliding with constant velocity.

Decay Laws and the Self-Organization of Aftershocks

Matthew Lee and Leon Knopoff
University of California, Los Angeles

We have previously reported a novel model of earthquake aftershocks based on the idea that the passing stress wave from the main shock introduces damage into the surrounding region, whereby the increased stress at the edge of the newly introduced cracks is enough to overcome the general decrease in stress to the region as a result of the main slip and produce decays of strength on a new time scale. Depending on the decay law used this model leads to aftershock sequences that self-organize to both a Gutenberg-Richter relation between the distribution of crack sizes and to an Omori law of aftershock rates, both with exponent values close to 1. Here we study the decay law in more detail. The decay law that leads to an Omori distribution is one where the material strength decays with time at a rate proportional to the locally applied stress to some positive power, α. We find there is a transition from a power law decrease in aftershock rate with time to a constant rate of aftershocks as α is varied. This puts a limit on the range of values of α that would produce acceptable results and can be compared with experiments providing a laboratory test for this model.

Seafloor Morphology of the San Clemente Island Fault

Mark R. Legg[1], C. D. Hollister[2], and P. Lemmond[2]
[1]ACTA Inc.
[2]Woods Hole Oceanographic Institute

Recent SeaBeam data acquired east of San Clemente Island, in the California Continental Borderland, allow more accurate definition of faulting along the San Clemente Island fault, a 120-km section of the San Clemente fault system. Numerous tectonic landforms, including scarps, linear valleys, benches, and sags, are aligned along the base of the east-facing

San Clemente Island escarpment. These tectonic landforms show active right-slip along a well-developed N40W-trending fault. A 22-km fault segment with more westerly trend shows convergent character, that may cause the relatively greater uplift of the adjacent southeast half of San Clemente Island. Other investigators (Ward and Valensise, 1996) modeled northeast-directed shortening on a southwest-dipping blind thrust fault beneath the island to account for the uplift of the Quaternary marine terraces, yet failed to constrain rates of strike-slip on the major San Clemente Island fault that must terminate the postulated thrust. In contrast, a 15-20 km northwest-trending graben truncates the southwest flank of Emery seaknoll, a Miocene (?)seamount volcano lying about 5-km to the northeast of the San Clemente Island fault. These prominent tectonic features with opposing tectonic character, suggesting both northeast-directed shortening as well as northeast-directed extension located in close proximity to the major strike-slip fault, imply that, like the modern San Andreas fault, the San Clemente Island fault is a very weak fault.

Crustal Thicknesses of the Northern Peninsular Ranges, Southern California, from Teleseismic Receiver Functions

Jennifer L. Lewis, Steven M. Day, and Harold Magistrale
San Diego State University
Jennifer Eakins and Frank L. Vernon
University of California, San Diego

A major SCEC focus is the development of a 3D seismic velocity model for southern California. An important element of the model is the structure of the crust-mantle boundary. While gravity and seismic refraction surveys in the Peninsular Ranges Batholith (PRB) have yielded poorly constrained and conflicting crustal thickness estimates, ranging from 26 km to 43 km, Moho P-to-S conversions (Ps) identified in recordings of teleseisms have provided reliable, well-localized crustal thickness estimates. Recently, Ichinose et al. (1996) used Ps arrivals from teleseismic receiver functions at the latitude of San Diego to infer a relatively flat deep Moho (~40 km) under the western PRB, and a steeply eastward shallowing of the Moho (~40 km to ~25 km) under the eastern PRB. We extend that study of PRB crustal thickness variations to ~100 km north, using broadband records from the ANZA and TERRAscope networks. Crustal thicknesses were estimated through analysis of teleseismic receiver functions at stations along a 60-km profile in the eastern PRB between the Elsinore Fault Zone and the eastern margin of the batholith. Observed Ps arrival times are combined with tomographic velocity models to image a northeastward thinning of the crust: the crustal thickness at the southwestern end of the profile is estimated to be ~37 km, thinning to ~28 km at the northeastern end. Moho topography does not mirror surface topography. The receiver function results show that the shallowest Moho exists beneath the highest surface topography in the eastern PRB. This may be indicative of isostatic rebound of the crust due to footwall unloading during Miocene extension.

Quantification of an Earthquake Cycle with Establishment and Destruction of Stress Correlations in the System

Cheng-Ping Li and Yehuda Ben-Zion
University of Southern California

Recent studies suggest that large earthquakes occur when a fault system reaches a critical state associated with the establishment of long range correlations of stress or other dynamic variables (e.g., Sornette and Sammis, J. Phys. I France, 1995; Ben-Zion, JGR, 1996). Here we quantify this process using stress and earthquakes histories generated by the model of Ben-Zion (1996) for a disordered strike-slip fault system in a 3D elastic half-space. The analysis is done on the central part of the model seismogenic zone, covering a depth range of 4 km to 8

km and horizontal extent of 55 km. For each depth interval of 0.55 km, we analyze the temporal evolution of the spatial distribution of stress using the following steps: (1) We compute the auto-correlation coefficients of the stress at each depth interval as a function of space offset. (2) We calculate the standard deviations of the auto-correlation functions and use these as estimates for the width of the stress correlation. To examine the evolution of stress correlation in different wavelength bands, we perform this analysis also in a spectral domain, using a spectral analysis called the Empirical Mode Decomposition (Huang et al., Proc. R. Soc. Lond. A, 1998). This method gives, like wavelet analysis, sharp identifications of energy distribution at any time in both the space and wavelength domains.

The results show non-repeating cyclic establishment and destruction of stress correlations on the fault with the following features: A cycle begins when each large event destroys the long range correlations of stress, leading to a sharp drop in the width of the correlation function. The combined occurrences of the subsequent small to intermediate size events increase the spatial correlation of stress on the fault. The correlation length of the evolving stress reaches a maximum value after 1/3 to 1/2 of the cycle time, when the ongoing model events establish "stress bridges" across the entire system. Then the correlation length fluctuates around the maximum value until one small event cascades to become the next large earthquake. This destroys the long range stress correlation and starts a new cycle. The above process may be used to define a large earthquake cycle on a spatially extended heterogeneous fault system. Continuing analysis of this process, combined with quantitative analysis of the associated seismicity patterns, may provide new target signals for statistical earthquake forecasting.

The Delineation of Landers Fault Zone Structure from Explosion-Generated Trapped Waves

Yong-Gang Li[1], John Vidale[2], Fei Xu[2], Robert Graves[3], and Keiiti Aki[1]
[1]University of Southern California
[2]University of California, Los Angeles
[3]Woodward-Clyde, Pasadena

Fault zone trapped waves generated by near-surface explosions and recorded by seismometers deployed along and across the Johnson Valley fault allow us to delineate the shallow seismic structure near the 30-km-long Landers southern rupture. Fault zone trapped waves with relatively large-amplitude at 1-2 Hz and long-duration wavetrain were recorded only when both the explosions and seismometers were close to the fault. Amplitudes of trapped waves also decreased with distance between the explosion and station along the fault, giving an apparent Q of ~18. The dispersion of trapped waves on the along-fault profile results a shear velocity of 1.0 km/s for the shallow part of fault zone and 1.8 km/s for the wall rock. The explosion-excited trapped waves are similar to those generated by aftershocks, but have lower frequencies and travel more slowly, suggesting that the fault zone has lower velocities, lower Q, and broadens as it approaches the surface. Using measured Q values and group velocities as constraints allowed us to fairly tightly determine the model parameters and reduce trade-offs among model parameters in the numerical modeling of trapped waves on cross-fault and along-fault profiles. Calculations of 3-D finite-difference synthetics further reveal a depth-varying fault structure.

Improvements to the UCSB Strong Motion Database

Grant Lindley, Alexei Tumarkin, and Ralph Archuleta
University of California, Santa Barbara

The UCSB Strong Motion Database (http://smdb.crustal.ucsb.edu/) has been significantly improved over the last year in the amount and type of data available, the access methods, and the access speed. The database now contains 5559 strong motion traces, up from 3745 traces, and now includes both corrected and uncorrected data. An interactive Java map access method has been added bringing to six the number of access methods available. The map

access method allows the user to query the database by selecting earthquakes or stations directly from a map. Other access methods have been expanded and improved to allow for easier use of the database.

Additional parameters have been added to the database, as requested by database users. These parameters include the accelerogram trigger time and the closest distance to the fault where reasonable fault parameters could be estimated.

Quality control has been conducted to complete the database and to confirm the accuracy of database parameter values. This has resulted in additional parameter values, especially for earthquake focal mechanisms and response spectral amplitudes.

A Sun Ultra 10 with a 300 MHz UltraSPARC processor, 17 GB of disk space, and 640 MB of RAM has been purchased. This computer now has a dedicated connection to the UCSB FDDI campus backbone through an ethernet switch. Access times have improved by approximately a factor of three.

The database is now seeing steady use. Over the last year there have been 54,657 Web pages downloaded (150/day), 2940 MB of strong motion data downloaded from UCSB (8 MB/day), and 3794 strong motion data files downloaded from USGS and CSMIP FTP sites via the Strong Motion Database (10 files/day).

Effects of Randomization of Source Parameters for Estimating Strong Ground Motion with Empirical Green's Functions

Pengcheng Liu, Ralph J. Archuleta, and Jamison H. Steidl
University of California, Santa Barbara

The complexity of the earthquake rupture convolved with complex path effects and site response produces the high-frequency strong ground motion. It is difficult to model the detailed source process and wave propagation deterministically in such a way as to reproduce acceleration waveforms that match in both phase and amplitude. However, we can avoid some of these difficulties in the estimation of strong ground motion by randomizing some source parameters and by using small earthquake recordings as empirical Green's functions. This procedure can account for the geometry between the rupture direction and the observers. It can also be extended to use all available EGFs, therefore the estimation is not biased by a single record.

Using Monte Carlo simulation, We have estimated the mean values and the standard deviations (~30%) of peak acceleration, Fourier amplitude spectra, and response spectra for the 1994 Northridge earthquake. In most cases the estimated results are in good agreement with the observed strong-motion records. Prediction of the UC Santa Barbara campus and Santa Barbara Natural History Museum are similar and give reasonable average ground motion parameters when compared with Northridge.

Earthquake Cycle, Faults, and Seismicity Patterns in a Rheologically Layered Lithosphere

Vladimir Lyakhovsky[1], Yehuda Ben-Zion[2], and Amotz Agnon[1]
[1]The Hebrew University, Jerusalem
[2]University of Southern California

We study the coupled evolution of earthquakes and faults in a model consisting of a seismogenic upper crust governed by damage rheology, over a viscoelastic substrate. The damage rheology has two types of functional coefficients: (1) a "generalized internal friction" separating states associated with material degradation and healing, and (2) damage rate coefficients for positive (degradation) and negative (healing) changes. The evolving damage modifies the effective elastic properties of material in the upper crust as a function of the ongoing deformation. This simulates the creation and healing of fault systems in the upper seismogenic zone. The seismogenic upper crust is coupled viscoelastically to the substrate where steady plate

motion drives the deformation. The calculations employ vertically averaged variables of the thin sheet approximation for the viscous component of motion, and a Green function for a 3-D elastic half-space for the instantaneous component of deformation.

To focus on basic features of a large strike-slip fault system, we start with simplified geometry of the seismogenic crust by prescribing there initial conditions consisting of a narrow damage zone in an otherwise damage-free plate. For this configuration, the model generates an earthquake cycle with distinct inter-, pre-, co-, and post-seismic periods. Model evolution during each period is controlled by a subset of parameters, which we constrain using geophysical, geodetical, and seismological data. In the more generic case with random initial damage distribution, the model generates large crustal faults and subsidiary branches with complex geometries. The results indicate that low healing rate, describing systems with relatively long memory, leads to the development of geometrically regular fault systems, and the characteristic frequency-size earthquake distribution. Conversely, high healing rate (relatively short memory) leads to the development of a network of disordered fault systems, and the Gutenberg-Richter earthquake statistics. The statistics depend on the space-time window of the observational domain, i.e., the response is non ergodic. For some parameters, the results exhibit alternating overall switching of response, from periods of intense seismic activity to periods during which the deformation occurs aseismically and back.

2D and 3D Simulations of Multi-Segment Thrust Rupture

Harold Magistrale and Steve Day
San Diego State University

Geometrical structures, such as fault-plane offsets and bends, can segment fault systems, and may limit the extent of individual earthquake ruptures. Seismological and geological observations suggest that the thrust faults under and nearby the densely populated Los Angeles basin are segmented by sharp bends (lateral ramps) and tear faults that offset the thrust segments. As part of the SCEC Group G effort to address the evolution of seismicity and stress, we evaluate the effectiveness of these offsets in retarding rupture. We use a finite difference method to simulate rupture of segmented thrust faults, in two and three dimensions. An important, and novel, element of the simulations is their incorporation of orthogonal, intersecting faults to model the interaction of the thrust fault segments with an offsetting tear fault. The model has two parallel thrust fault segments, each 10 km in length along strike, offset by various distances, with and without a tear fault present. The direction of tectonic loading (maximum principal stress) is assumed to be horizontal and parallel to the tear fault, so that there are applied shear and normal stresses on the thrust segments, but no direct tectonic load on the tear fault. We varied the initial shear stress conditions and the static frictional strength of the faults, performing simulations for a range of stress drops and values of the strength parameter S. With a tear fault present, rupture can jump offsets of several km (versus only several hundred m without a tear fault). Our simulations are consistent with observations of well documented thrust earthquakes which indicate that, with a tear fault or lateral ramp present, offsets up to 2 km wide usually present little impediment to rupture, and offsets of 2 to 5 km are more significant barriers that may or may not rupture. The segment boundaries of Los Angeles area thrust fault segmentation models are offsets of up to about 5 km; some of the offsets are occupied by lateral ramps and tear faults defined by surface fault traces or seismological observations. For blind thrusts, some of the fault offsets are inferred from offsets in the fold axes above the thrusts, and the presence of lateral ramps and tear faults is uncertain. The simulations indicate that the presence of a tear fault or lateral ramp linking offset thrust fault segments greatly abets multi-segment rupture, so it is critical to accurately characterize the nature of the thrust fault segment offsets.

A Standard Three-Dimensional Seismic Velocity Model For Southern California: Version 1

Harold Magistrale[1], Robert Graves[2], and Robert Clayton[3]
[1]San Diego State University
[2]Woodward-Clyde, Pasadena
[3]California Institute of Technology

A primary task of the 1998 SCEC Science Program is the development of a single standard 3D velocity model capable of supporting strong ground motion simulations, tectonic studies, tomographic imaging, earthquake location, and other research needs. Version 1 of the model fits a range of geological and geophysical observations. It consists of the major populated basins (Los Angeles basin, Ventura basin, San Gabriel Valley, San Fernando Valley, and San Bernardino Valley) embedded in a crust with velocity smoothly varying with depth, over a constant depth Moho. The model is parameterized as a set of objects and rules that are used to generate any 3D mesh of seismic velocity and density values (at length scales appropriate for different uses). The detailed basin portion of the model has over 70 defined surfaces that generally represent lithological interfaces. This parameterization is convenient to store and update as new information (e.g., oil well sonic logs) and verification results become available.

Version 1 of the model will be tested by a variety of waveform modeling, tomographic studies, and new data releases that will provide constraints to be incorporated into Version 2. The model is available on the SCEC Data Center at http://www.scecdc.scec.org.

Probabilistic Seismic Hazard Analysis of Southern California

Mehrdad Mahdyiar
VortexRock Consultants, Inc.

The Phase III report makes important contributions to the practice of seismic hazard analysis in southern California. The Phase III working group, based on the review of the regional earthquake ground motion and site conditions data, has developed a regional site condition map and the related site response amplification factors for seismic hazard analysis. It is the objective of this study to investigate the effects of this new information on the probabilistic seismic hazard analysis (PSHA) of southern California.

The Phase III report defines three site categories, Quaternary (Q), Tertiary (T), and Mesozoic (M), for characterizing site conditions for the PSHA. Each site category is identified by a shear wave velocity for its top 30-m materials. The report provides site response amplification factors for these three site categories as a function of frequency and peak ground acceleration. Specific amplification factors, for long period motions, are also introduced to account for the basin-effects on earthquake ground motions.

The CDMG/USGS fault database for southern California, as is reported on the USGS web-site, is used for the analysis. The model and the PSHA programs are validated by reproducing hazard curves from the CDMG report and the PGA hazard map for the entire region of southern California as is published on the USGS web-site.

Three attenuation equations, as recommended by the working group, are used for the analysis. The SCEC's site amplification factors are reported as correction factors for the Geomatrix rock-site attenuation equation to account for different site conditions. Here, we refer to the modified Geomatrix attenuation equation, based on the SCEC's site amplification values, as Y1 and Y2 equations. The Y2 equation reflects the basin-effects on ground motions and is defined only at 3.0 s period. Sites along three cross sections crossing major faults in southern California are selected for the PSHA. We use spectral acceleration values with 10% probability of exceedance in 50 years to compare and evaluate the results of the PSHA based on different attenuation equations and site condition information.

The results of the analysis are presented by a number of hazard plots over different cross sections. This provides direct comparison between the results of the PSHA based on different attenuation equations and site condition information. The largest differences between the PSHA

results based on the Y1- and generic Geomatrix rock/soil site attenuation equations are observed for 0.3s spectral values for T-site condition category. The Y1 equation calculates about 30% higher SA values based on the Geomatrix soil-site attenuation equation. For the Q-site condition category at 0.1 and 0.3 s periods, Y1 and the generic Geomatrix soil-site equations give rather similar hazard values at most sites. At 1.0 and 3.0 s periods, Y1 equation gives about 25% lower hazard values than the Geomatrix soil-site equation. Including the basin effects for the sites within the basin, i.e. using Y2 attenuation equation, the hazard values at 3.0 s period become rather close to the corresponding Geomatrix soil hazard-values. However, the basin effects in the Y2 equation is depth dependent and at some locations Y2 equation calculates higher, up to 50% higher, SA values than the generic Geomatrix soil-site equation. This is an important consideration for the design of large-scale structures.

Abrahamson/Silva attenuation equation calculates higher ground motion values at sites over the hanging walls of the thrust/reverse faults. The results of this study indicate that the hanging-wall effects at sites close to reverse/thrust faults are significant. The hanging-wall effects are in the same order of magnitude and in cases higher than the site condition effects on the PSHA.

Investigating Earthquakes through Regional Seismicity: http://www.scecdc.scec.org/Module/module.html

John Marquis, Katrin Hafner, and Egill Hauksson
California Institute of Technology

We present version 1.0 of a web-based module for earth science education. With the unifying concept of "The earth is constantly changing", this module has been designed for use both in the classroom (high school and undergraduate levels), as part of an earth-science curriculum, or standalone, for use by the general public interested in a user-friendly resource for basic seismological information. The content and format of this module have been reviewed by scientists and educators alike, and portions of the module have been field tested in high school and community college settings.

Because the module is web based, it is more than just a static educational product. Version 1.0 of the module consists of a single section, entitled "What is an Earthquake?". This section consists of a sequence of text "pages" -- with explanatory maps, diagrams, and other inline images -- hyperlinked to activities, in which students can develop an understanding of the concepts in a more interactive way. Many of these activities are, in turn, linked to separate on-line resources (e.g. fault maps), and interfaces that provide access to seismological data archived at the SCEC Data Center. The ability to learn about earthquakes using a continuously updated storehouse of latest earthquake data provides an educational experience that relates to the "real world".

The modular design of this product allows future sections to be easily appended. A second section, entitled "The Distribution of Earthquakes", will be released at the Fall AGU Meeting in December, and version 2.0 of this module, due in 1999, will include a third section ("Measuring Earthquakes") currently in the planning stage.

Partial Paleoseismic Record of the San Andreas Fault at City Creek, near San Bernardino, California

Sally F. McGill and Dawn Grant
California State University, San Bernardino
Stephen G. Wells
Desert Research Institute, Reno, Nevada

We report here the results from a trench excavated across the San Andreas fault within the flood control channel of City Creek, in Highland, California. The excavation was located just north of Highland Avenue and just east of state Highway 330, about 18 km northeast of downtown San Bernardino. The trench crossed the South Branch of the San Andreas fault zone,

which is the dominant strand of the fault (Sieh and Grant, 1994). Only one well-documented faulting event was visible within the trench. Calibrated radiocarbon dates on two detrital charcoal samples bracket the date of this event to between AD 1020 and AD 1260, although the younger limit on the date of the earthquake is not absolute because the age of any detrital charcoal sample may be older than the layer from which it was collected. Although there were other discontinuities in the stratigraphy, none of them could be clearly associated with faulting. Thus at the City Creek site there is no evidence for any earthquakes younger than AD 1020-1260. This is in striking contrast to the paleoseismic records at Wrightwood and Pitman Canyon, where five and four earthquakes, respectively, have been documented since ~ AD 1450 (Fumal and others, 1993; Seitz and Weldon, 1994). In addition, two faulting events have been documented at Plunge Creek since AD 1325-1410 (McGill and others, 1998; see also Dergham and McGill, this volume). We suspect that at least some of these younger earthquakes did rupture the San Andreas fault at City Creek, but that the evidence for these earthquakes has been destroyed. In the northern half of the trench, the faulted strata have been eroded by a younger channel which was then filled with bouldery gravel. Analysis of aerial photographs indicates that the main strand of the fault may intersect the trench within this younger channel. No faults were visible within the bouldery channel fill, but it is possible that this young channel incised and filled after the most recent earthquake and that it destroyed evidence for faulting events that may have occurred after AD 1020-1260.

Dynamics of a Three-Dimensional Fault-Patch Model of Earthquakes

Seth McGinnis
University of Colorado

We have developed a computer model, suitable for the study of large-scale systems, that can simulate the dynamics of fully three-dimensional earthquake fault systems. In this model, a fault system is composed of patches of dislocation which are allowed to have arbitrary orientation and spatial arrangement, a significant advancement over previous modeling programs which allow only vertical patches as fault elements. The patches interact via 3D elastic stress transfer, rather than simple linear force transfer. When a patch slips, transferred stress is modeled as due to a point source, and the formulations of Okada (1992) for strain due to finite shear dislocation allow us to calculate the compensatory stress resultant on the patch itself.

To compare the fault-patch model with a model whose statistics are known, the initial configuration studied is a regularly-spaced planar set of patches parallel to the free surface of the halfspace. This configuration is dynamically similar to slider-block earthquake models. The fault-patch model shows the expected power-law scaling in the magnitude-frequency relation, but in contrast to other (short-range) models, the cluster of fault elements involved in an earthquake events is, due to the infinite-range interactions, ramified and non-compact. The use of a point-source model for stress transfer speeds computation dramatically.

Future research will study the effects of three-dimensional fault geometry on the dynamical evolution of the model; introducing a single 'fold' into the planar geometry changes the system in such a way that it can no longer be modeled by a simple two-dimensional model. The three-dimensionality of the model will also be studied with structures like the 'Z' (two-fold) and 'Y' (vertical triple-junction) configurations.

Steady, Balanced Rates of Uplift and Denudation in the Santa Monica Mountains, California

Andrew Meigs
Oregon State University

Topographic change in regions of active deformation is a function of rates of uplift and denudation. The rate of topographic development and change of an actively uplifting mountain range, the Santa Monica Mountains, southern California, was assessed using landscape attributes of the present topography, uplift rates, and denudation rates. Landscape features were

characterized through analysis of a digital elevation model (DEM). Uplift rates at time scales ranging from 104 to 106 years were constrained with geologic cross-sections and published estimates. Denudation rate was determined from sediment yield data from debris basins in southern California and from the relief of rivers set into geomorphic surfaces of known age. First-order morphology of the Santa Monica Mountains is set by large-scale along-strike variations in structural geometry. Drainage spacing, drainage geometry, and relief to a lesser extent, are controlled by bedrock strength. Dissection of the range flanks and position of the principal drainage divide are modulated by structural asymmetry and differences in structural relief across the range. Topographic and catchment-scale relief are ~200 to 600 m. Mean denudation rate derived from the sediment yield data and river incision is 0.5 ± 0.3 mm/yr. Uplift rate across the south flank of the range is ~0.5 ± 0.4 mm/yr and across the north flank is 0.24 ± 0.12 mm/yr. At least 1.6 to 2.7 Myr is required to create either the present topographic or catchment-scale relief based on either the mean rates of denudation or uplift.. Although the landscape has had sufficient time to achieve a steady state form, comparison of the time scale of uplift and denudation rate variation with probable landscape response times implies the present topography does not represent the steady state form.

Inverting Fault Zone Trapped Waves with Genetic Algorithms

Andrew J. Michael
United States Geological Survey
Yehuda Ben-Zion
University of Southern California

Fault zone (FZ) trapped waves can help constrain the seismic velocities and attenuation of the rocks in and around the FZ as well as the width of the FZ. We are developing a genetic algorithm inverse approach to extract this information from the waveforms along with realistic confidence bounds. Strong trade-offs between parameters such as FZ width, propagation distance, velocity contrasts, attenuation, and source and receiver location have been observed in sets of synthetic seismograms [Ben-Zion, 1998, JGR]. This creates problems for both forward modeling and traditional optimization methods which genetic algorithms can overcome.

For instance, forward modeling results suggest that these waves can accurately constrain various parameters because small changes in single parameters can make large changes in the synthetic waveforms. With the strong trade-offs between various parameters there may be multiple sets of parameters that yield similar synthetic seismograms, but without a systematic search this will not be completely explored.

Using an inverse method allows us to test a wider variety of models in an objective manner and develop confidence bounds on the best result. We quantify the fit function as the correlation coefficient between the observed and synthetic waveforms. Synthetics are computed with a generalized version of the solution of Ben-Zion and Aki [1990, BSSA] for a scalar wavefield in a structure consisting of two FZ layers between two quarter spaces. A grid search inversion shows that good fits can be obtained for a wide range of values in any one parameter by varying the other parameters. Thus, the strong trade-offs between parameters do undermine the forward modeling results as expected. The grid search results also reveal that the correlation coefficient is a complex function of the fault zone parameters. This creates problems for traditional optimization techniques.

While a grid search is a very systematic exploration of the parameter space, genetic algorithms are more computationally efficient because less time is spent on models with poor fits. The genetic algorithm also maintains a population of models and thus provides information about a large set of acceptable models that can be used to infer the confidence bounds on the best model. To decide which models belong inside a particular confidence level requires knowing how noise affects the correlation coefficients. Most of the "noise" in the fault zone trapped phases are actually the signal of other seismic phases. Thus, we will use observed seismograms without fault zone trapped waves to provide a model of noise.

Structural Analysis of Active Fault-Related Folds in the Elysian Park and Puente Hills Blind Thrust Systems, Eastern LA Basin

Karl J. Mueller[1], Robert E. Crippen[2], and Mike Oskin[3]
[1]University of Colorado, [2]Jet Propulsion Laboratory
[3]California Institute of Technology

We combine digital elevation models and structural analysis using wireline logs to define the geometry of blind thrust segments and surficial fault-related folds in the Coyote oilfields, eastern LA Basin and in the Boyle Heights area, northeast LA Basin. The south-vergent blind faults which drive uplift of the Coyote folds are interpreted as part of the Puente Hills blind thrust system, and comprise a segment which lies adjacent to the rupture associated with the 1987 M 6.0 Whittier Narrows earthquake.

Our analysis indicates the blind thrusts underlying Coyote dip ~ 25 degrees at depth where they accommodate partitioned shortening across the transpressive Whittier fault. Steeper updip segments of the blind thrusts dip 45-70 degrees where they are associated with fault-related folding in the Coyote oilfields. A west-facing tear fault imaged at the ground surface using anaglyphs created from a digital elevation model is interpreted as a possible segment boundary between the west and east Coyote structures. We model west Coyote as a fault-bend fold based on the dip of pregrowth strata in its forelimb, stratigraphic architecture in the upper Fernando Formation and the morphology of folded sediments at the surface. We argue that the structures at Coyote are a potential source for M6.0 Whittier Narrows-sized earthquakes in the densely urbanized eastern Los Angeles Basin. Our ongoing efforts are aimed at a more complete subsurface stuctural mapping program, in addition to identification of the ages of young deposits deformed in the folds. These data hold the potential to quantify rates of shortening across these active blind thrusts, in addition to guiding analyses of strong ground motions for scenario earthquake studies.

For work funded by SCEC in east Los Angeles, we present revised cross sections tied to mapping of late Quaternary deposits folded at the surface. Our structural analysis indicates these steeply dipping faults collectively accommodate shortening across the monoclinal south-facing limb of the Elysian Park Anticline. At least one structure is a candidate for reactivation of a Neogene normal fault based on thickness changes in the Miocene section. Little evidence for lateral propagation of the surficial fault-related folds supports this idea. Shortening across east LA has evolved as a southward propagating thrust belt, buttressed against the strike slip Santa Monica and Raymond faults to the north. Ongoing map view reconstructions and evidence for west to east younging of the onset of shortening is used to assess the role of lateral "escape" along strike slip faults in lengthening the Elysian "thrust belt".

A Preliminary Evaluation of the Maximum Depth of Earthquakes in Southern California

Julie J. Nazareth and Egill Hauksson
California Institute of Technology

The significant variations in the maximum depth of small earthquakes in southern California reflects the lithological and tectonic complexity of the crust of the region. We wish to understand what geophysical and geological conditions influence the maximum depth of seismicity in the hope that these relationships will provide constraints for the depth of the brittle-ductile transition beneath southern California. As a starting point, we investigate the maximum depth of earthquakes regionally, and locally along the major faults in southern California.

We use earthquakes recorded by the Southern California Seismic Network (SCSN) between 1991 and 1998. Hypocenters are located using a 3-d velocity model, and are sorted into bins. Regional bins are 1 degree by 1 degree in latitude and longitude, and are constructed without reference to the location of faults or other geological features. Local bins are constructed by projecting earthquakes from 5 km on either side of the fault. The bins are classified as deep,

intermediate, or shallow. Depth values greater than 15 km are considered deep, with intermediate values between 10 and 15 km, and shallow as less than 10 km. We define the maximum depth of earthquakes in a bin as the depth above which 95% of earthquakes occur (the 95% depth).

Regions with the 95% depth considered deep are in general characterized by compressional tectonics and rapid rates of sedimentation. The intermediate 95% depth classification covers much of southern California. Most of these areas are within major stable tectonic blocks and include the major strike-slip faults. Parts of the San Jacinto fault in the northeastern Peninsular Ranges is an exception, having deep 95% depths in a strike-slip regime. The 95% depth is shallow for the Salton Sea and the Brawley Seismic Zone, consistent with the unusually high heat flow in that region.

Time-Delayed Fracture Criterion for Burridge-Knopoff Model

Xiao-xi Ni and Leon Knopoff
University of California, Los Angeles

When a mass fails in the conventional Burridge-Knopoff model, it transmits stress its adjacent neighbors immediately. On a fault where the stress is at a critical stage everywhere along the fault, infinite velocities of rupture propagation can occur which is evidently unrealistic for real media. We introduce a time-delayed fracture criterion for the Burridge-Knopoff model which guarantees that the velocity of the rupture front is less than or equal to the speed of sound. The new fracture criterion is used to test against a case problem which yields an analytical solution. The numerical simulation from the Burridge-Knopoff model shows considerable oscillations in particle velocity close to the tip of the crack. The oscillation is attributed to the discontinuity of dislocation at the crack tip. A damping term is introduced in the model to eliminate the oscillations at the tip of the crack; the effects of the damping have a scale size that is short compared with the lattice spacing. The physics of the viscosity shows that it is equivalent to a strength-weakening property and hence that such weakening can damp out lattice oscillations. Numerical simulations with the Burridge-Knopoff model fits an analytical solution well. Results show that there are more large events in the case with the new fracture criterion than with the old fracture criterion.

Resolution of Site Response Issues in the Northridge Earthquake (ROSRINE): Progress Report

Robert Nigbor[1], Robert Pyke[2], Cliff Roblee[3], John Schneider[4], Walt Silva[5]
[1]Agbabian and Associates
[2]Consultant
[3]California Department of Transportation
[4]Impact Forecasting
[5]Pacific Engineering and Analysis

ROSRINE is a collaborative research project ultimately focused on improving engineering models for estimation of earthquake ground motions. The central component of this project is the collection, synthesis, and dissemination of high quality subsurface data obtained primarily from sites that recorded strong ground shaking during the 1994 Northridge Earthquake.

To date 42 sites have been investigated. Results are available on the project web site (http://rccgo1.usc.edu/Rosrine. These include geologic logs, P- and S-wave velocity profiles, electric logs, and laboratory testing results for selected soil samples. Results show that many of the sites have been previously misclassified.

Ultimately these synthesized data will be used to constrain a program of ground-response analyses focused on evaluating the contributions of source, path, and site parameters on the variability of observed ground motions.

3-D Simulation of Asymmetric Ground Motion from Dipping Faults

David D. Oglesby, Ralph J. Archuleta, and Stefan B. Nielsen
University of California, Santa Barbara

Due to the asymmetric geometry of dipping faults, dynamic simulations of earthquakes on such faults produce asymmetric ground motion near the fault. The ground motion from a thrust/reverse fault is larger than that of a normal fault by a factor up to two or more, given identical initial stress magnitudes. A strike-slip fault with the same stress magnitude will have ground motion in between these two extremes. In all three types of earthquake, the motion of the hanging wall is larger than that of the footwall. The asymmetry between normal and thrust/reverse faults results from time-dependent normal stress caused by the interaction of the earthquake-generated stress field with the earth's free surface. The asymmetry between hanging wall and footwall results from the asymmetric mass and geometry on the two sides of the fault.

Velocity Structure of the LA region at Differing Spatial Granularity: Contributions to the Group D 3-D Velocity Project

David Okaya, Nicola Godfrey, Tracy Pattelena, and Thomas Henyey
University of Southern California

We contribute the following velocity information to the Group D regional velocity volume:

(a) 2-D velocity slices at 1 km pixel resolution along the LARSE transects;

(b) 2-D velocities at 50 m pixel resolution of the shallow surface above the Northridge epicenter from industry seismic data;

(c) 1-D velocities from sonic wells in the San Fernando valley.

The LARSE seismic transects do not have a rich series of crustal phases due to the diminished signal-noise ratio of urban LA. This has required us to develop additional algorithms of velocity adjustment consistent with the velocity inversion method of Hole (1992). A similar approach was used for refraction arrivals which are present in the raw data of the industry reflection profiles in the Northridge epicentral region of San Fernando Valley. Within this SCEC Summer Internship project, Vp and one example of Vs structure was obtained for three 12 km-long slices to depths of 500 m at a resolution of 50 m. The calculated Poisson's and Vp/Vs ratios differ with geological structure. Well logs in this region for which we have sonic logs provide 1-D (spot) velocity-depth information which are consistent with the high resolution velocity results. A related study in collaboration with Tom Wright will provide the geometrical shape of the western SF basin; the above velocity information can be used to define a velocity structure for the basin.

2-D and 3-D Amplification Effects in Santa Monica, California

Kim B. Olsen and Carmen M. Alex
University of California, Santa Barbara

We used finite-difference simulations of 10-Hz P-SV and SH waves to estimate the contribution from the deep basin structure to the large ground motion amplification in Santa Monica, California, observed for seismic waves incident from the north. Our simulations of a 17-km deep Northridge aftershock with epicenter 30 km north of Santa Monica show that focusing at the lens-shaped boundary of the sediments can only account for less than half the amplification observed in the area that was heavily damaged during the 1994 M 6.7 Northridge earthquake. The focusing in the simulations caused amplification of up to 1.6 times in a zone 0.65-2.4 km south of the Santa Monica fault and de-amplification at sites just south of the fault where some of the largest amplification is observed in the data. These results suggest that features omitted in the modeling, namely shallow basin edge effects and reverberations in the

near-surface low-velocity sediments account for a significant part of the anomalous amplification in Santa Monica.

We correlate the location of red-tagged buildings in Santa Monica after the Northridge earthquake with the underlying basin structure using isosurfaces of the 3-D model developed by Magistrale et al. The red-tagged buildings are primarily located above the deepest part of the basin, just south of the Santa Monica fault. We use this model and a finite-fault realization of the 2-rake, 3-window slip distribution of the Northridge earthquake by Wald et al. (1996) to estimate the contribution to the amplification from focusing at the lens-shaped boundary of the sediments in three dimensions.

Modeling Dynamic Rupture in a 3D Earthquake Fault Model

Kim B. Olsen[1], Raul Madariaga[2], and Stefan Nielsen[1]
[1]University of California, Santa Barbara
[2]Ecole Normale Superieure, Paris

We have developed a 4th-order 3D staggered-grid finite-difference method with a novel implementation of boundary conditions on the fault capable of modeling any general friction law, including slip-weakening and rate-dependence, for spontaneous rupture propagation along an arbitrarily loaded planar fault. Our results show a simple scaling of the rupture as a function of slip-weakening distance, asperity size, and grid size. The degree of resolution improves as the slip weakening distance increases, and we find that numerical simulations are stable and reproducible for slip weakening distances larger than about 4 in non-dimensional form. Rupture is controlled by a non-dimensional number which is a function of a characteristic length, the stress load, and the energy release rate on the fault. An essential requirement for rupture to grow beyond the asperity is that this non-dimensional number is larger than a critical value. For smaller values rupture does not grow beyond the initial asperity. For larger values rupture grows indefinitely at increasing speed. This is a simple example of a pitch-fork bifurcation, with one complication: if the parameter is larger than 1.3 times the critical values the rupture front in the in-plane direction jumps ahead to speeds higher that the shear wave speed. The rupture front acquires an elliptical shape elongated along the in-plane direction. This result explains why only a narrow range of the slip weakening distance (near 0.5 m) and the yield stress (near 120 bars) was found to generate dynamic ruptures with synthetics resembling data for the 1992 Landers earthquake (Olsen et al., 1997).

We have also implemented a dipping free surface boundary condition in the 3-D finite-difference method, which we use to simulate the 1994 Northridge earthquake. The simulation uses the 1-D crustal model by and prestress distribution computed from the slip inversion study by Wald et al. (1996).

The Quaternary Fault Structure of a Left-Stepover Within the San Jacinto Fault Zone, Riverside County, California

Nate W. Onderdonk
University of California, Santa Barbara

Detailed mapping of a segment of the San Jacinto fault zone has revealed a previously unmapped left-step fault structure at the juncture of the Hot springs fault and the Claremont fault. The recognition of additional faults and geologic relationships indicate that older interpretations of the Hot Springs fault splaying off the Claremont fault are incorrect. The new mapping describes a left-step structure which is represented by the local geomorphic expression, faulting style, and fault geometry. The sharply elevated area between the Hot Springs fault and the Claremont fault provides striking geomorphic evidence of shortening and uplift within the left-step, and geologic relationships indicate at least 2,000 feet of uplift has occurred in the past one million years. The two main types of deformation structures present include thrust faults and folds striking approximately east-west at the boundaries of the uplifted area, and strike-slip faults

which strike northwest. These faults fit simple-shear models both in orientation and fault type. This new mapping of the juncture between the Hot Springs fault and the Claremont fault presents a more complete view of the structure of this seismically active area and may contribute to a better assessment of possible earthquake hazards.

Active Parasitic Folds on the Elysian Park Anticline, Los Angeles, California: Implications for Seismic Hazard in Central Los Angeles

Michael Oskin and Kerry Sieh
California Institute of Technology

We characterize the seismic hazard of the Elysian Park fault, a blind reverse fault beneath central Los Angeles, by analysis of the Elysian Park anticline, which overlies it. New shallow-subsurface geotechnical data, combined with other surficial stratigraphy and geomorphology reveal that the Elysian Park anticline is an active, 20-km-long structure. From their style and rates of deformation, we estimate a contraction rate of 0.8 ± 0.2 mm/yr for parasitic folds on the southern limb of the anticline. This rate provides a basis for estimating a rate of contraction of the entire Elysian Park anticline, which, in turn allows us to estimate a 1.1 ± 0.3 mm/yr rate of slip on the underlying fault. At this rate of slip, rupture of the Elysian Park fault could produce a nominal Mw 6.5 to 6.8 earthquake every 1000 to 4000 years, on average. Although this nominal Elysian Park earthquake recurs infrequently, its size and recurrence interval are similar to those determined for the sources of the destructive 1971 San Fernando and 1994 Northridge earthquakes.

Near Fault Ground Motion Simulation Using the Hybrid Green's Function Method

Arben Pitarka[1], Paul Somerville[1], Robert Graves[1], Katsuhiro Kamae[2], and Kojiro Irikura[2]
[1]Woodward-Clyde, Pasadena
[2]Disaster Prevention Research Institute, Kyoto

The Green's function methods using either empirical or synthetic Green's functions have been used extensively to model or simulate high-frequency strong ground motion from large earthquakes. The recently proposed hybrid Green's function method has been also tested against near-fault broad-band ground motion data. The tests have shown that the technique should be improved in order to better represent the effect of the radiation pattern in the intermediate (1-3 Hz) and high (> 3 Hz) frequency ranges. We implemented a technique that generates a frequency dependent radiation pattern of S-waves based on theoretical and average radiation coefficients calculated for the low and high frequencies, respectively. By this technique the effect of the radiation pattern gradually becomes random at high frequencies. We will show results of comparisons between the Hybrid Green's function method modified for the frequency-dependent radiation pattern effect and the Green's function method that uses an empirical representation of the radiation pattern. We also will show comparisons of simulated and recorded broadband near-fault ground motion from Kobe earthquake.

Broadband Seismic Data from TriNet and TERRAscope

Jascha Polet and Egill Hauksson
California Institute of Technology

The TriNet network (including TERRAscope) currently consists of over 60 stations with broadband and strong motion sensors. An additional 30 stations have strong motion sensors only. Continuous broadband data for all STS-1 and STS-2 sensors are archived and sent to the IRIS/DMC data center as part of the continuous TERRAscope data set. These data will be

available on-line from the SCEC/DC when it upgrades to the new Oracle database. At present the SCEC data center archives triggered broadband, long period, short period and strong motion data for local as well as teleseismic events. We will show examples of TriNet data for both kinds of events. Quality control for the TriNet stations involves checking the polarity of all channels with the help of teleseismic signals and an analysis of the overall noise level. Currently under development is a cross-correlator code, which will compare teleseismic P-waves across the network and should be useful for analysis of timing problems as well as data quality and the computation of noise spectra for all stations.

Implementing California's Seismic Hazard Mapping Act in Portions of Los Angeles, Ventura, and Orange County, California

C. Real, A. Barrows, M. DeLisle, T. McCrink, M. Petersen, M. Reichle, and T. Smith
California Department of Conservation, Division of Mines and Geology

With support from FEMA, California's Seismic Hazard Mapping Program has completed a three-year seismic zonation project covering portions of Los Angeles, Ventura, and Orange counties. "Zones of Required Investigation" for areas having a potential for liquefaction or landslides, were designated for 39 7.5 minute quadrangles covering approximately 6,200 square kilometers of land. Although most of the land is already urbanized, new construction volume is high due to infill and redevelopment. California law requires that proposed projects located within seismic hazard zones have a geotechnical investigation at the project site that validates the level of hazard, and recommends appropriate countermeasures in order to obtain a permit for construction. Program staff has met with over 100 affected jurisdictions to discuss the purpose of the maps, their basis, and legal requirements for implementation. "Guidelines for Evaluating and Mitigating Seismic Hazards in California" were published, and a three-day course on "Evaluation and Mitigation of Seismic Hazards", co-sponsored by UC Berkeley and the SCEC, was presented to local regulators. UC Berkeley repeated the course for the geotechnical consulting industry in the Los Angeles and San Francisco Bay regions. SCEC helped form an "Implementation Committee", representing the six-county southern California region, to recommend detailed procedures that will assist local agencies with implementing the state guidelines. These efforts are expected to raise the quality of standard geotechnical practice with regard to earthquake hazards in California.

Several new data sets have, or will soon, become available as a result of the seismic zonation program. CDMG partnered with the USGS to assess the ground shaking potential, building on the SCEC hazard model for the region. Collaboration with the USGS' Southern California Areal Mapping Program resulted in a new generation of 7.5 minute geologic quadrangles for the project area. These maps include more detailed differentiation of Quaternary units for purposes of assessing earthquake hazards. Level-II 10-meter digital elevation models were obtained from the USGS, and were updated to reflect modern topography in urbanized areas using photogrammetric and radar-derived elevation measurements provided by NASA/JPL. In addition, assessment of regional liquefaction potential resulted in a digital database containing over 10,000 geotechnical borehole logs. Work is currently underway to make all of these data sets accessible over the Internet.

Relocating the Southern California Seismic Catalog Using the L1-norm and Source Specific Station Terms

Keith Richards-Dinger and Peter Shearer
University of California, San Diego

We relocate over 300,000 earthquakes recorded by the Southern California Seismic Network (SCSN) between 1981 and 1997 using an L1-norm, grid-search approach on a smooth 1-D velocity model. Predicted travel times from each of the >200 stations of the network are

precomputed to a grid of points covering the region to a depth of 30 km with a 2 km spacing between adjacent points. Events are located by searching for the grid point that minimizes the L1-norm misfit to the archived P and S picks obtained by the network analysts. To achieve finer resolution we use cubic interpolation of travel times between grid points. Station terms are incorporated into the location procedure in several stages. First, we relocate a spatially distributed, well-recorded set of 5,200 events, iterating several times to obtain a stable set of hypocenters and station terms for these events. In this case the station terms are simply the median of the residuals at each station. Next, we relocate the entire catalog of >300,000 events using these station terms. The resulting locations exhibit greater clustering and coherence than the original SCSN catalog locations. The station terms in this case compensate for velocity differences in the shallow crust below each station, but cannot account for more complicated three-dimensional velocity structure. Finally, we allow the station terms to vary as a function of source location in the following way: we calculate a separate correction for each source-receiver pair as the median of the residuals from the source's 50 nearest neighbors (as determined by a Delaunay tessellation) to the station. Again, we perform several iterations of hypocenter relocation and station term estimation. This technique achieves relative location accuracy comparable to master event methods for large distributed areas of seismicity. Our final locations exhibit much greater clustering and coherence than the original SCSN catalog locations, permitting better delineation of fault structures in southern California.

Crust and Mantle Structure Beneath the San Gabriel Mountains: Preliminary Constraints from Topography, Gravity, and Seismic Data along LARSE Line 1

Mousumi Roy
University of New Mexico
Robert W. Clayton
California Institute of Technology

The San Gabriel mountains are an east-trending belt of high topography in the central Transverse Ranges, southern California. Crust and mantle structure beneath the mountains and compensation mechanisms for high topography in this region are not well understood. In this study we present a preliminary 2-D analysis of topography, gravity, depth-to-Moho, and seismic velocities obtained in a profile across the San Gabriel mountains, along LARSE line 1. We use an empirical relation to convert Vp obtained from a crustal tomographic model to density within the crust. From this, we infer the local density structure in the Los Angeles basin and beneath the San Gabriel mountains and southern Mojave desert. We then use our crustal density model, together with seismically measured Moho depths and gravity data, to investigate the implications of simple local and regional compensation models of the San Gabriel mountains.

Analysis of Simulated Ground Motion Parameters Produced by a Simultaneous Rupture of the Hollywood and Santa Monica Faults due to a M_w 7 Earthquake on Each Fault

Chandan K. Saikia and Paul G. Somerville
Woodward-Clyde, Pasadena,

We have simulated ground motion time histories at eighteen urban centers with tall buildings (8 to 54 stories) located along the Santa Monica Mountain fault systems for earthquakes occurring on the Hollywood and Santa Monica faults. These urban centers include many sites in Los Angeles, Westwood, Beverly Hills, Glendale, Sherman Oaks and Santa Monica where the CSMIP strong motion stations are also located. These simulated ground motions include both long-period and short-period motions. Long-period motions are deterministic and short-period motions are stochastic. Time histories are simulated for earthquakes of magnitude Mw of 7 ($Mo=3.4x10^{26}$ dyne-cm) on each fault with 52 km x 18 km dimensions for 9 hypocenters using 10 randomly generated slip models. The Hollywood fault is a shallow fault coming to a depth of 0.4 km and has a dip of 70 deg and a strike of 257.5 deg.

Its rake is 5 deg. The Santa Monica fault strikes at 266 deg and has a shallow dip angle (20 deg). The rake of this fault is 90 deg. We have simulated time histories for these two earthquakes separately. We used a velocity model which is includes layers having the velocities comparable to the basin materials. Our presentation will illustrate statistical variations of these ground motions due to different rupture directivity scenarios including a scenario involving a simultaneous rupture of the two faults.

Seismological Observation of Discrete Hierarchical Fractal Structures in the San Andreas Fault Zone at Parkfield, California

Charles G. Sammis[1], Robert Nadeau[2], and Lane Johnson[2]
[1]University of Southern California
[2]University of California, Berkeley

A recent study of repeating earthquakes on the San Andreas fault in central California by Nadeau and Johnson [1998] found that the smallest events occurred on patches having a linear dimension on the order of 0.5 m., displacements of about 2 cm. and stress drops on the order of 2000 MPa, roughly ten times larger than rock strengths measured in the laboratory. The stress drop for larger events was observed to decrease as a power law of the seismic moment reaching the commonly observed value of 10 MPa at about magnitude 6. These large strengths are shown here to be consistent with laboratory data if the preexisting microcracks are all healed. A hierarchical fractal asperity model is presented which is based on recent laboratory observations of contact distributions in sliding friction experiments. For this model, a fractal dimension of D=1.0 is shown to be consistent with the observed power law decrease in stress drop and increase in displacement with increasing event size. The spatial distribution of hypocenters in the Parkfield area is shown to be consistent with this model, and with a hierarchical clustering of asperities having a discrete rescaling factor of about 20. This rescaling factor is consistent with the change in scale observed during shear localization in granular layers in the laboratory.

Earthquake Depth Estimation

Brian Savage and Don Helmberger
California Institute of Technology

Recent source depth determinations using TERRAscope data are not always consistent with those reported in the SCSN catalog. For a population of over 300 events, SCSN reports an average depth of 5.6 ± 4.4 km, while those from waveform modeling yield depths of 11.9 ± 3.7 km. The discrepancy in depth could be due to a bias in either because of the tradeoff between origin time and depth (SCSN) and inadequacy of shallow Green's functions (modeling). Since the nearest station plays a crucial role in SCSN's determination, S-P travel times, we have initiated a program to systematically model the nearest Tri-Net station assuming local models.

In this preliminary stage, we have constructed a library of plausible models and searched through their associated synthetics to best match the waveform data. We assume the event location and mechanism are known and estimate depth and source durations of the P and SH pulses. Example applications of this approach will be presented where it appears that the phase SP is commonly misidentified as S, which can lead to shallow depth estimates in SCSN reports.

Southern California Earthquake Center Crustal Deformation Velocity Map V2.0

SCEC Crustal Deformation Working Group*
*contact: Zheng-kang Shen, Dept. of Earth and Space Sciences, UCLA

The Crustal Deformation Working Group of SCEC recently released its crustal deformation velocity map v2.0 (http://www.scecdc.scec.org/group_e/release.v2). The new solution results from an analysis of nearly all of the EDM, VLBI, and SCEC archived GPS data acquired for southern California between 1970 and 1997. The map and accompanying table include 363 stations for which the uncertainty in horizontal velocity is less than 5 mm/yr. For

stations close to the Landers epicenter, we have provided estimates of both the pre- and post-Landers velocities.

The most important differences between Release 2.0 and Release 1.0 (October 1996) are the direct use of the VLBI data and the addition of GPS data from continuous observations since 1992, post-Landers surveys of the epicentral region, a 1992 survey of about 60 stations in and around the Los Angeles basin, and a 1997 resurvey of about 60 stations in the southern San Andreas system. These additions have added 76 stations to the map and have reduced 2/3 of the station velocity uncertainties to about 1 mm/yr.

The Importance of Pretreatment in High Resolution C-14 Dated Paleoseismic Sites Along the Southern San Andreas Fault, California

G. G. Seitz[1], R. M. Langridge[1], Thomas E. Fumal[2], and Ray J. Weldon II[1]
[1]University of Oregon
[2]United States Geological Survey, Menlo Park

C-14 dated peat-bearing stratigraphic sections along the southern San Andreas Fault (SAF) provide the highest age resolution of long earthquake event series, and for this reason have been extensively studied. While most C-14 dates at the 3 best-dated sites, Pallett Creek (75 samples), Wrightwood (80), and Pitman Canyon (26) are stratigraphically consistent and provide temporal resolution with precision of 20 to 50 years, about 1/3 of the dates are stratigraphically and temporally inconsistent (bad) with the consistent (good) dates. We have discovered that the principal cause of bad dates is sample pretreatment. Essentially all of the bad dates received acid/alkali/acid (AAA) pretreatment, whereas the good ones are made up mainly of samples with acid only (AO) pretreatment and a small fraction of the AAA treated samples.

The presence of visible detrital material in the sections and the fact that most bad samples are too old, suggest that AAA removes the in situ organic material, leaving a residue rich in detrital material. However, a few of the AAA samples are too young, and two dates on plant matter picked out of peats are too young, so AAA pretreatment can also produce anomalously young ages, probably in layers rich in younger roots. Because AO chemically removes the fulvic acid component (that makes up about 20% of the organic material) and the AAA pretreatment also removes the humic acid (that makes up about 60%), the AO samples may produce consistent results because there is enough humic acid to mask whatever insoluble residue is in the sample (in some cases much of the insoluble residue is physically removed in a AO treatment).

These results suggest that 1) it is very important to pay attention to how samples from these kinds of sites are pretreated, 2) that pretreatment must be reported so that the dates can be evaluated and consistently compared between sites, and 3) that dating of a particular organic fraction (almost certainly the humic acid) may produce even more consistent and precise dates for these sites.

New Methods of Defining Concealed Earthquake Sources: Applications to the Southern Puente Hills and Oceanside Blind-Thrust Systems, Los Angeles

John H. Shaw[1], Peter M. Shearer[2], Karl J. Mueller[3], and Carlos Rivero[1]
[1]Harvard University,
[2]University of California, San Diego
[3]University of Colorado

We combine industry seismic reflection profiles, well data, precisely relocated seismicity, and paleoseismic investigations to define active blind faults in Los Angeles. Damages exceeding $35 billion from the 1994 Northridge (M 6.7) earthquake, combined with recent evidence of larger (M 7+) events in the geologic record, have focused attention on the hazards posed by thrust faults to this region. We offer compelling images of active blind-thrust faults beneath the metropolitan, linking precisely located earthquakes, direct fault images, and near-surface folds that characterize deformation above blind thrusts. The Puente Hills blind-thrust system is imaged

in seismic reflection profiles and expressed at the surface by anticlines forming the Santa Fe Springs and Coyote Hills. We demonstrate that a segment of this fault caused the 1987 Whittier Narrows (M 6.0) earthquake by precisely relocating the earthquake mainshock and aftershocks using waveform cross-correlation techniques with new station correction terms and velocity control from wells. These revised locations are coincident with the projection to depth of the fault-plane imaged in reflection profiles, offering a compelling linkage between the Puente Hills blind thrust and the earthquake. The Whittier Narrows earthquake ruptured less than 10% of the total area of the Puente Hills thrust system, and thus remaining fault segments could generate much larger earthquakes (M 6.5-7.0+).

In offshore and coastal Orange County, we demonstrate that a large normal fault (the Oceanside detachment) has been reactivated as a blind thrust. The gently east-dipping Oceanside fault is imaged in reflection profiles, and produces contractional folds that deform the seafloor. Back-thrusts above the Oceanside detachment form asymmetric, northeast vergent anticlines along the coast, including structure of the San Joaquin Hills. Recent SCEC-sponsored studies in the San Joaquin Hills proposed that an active blind thrust, with an inferred southwest dip, lays beneath this region. Our results support the existence of this fault. However, we suggest that the inferred southwest-dipping fault is limited to the upper 3 or 4 km of the crust, below which it roots into the gently east-dipping Oceanside thrust forming a structural wedge. This implies that the Oceanside thrust, which appears to extend deep into the crust, is an active and potentially important earthquake source beneath Orange County.

Los Angeles Physics Teachers Alliance Group (LAPTAG) Seismograph Project

Gerry Simila
California State, Northridge
Walter Gekelman
University of Southern California

LAPTAG is an alliance of over 20 high schools, and one of their science projects involves an inexpensive PC-based seismometer. A 10 school network has been established. The goal of this project is to teach students how science is conducted in teams. The student earthquake data files are transferred and combined at UCLA (http://coke.physics.ucla.edu/laptag). A review of last years student projects is presented.

SCEC Borehole Instrumentation Initiative

Jamison Steidl and Ralph Archuleta
University of California, Santa Barbara

The variability of observed ground motion and damage patterns over short distances produces a large degree of uncertainty in our ability to predict shaking from future earthquakes. Part of the variability is caused by the local near-surface site conditions. Installing borehole instrumentation below the surface soil layers allows us to remove the near-surface site effect at a few select stations. These borehole stations produce data that has not been distorted by the effect of the surface materials. This will allow for direct estimation of site effects and provide a test for the calibration and improvement of physical models of soil response. It will also give us a much clearer picture of the incident ground motion, which can be used to study the earthquake source process and the regional crustal structure in more detail. In addition the borehole data can be used as empirical Green's functions (the input motion) for predicting ground shaking at surface sites in the region surrounding the borehole station.

This marks the second year of the SCEC borehole instrumentation initiative. The long-term objective of this project is to instrument three borehole sites per year in the Los Angeles region. Currently five sites have been selected and are now in the final stages of deployment. All five of the sites have been drilled, logged for wave velocity, and cased for deployment of the

downhole instrumentation package. The five sites include: 1) Stone Canyon Reservoir, 2) Wonderland Avenue School in Laurel Canyon, 3) Mira Catalina School in Palos Verdes, 4) Griffith Park Observatory, and 5) Obregon Park. Collaboration and cost sharing between the ROSRINE project, the Caltech/USGS seismic network, and CDMG's strong motion instrumentation program have helped make this project a success. Data from the Griffith Park Observatory station is already being provided in real-time to the Caltech/USGS Southern California Seismic Network (SCSN) and is being stored online at the SCEC data center. The other four stations should be online before the end of 1998.

Fault Zone Geometry and Historic Displacement Along the Cholame Segment of the San Andreas Fault, Southern California

Elizabeth M. Stone[1], J. Ramon Arrowsmith[1], Dallas D. Rhodes[2], and Lisa B. Grant[3]
[1]Arizona State University
[2]Georgia Southern University
[3]University of California, Irvine

The Cholame segment of the San Andreas Fault (SAF) is the transitional zone between the Parkfield segment to the north (containing both creeping and locked zones) and the locked Carrizo segment on its southern end. Unlike both the Parkfield and Carrizo segments, where the SAF is typically a single well defined trace, the geometry of Cholame segment fault strands is variable on a kilometer scale.

Starting at SW 1/4, sec 22, T28S, R18E for a distance of 2 km southeast, the fault zone contains two parallel recently active strands. Along the next 2 km stretch farther to the southeast, the fault zone contains only one active but discontinuous strand, each trace of which strikes up to 10 degrees from the trend of the SAF, and is <1 km in length. The next 1 km to the southeast, the scarps are less sharp and the fault zone is characterized by alternating en echelon highs and lows approximately 40 m long, 20 m wide, and 2 m high adjacent to the fault. The fault zone becomes even more subdued for the next km where there is no surficial evidence for an active trace. This area is characterized by linear valleys and sag ponds. In some locations, up to five valleys occupy the width of the fault.

Preliminary analysis of data from 1855 and subsequent surveys in several locations across the SAF indicate that several meters displacement occurred in 1857 over a 1.6 km-wide zone spanning the Cholame segment. There are large uncertainties in the reliability and precision of the measurements. Additional analysis and paleoseismic data are needed to reduce the uncertainty. Mapping along the central Cholame segment has yielded three possible sites for paleoseismic trenching and measurement of offset. All three sites are located on active alluvial fans emanating from the Temblor Range. Alluvial deposits at Bitterwater Canyon interfinger with fluvial sediments from Bitterwater Creek. The Las Yeguas fan terminates in a poorly drained depression that may have accumulated peat. The southern Cholame site is at the proximal end of a fan and therefore should only contain its alluvial deposits. Paleoseismic and structural data collected on this segment will allow better characterization of the earthquake potential of the central San Andreas fault zone.

Study of Weak and Strong Ground Motion Including Nonlinearity From the Northridge, California, Earthquake Sequence

Feng Su, John G. Anderson and Yuehua Zeng
University of Nevada, Reno

This paper presents a new method to estimate S-wave site response relative to a regional layered crustal model. The method is useful for site specific strong motion prediction since the estimated site response functions are referenced to an idealized regional layered model for which we know the ground response exactly. We applied this method to the Northridge earthquake sequence. We determined the site amplifications, from aftershocks with magnitudes 2.6 to 4.3,

at 21 stations which were co-located with strong motion stations. These site response functions were then used to modify synthetic seismogram calculated for the Northridge mainshock in the same regional layered crustal model and thus obtain site-specific ground motion estimates. These site specific synthetic seismograms have higher correlation to observations in comparison to the synthetic seismograms without weak motion site correction. They have similar amplitude and frequency content to the observations, especially at sites with recorded peak ground accelerations below 0.3g. At sites with larger ground motions, however, this approach overestimates the strong motion. The differences are made clear when we estimate site response functions from the strong motion records and compare them with those from weak motion records. We express the differences as the average ratio of the weak to strong motion site response (AWS Ratio). When the ground motion is low, the AWS Ratio is near unity, indicating that the weak and strong motion site responses agree with each other within the uncertainty. However, The AWS Ratio increases as the ground motion amplitude increases. The difference in weak and strong motion site responses becomes significant at stations where peak acceleration was above 0.3g, peak velocity was above 20 cm/sec, or peak strain was above 0.06% during the mainshock. This result demonstrate directly from the ground motion observations the relationship between nonlinear site response and peak ground motion parameters. The nonlinearity is present on soft rock sites as well as on sediment sites.

Seismic Velocity Structure Derived from Sonic Logs and Industry Reflection Data in the Los Angeles Basin, California

M. Peter Suess and John H. Shaw
Harvard University

We describe seismic velocities in the Los Angeles basin using a database of more than 150 sonic logs, check-shot surveys, and 5000 stacking velocity measurements from industry reflection profiles. These formerly proprietary data offer extremely precise and accurate measures of P-wave velocities. We present our results in the form of empirical depth/velocity relations for Tertiary stratigraphic units in the basin, along with 1-D velocity functions at various locations in the basin, including the positions of four Southern California Seismic Network (SCSN) stations. In SCEC-related efforts, these new velocity data have been used to: 1) precisely relocate seismicity using waveform cross-correlation techniques; 2) process industry and LARSE1 seismic reflection data to define earthquake sources; and 3) calibrate and test current 3D velocity models of the basin, which are used for the numerical simulation of earthquake wave propagation and the prediction of hazardous ground shaking. Velocity functions and raw data from selected wells will be made available to the SCEC community via the WWW.

Oxygen Isotope Correlation of Marine Terraces and Calculation of Uplift Rates, Santa Barbara, California

Molly A. Trecker, Larry D. Gurrola, and Edward A. Keller
University of California, Santa Barbara

Resolving the chronology of marine terrace sequences is critical for determining uplift rates along tectonically active coastlines. Unfortunately, lack of suitable dating materials often makes this difficult. We have developed and locally calibrated a method of correlating undated terraces to those of known age using oxygen isotopic signatures preserved in marine terrace mollusks. U-series dated terraces at Isla Vista (47 ka ± 500 yr) and Santa Barbara City College (SBCC) (70 ± 2 ka) provide age control for the isotopic data. Our data, from fossil shells of *Olivella biplicata*, indicate that oxygen isotopic signatures preserved by organisms of different ages are distinct, and can be used to correlate undated terraces to those of known age. We have begun to apply this method to increase resolution of uplift rates in the Santa Barbara area. Using the U-series date from SBCC, coupled with oxygen isotopic data and geomorphic correlation we calculate a rate of uplift ranging from 0.62 ± 0.03 mm/yr (where the elevation of the first emergent terrace is 41 m) to 0.54 ± 0.05 mm/yr (where the elevation of the first emergent terrace

is 36 m) for marine terrace flights preserved on the Mesa hills anticline located in the city of Santa Barbara. Also, preliminary data from terraces at Ellwood Beach and More Mesa indicate that these terraces can be correlated to the Isla Vista terrace, revealing a wide range of uplift rates over a short distance. These examples illustrate the utility of oxygen isotope correlation as a means of resolving uplift rates.

Ground Motion Prediction With Energy Constraints

Alexei Tumarkin
University of California, Santa Barbara

The radiated energy is a very important observational characteristic of seismic sources (Gutenberg and Richter, 1956). While the seismic moment constrains the level of radiation at the lowest frequencies, the energy is determined by the total spectral power. More precisely, the energy is an intermediate-frequency constraint, as Vassiliou and Kanamori (1982) showed that most of the energy is contained below 1-2 Hz. With the recent advances in compiling energy estimates for major earthquakes in the world (e.g., Choy and Boatwright, 1995), there is now a real chance to verify whether the total radiation of models of earthquake sources is realistic (Anderson, 1997; Shaw, 1998; Tumarkin, 1998). The most convenient way of calculating the radiated energy for general models of extended earthquake sources was suggested by Rudnicki and Freund (1981). It is based on the knowledge of the slip-rate history on the fault at each moment. This information is readily available for most of the models. We present various results of energy and apparent stress calculations for kinematic models including their dependence on rise time and rupture velocity.

Pressure Solution Strain Associated With Seismogenic Faulting: the San Cayetano Fault

Jan Vermilye and Leonardo Seeber
Lamont-Doherty Earth Observatory, Columbia University

Diffused rock strain in the upper crust can be partitioned into an elastic, recoverable component and an inelastic, permanent component. The elastic strain is largely accounted for by seismogenic fault slip. A poorly known but possibly significant portion of the total strain may be diffused, permanent, aseismic deformation, particularly in proximity to large faults.

The San Cayetano fault is a seismically active reverse fault located in the western Transverse Ranges. We examined pressure-solution structures along six transects across the fault in order to evaluate the role that pressure solution plays in accommodating penetrative deformation. Macroscopic spaced solution cleavage and microscopic dissolution grain-shape fabrics were observed. Finite strains measured in sandstones show that grain-scale dissolution accommodates from 10-20% shortening in addition to shortening across cleavage planes.

The orientations for spaced solution cleavage planes as well as the orientations for the grain-scale pressure solution fabrics generally indicate N-S to NE-SW shortening directions. These are consistent with the present day compressional tectonic setting as expressed in Quaternary folding, earthquake focal plane solutions and in-situ stress measurements. Local variations for cleavage strike, along the fault trace, mimic changes in fault strike and local fold trends. The parallelism between the fault, folds, and cleavage planes suggest alternative "stress" and "strain" hypotheses for the evolution of the structures. In the "stress" hypothesis, the variations in strike reflect stress variations associated with the pre-existing fault. In the "strain" hypothesis, the strike changes are acquired during the evolution of the structures and distort an early, uniform, shortening fabric. Our data demonstrate that pressure solution records the effects of stress, strain, and fluid activity in the evolution of a young and active compressional structure. Investigation of this deformation may lead to a better understanding of the role that pressure solution plays in the overall strain budget, in the evolution of the structure, and in the seismic cycle.

ANZA Broadband Seismic Network and Portable Real-Time Telemetry Arrays

Frank Vernon and Jennifer Eakins
University of California, San Diego

The ANZA network enhances the broadband coverage provided by the SCSN in southernmost California. ANZA stations are designed to operate in remote areas without supporting infrastructure such as AC power, telephone or computer communications. Each station can operate using solar power and all communications between stations and the IGPP are dedicated VHF, spread spectrum, or microwave radio links. Two ANZA stations have developed significant cultural noise over the past several years, and will be redeployed in the Borrego Valley to upgrade SCSN single component analog sites. The station SOL, in La Jolla, provides extended broadband coverage to San Diego county and the offshore region complementing the nearest TERRAscope stations at Barrett Junction (BAR) and Mt. Palomar (PLM), east and north of San Diego respectively. ANZA data is now received by TRINET and SCSN within ten seconds of real-time and is seamlessly integrated into their data streams. This technology developed for the ANZA network and the IRIS PASSCAL Broadband Array can be easily integrated to create portable stations with telemetry capable of sending data to TRINET in real time. This capability can greatly enhance the real-time data coverage during an aftershock sequence or other temporary deployments such as LARSE II.

Aseismic Creep along the San Andreas and Superstition Hills Faults with Uplift at Durmid Hill, Southernmost San Andreas Fault, CA Measured by Radar Interferometry

Paul Vincent, John B. Rundle, and Roger Bilham
University of Colorado
S. M. Buckley
Center for Space Research, University of Texas, Austin

ERS-1/2 radar images acquired 4.5 years apart from 8/4/92 to 1/24/97 and centered over the Salton Sea were analyzed using differential radar interferometry and image aseismic creep and uplift along the southernmost San Andreas fault as well as aseismic creep along approximately 5 kilometers of the Superstition Hills fault. Discontinuities in the interferometric phase coincident with the mapped trace of the San Andreas and Superstition Hill faults vary in magnitude and sign with the sign reversal occurring at Durmid Hill. The sign change at Durmid Hill is consistent with uplift of the southwest flank of Durmid Hill relative to the northeast flank and agrees with data from a leveling line crossing the fault at Durmid Hill. A series of synthetic interferograms were computed from elastic models, constrained by GPS, trilateration, creep measurements, and leveling data where various locking depths and slip rates at depth were investigated. These models show a progressive pattern of deformation with shallowing spreading depths imposed on the Brawley Seismic Zone (BSZ) which is modeled as an evolving spreading center that connects the San Andreas and Imperial faults. The model predicts uplift at Durmid Hill for a relatively narrow range of lithospheric thicknesses above the BSZ spreading center.

Nonlinear Site Response due to Low and High Frequency Base-Rock Motions

Mladen Vucetic
University of California, Los Angeles

To advance the understanding of the effects of local geologic and soil conditions on the intensity and characteristics of ground shaking and related damages for the area of Los Angeles, and to improve methods for dealing with these effects, a series of 1-D nonlinear site response analyses was conducted. The computer code DESRAMOD2, which is a modification of the original computer program DESRA-2, was utilized. The DESRA-2 and DESRAMOD2 models can calculate a nonlinear response of stratified soil profile composed of different layers of soil

due to the base excitation applied in the form of an accelerogram. The particular soil profiles used in this exercise were a couple of profiles from the SCEC Geotechnical Database.

To investigate the effect of the frequency content on the calculated ground surface motions, several base excitation inputs with different frequency contents but same peak acceleration values were used. The main purpose of this ongoing investigation is to examine how the accelerograms obtained from the SCEC linear 3-D basin response studies can be used for nonlinear site response estimations. The accelerograms obtained from the 3-D linear simulations are known to have frequencies lower than actual field frequencies recorded during past earthquakes.

The results show that the frequency content of the input excitation motion can have significant effect on the outcome of a nonlinear site response analysis.

Analysis of Long Period Ground Motion Variability Related to Uncertainty in the Los Angeles Region 3D Velocity Model

David J. Wald[1] and Robert Graves[2]
[1]United States Geological Survey, Pasadena
[2]Woodward-Clyde, Pasadena

We have continued to test both earlier and updated 3D earth structure models of the Los Angeles basin using data from the 1992 Landers earthquake. Two of the major modifications in the newer versions (models "A" and "A5") of the Magistrale model are the deepening of the structure of the San Fernando basin, particularly in the northern basin, and the calibration of the P-wave velocity structure against deep borehole sonic logs that have recently been made available by the USGS. The main effect of this velocity calibration is to noticeably reduce the velocities within the basin sediments, which effectively makes the basins deeper relative to the original Version 1 of the Magistrale model. Compared to the Graves model, the new versions of the Magistrale model now have similar sediment velocities in the deep portions of the basins, and slightly lower velocities in the middle and shallow portions of the basins. Simulation results for the Landers earthquake indicate that the new Magistrale models do progressively better in reproducing the peak, long period ($T > 2$ sec) amplification pattern in the San Fernando, Los Angeles, and the San Gabriel basins. The new models produce a much better match in the San Fernando Valley than was obtained with the original Magistrale model. We have also made further progress in our analysis of the Northridge mainshock. We are computing the response for the newest version of the Magistrale model (A6) for the Northridge event, and these results will be compared with those already obtained using the Graves model. Similar analyses to that conducted for the Landers earthquake data is planned and the preliminary results will be presented. These ongoing validation analyses provide a means of charting the progress of the SCEC 3D model development. (See Wald, Graves, and Kohler Abstract for further results).

Teleseismic Waveform Amplitude Variations in the Los Angeles Basin: An Independent Check of 2D and 3D Earth Structure Models

David J. Wald[1], Robert Graves[2], and Monica Kohler[3]
[1]United States Geological Survey, Pasadena
[2]Woodward-Clyde Federal Services
[3]University of California, Los Angeles

Waveform data from a recent, high-density seismic array show a large variation in teleseismic P- and S-wave amplitudes across the Los Angeles basin. Since the relatively long-period (>1 sec) waveforms have nearly identical raypaths, the amplitude variations can be directly attributed to basin amplification. The recordings, made by the 18 stations of the 1997 Los Angeles Basin Passive Seismic Experiment (LABPSE), have an average spacing of 3 km, and span the San Gabriel Valley and deeper central Los Angeles sedimentary basins from Azusa to Seal Beach. Teleseisms from events with M>5.5 exhibit a P-wave amplitude ratio of up to 4:1 for stations near the deepest portion of the Los Angeles basin (where sediments are ~7 km thick)

relative to the northernmost crystalline rock San Gabriel Mountain station. S-wave amplitude ratios are as much as 6:1. Some of the largest ratios, however, are seen at the southernmost edge of the basin (e.g., Seal Beach), even though sediments have thinned to about 3 km. The observed P waveforms also show a clear high-frequency shift at sites with large amplifications, indicating that while the overall sedimentary thickness is important, the majority of the amplitude variations are controlled by the nature of the shallowest structure. Two-dimensional, finite-difference modeling suggests that recent high-resolution upper crustal velocity and 3D models may not adequately predict the observed large amplification or frequency shift, particularly at the southernmost portion of the Los Angeles basin. This experiment illustrates that high-density arrays, intended for local/regional wave propagation and deeper mantle studies, are also quite suitable for independent validation of the structural elements of previously obtained 2- and 3-D crustal velocity models intended for estimation of strong ground motions in hazards analysis.

Evaluation of Two Methods for Estimating Linear Site Response Amplifications in the Los Angeles Region

Lisa A. Wald and Jim Mori
United States Geological Survey, Pasadena

We have evaluated two methods of estimating linear site response amplifications and the standard index for classifying sites by comparing the results of each technique to observed ground motions at 32 sites in the Los Angeles region. Using velocity and density profiles from 32 boreholes, we evaluated the use of the average 30-meter shear-wave velocity and associated site classifications, the quarter-wavelength method, and the Haskell propagator matrix method. We correlated the average 30-meter shear-wave velocity and NEHRP site classification at the borehole sites co-located within 360 m of a site with observed ground motion. The observed data follow the expected trend of higher ground motion amplifications for lower average shear-wave velocities, but there is a significant degree of variability. Also, there is a great deal of scatter in the observed amplifications within each NEHRP class. We used the velocity and density information in the database to calculate the average frequency-dependent site response in the frequency ranges 1-3 Hz, 3-5 Hz and 5-7 Hz for a one-dimensional flat-layered structure using the Haskell propagator matrix method and the quarter-wavelength method. There is a general correlation with the ground motion data, however, once again there is a great degree of scatter. Even though all techniques considered give results that follow the expected trend of higher amplifications for softer sediments, the "predicted" site response at any particular site may not be representative of the shaking that will actually occur during an earthquake. The disparity between observed and predicted amplifications appears to be a result of oversimplification inherent in the amplification estimation methods, such as the use of average or assumed values for the site conditions in the absence of measured values, the "smoothing" effect of using an average velocity, limiting the properties considered to the uppermost 30 m of material, and complexities in the wave propagation that are not addressed by these methods.

San Francisco Bay Area Earthquake Simulations

Steven Ward
University of California, Santa Cruz

The United States Geological Survey is now involved in revising its 1990 probability estimates (WGCEP/90) for large earthquakes in the San Francisco Bay Area. I have been contributing to this process by fielding improved synthetic seismicity calculations of the type that I had originally developed for use in southern California.

Improvements in the theoretical formulation of the synthetic seismicity calculations now allow for the inclusion of a finite speed of signal propagation (Vp) while still keeping within a quasi-static framework. These improvements remove objections to quasi-static models based on "instantaneous response" arguments and allow for a specific interval Dt to be associated with

each step in a rupture simulation. Moreover, by adopting a linear, velocity-weakening friction law, I can now write explicit expressions relating critical slip velocity, critical slip distance and minimum patch size for run-away failure in terms of Vp, Dt and the difference between local static and dynamic fault strengths.

Figure 1 (1906_rupt.GIF) exemplifies a rupture calculation on a 550 km long stretch of the San Andreas Fault from the Mendocino Fracture Zone (MTZ, left) to San Juan Bautista (SJB, right). In Figure 1, the green color represents the static strength of the fault. Static strength is a fixed physical characteristic except at points where slip is actually occurring during an earthquake. This model assumed a constant 20 bar static strength except in northern Mendocino where 30 bars was adopted. The yellow color represents the current stress on the fault. Current stress is not a fixed physical characteristic. Current stress changes between, and within rupture events. In this case, the initial distribution of stress (yellow, top line) was selected so that the synthetic quake reproduced the surface slip of the 1906 San Francisco earthquake (squares, bottom) as inferred by the geodetic analysis of Thatcher (1997). As did the 1906 event, the model earthquake nucleates north of the Golden Gate (GG) and propagates bi-laterally toward the north and south. Time since nucleation is listed to the left, and red coloring highlights those parts of the fault that are actively sliding. The curves at the bottom of the Figure plot the evolution of slip at 2-second intervals. Note that the "Fort Ross" slip deficit near km #250, can be generated by an initial stress selection alone, without resort to along-strike changes in permanent strength. A single observation of surface slip can go a long way toward constraining a fault's static strength distribution, a key factor in long-term seismicity simulations.

Individual fault models such as Figure 1 can be grouped to form the entire San Andreas Fault system. This system can then be set into motion to generate a full set of earthquake statistics over a several thousand year interval. Figure 2 (bay.area.sim1.GIF) shows, in map view, a 1172 year simulation of M>6 earthquakes on the major faults of the San Francisco Bay Area. The included faults appear in red in the upper left panel. The "movie" frames are not regularly spaced in time, but update on the occurrence of an M>7 event listed to the upper right in each frame. Red coloring marks M>7.5 earthquakes; orange coloring, 7<M<7.5; and the thick and thin black lines, 6.5<M<7 and 6<M<6.5 respectively. At the lower left in each panel is time in years since the start of the simulation. Final and intra-rupture slip history for each earthquake (like those illustrated in Figure 1) are cataloged separately. As a basis for forecasts, these long-term seismicity models supply every imaginable earthquake statistic while simultaneously satisfying all geological slip rate constraints. Due to the region's closely spaced, sub-parallel distribution of faults, the behaviors of San Francisco Bay Area earthquakes are likely to be more strongly affected by stress interaction than earthquakes in any other place in the world. Given this, I believe that meaningful progress toward updating the WGCEP/90 Bay Area earthquake probabilities can be made only with the guidance provided by physically-based and region-wide earthquake simulations.

Paleoseismic Evidence for Surface Ruptures on the Raymond Fault, San Marino, Los Angeles County, California

Kristin Weaver and James F. Dolan
University of Southern California

The Raymond Fault is a west-south-west-trending, left-lateral strike-slip fault that extends for 20 km beneath the San Gabriel Valley, northeast of Los Angeles. Previous work has shown that the most recent surface rupture on the Raymond fault occurred between 1000 and 2000 (probably 1000 -1500) years ago, and that it therefore did not rupture with the Hollywood fault during the Hollywood fault's most recent surface rupture (5000-10,000 years ago). To find evidence for the penultimate and older events on the Raymond fault we excavated a 28 meter-long, four meter-deep trench down the median strip of Sierra Madre Boulevard in San Marino, CA across a fault strand identified by a transect of bucket-auger holes during August, 1998. The trench exposed two main faults that cut to the base of a man-modified A horizon . The northern fault is a 1.5 m-wide zone of several vertical to near-vertical, anastamozing faults with

predominantly strike-slip motion, indicated by the juxtaposition of brown sandy silt units to the south of the fault zone with beige fine- to coarse-grained sands and pebble to cobble gravels to the north. South of the vertical fault zone lies a 45°-north-dipping, thrust fault with 1.6 m of dip-slip, indicated by reconstructing a series of black- to blue-gray marsh deposits. The marsh deposits overlie iron-oxide-stained sandy gravels and are in turn overlain by a series of beige-gray silts and wedge-shaped, beige iron-oxide-stained sand units. The southern end of the trench contains horizontal, interfingering beige and iron-oxide stained sands and gravels with gray-beige silty fine-grained sands.

Although the section of the stratigraphic column that would have contained the most recent event was previously destroyed, we have found evidence for at least five older events. The oldest well-defined surface rupture is defined by four faults at the bottom of the trench that terminate at the base of a beige, iron-oxide-stained sand and pebble gravel unit. This event tilted some of the sands and gravels cut by the fault strands, but was predominately a strike-slip event, as indicated by abrupt thickening, thinning and disappearance of different sedimentary layers. Three other paleo-surface ruptures are indicated by geometrical relationships between a series of alternating silts and sands. Advanced charcoal dates indicate that these four earthquakes occurred during the Pleistocene. The youngest well-exposed event is expressed by a series of fracture fills that terminate at a near-horizontal horizon. Abundant charcoal collected from numerous horizons will provide better age constraints on these paleo-earthquakes.

The Southern California Integrated GPS network (SCIGN): Status Report

Frank H Webb[1], Yehuda Bock[2], Kenneth Hudnut[3], and Bill Young[4]
[1]Jet Propulsion Laboratory;
[2]University of California, San Diego
[3]United States Geological Survey, Pasadena
[4]League of California Surveying Organizations

The Southern California Integrated GPS Network is a collaborative project to install and operate 250 continuously operating GPS stations in and around southern California with an emphasis on understanding the earthquake hazard and tectonics of the Los Angeles basin. The major phases of the installation of SCIGN are: Site selection, network installation, network operation, network analysis, and product delivery to the user community. The major participants include NASA/JPL, the United States Geological Survey, and the University of California San Diego, operating under the umbrella of the Southern California Earthquake Center (SCEC). Chief sponsors are the W. M. Keck Foundation, the National Science Foundation, NASA, and the USGS. Because of the time required to design, install and build the network, each phase of the project is being developed and deployed concurrently. We will present an overview of the project, including a review of the network status, operating plan, results to date, and a description of how users can access the data.

Basin Structure of the Western San Fernando Basin from Industry Seismic Profiles and Well Logs

Tom Wright[1], David Okaya[2], Robert Yeats[3], and Julie Francis[2]
[1]Consultant
[2]University of Southern California
[3]Oregon State University

Well logs and seismic profiles in western San Fernando Valley were integrated in order to identify the geometrical shape within the SF basin. Stratigraphic horizons of several well logs made available to SCEC were interpreted and cross-referenced to earlier nearby studies of Shields (1977) and Tsutsumi and Yeats (in review). In order to then tie this information to the

seismic profiles, depth/two-way time curves were carefully constructed from sonic logs taken from wells nearest the profiles. Corrections included taking into account the deviations of the wells from the true vertical. These stratigraphic horizons were subsequently identified in the seismic profiles. Structural "depth-to" maps are being constructed of five stratigraphic levels as well as the basin bottom. The basin is asymmetric to the north with the Northridge Hills anticlines as prominent subsurface structures. Available velocity information suggests that the Northridge Hills provide some but not extreme velocity heterogeneity to the basin velocity structure.

Soup-to-Nuts Modeling of Nonlinear Soil Layer Response to Strong Ground Motions

H. Xu[1], Steven M. Day[2], and J. Bernard Minster[1]
[1]University of California, San Diego
[2]San Diego State University

We present a nonlinear wave propagation model, based on the endochronic theory, which offers the following desirable characteristics:

1. It is an integrated modeling capability, that includes 3D nonlinear wave propagation and 3D nonlinear soil response, "all in one package". The validity of the nonlinear solutions can be tested systematically, including its asymptotic behavior in the limit of weak motion.
2. The model parameters are derived in a very straightforward, systematic fashion from laboratory measurements, and the approach is effective for rock as well as for soil behavior.
3. The method is validated by systematic comparisons of the results against analytical and perturbation solutions in 1D, 2D and 3D problems, for linear and nonlinear elastic and anelastic rheologies, and for inelastic endochronic rheologies, in a progression where each step is fully documented and understood.
4. The accuracy of different numerical schemes is compared in a 2D half space simulation suite, which reveals heretofore undocumented difficulties encountered with "pseudospectral" methods in modeling surface waves.
5. The numerical modeling is readily amenable to automatic parallelization on massively parallel supercomputers, which are necessary for 3D simulations. The MPI block transpose technique is demonstrably effective for such applications.

We will present realistic simulations using soil models applicable for structures in the Bay area, and show how a low order parametric model is capable of simulating realistic ground motion histories.

Complex Contractional Structure of the San Andreas Fault Zone near San Gorgonio Pass and Implications for Future Large Earthquakes

Doug Yule and Kerry Sieh
California Institute of Technology

We have used geologic mapping, thermochronometry, and patterns of crustal seismicity to constrain better the three-dimensional geometry of the active San Andreas fault zone in the region of San Gorgonio Pass, southern California. This analysis allows us to construct a structural model that is useful for forecasting the nature of large earthquakes there. The dextral-reverse nature of the fault zone within this 15-km-wide contractional stepover was recognized by earlier workers. What we have focused upon is the determination of which faults and folds are currently active and the characterization of their style of deformation. The dominant structure within the stepover is the San Gorgonio Pass-Garnet Hill fault system, a dextral, reverse fault assemblage that dips moderately northward. A small piece of this system generated the M5.9 North Palm Springs earthquake in 1986. Within the hanging wall block are subsidiary active

normal and strike-slip faults. These faults relate in complex and diverse ways to the strike-slip faults that bound the stepover.

An analysis of crustal seismicity allows us to constrain the geometry of this system in the subsurface and to relate it to the bounding strike-slip strands of the San Andreas fault at depth. A 5 to 7 km high east-west striking step in the base of crustal seismicity defines the down-dip projection of the San Gorgonio Pass-Garnet Hill fault system beneath the San Bernardino Mountains. Our structure-contour map of the fault depicts it merging gradually eastward with the steeper right-lateral faults east of the stepover. At the western edge, however, the San Gorgonio Pass fault is not smoothly connected to the bounding strike-slip fault. Instead, the bounding fault dies out southward as a strike-slip tear in the hanging wall block of the San Gorgonio Pass fault.

We interpret the large step in the base of seismicity as an indication that the mid-crustal brittle-plastic transition is offset several kilometers by dip slip on the San Gorgonio Pass-Garnet Hill fault system. U/Th thermochronometry support our interpretation that this south-under-north doubling of the crust has created the region's 3 to 3.5 km of topographic relief. We conclude that future large earthquakes generated by the San Andreas fault zone in this region will have complex, but specific multiple sources with dimensions of 1 to 20 km. Despite their complexity, the most important of these sources have now been mapped; thus the construction of realistic source models should now be possible.

A Simplified Approach to Basin Effects

Yuehua Zeng
University of Nevada, Reno

In this paper, we seek to develop and apply a simplified method that characterize the differences between predictions of a reference genetic crustal model and a complex basin structure. Our approach uses a simplified ray method combined with the surface wave technique to compute the trapped waves along the basin boundary.

Our study show that inside the basin, the synthetics obtained using the Gaussian Beam method to sum up the contribution from multiple reverberations of rays within the basin layer approximate more precise numerical methods like the analytical or finite difference methods very well. At the edge of the basin, the wave field is dominated by the trapped Stoney type waves propagating along the basin boundary that are excited by the incident waves to the basin as well as the reflected waves from the basin. The attenuation of this trapped basin boundary wave strongly depending on the curvature of the basin boundary and its wave length in addition to the intrinsic and scattering attenuation.

Using this simplified method, we simulated the basin response for the South San Francisco Bay model (Brocher and Jack, 1997). The input motion uses strong ground motions of the Morgan Hill earthquake, Loma Prieta earthquake and simulated seismogram from a scenario earthquake on the Hayward fault. The basin responses are, in general, very complicated. By comparing the results from different sections of the South Bay, we found that the average responses across the basin show no correlation with the impedance contrast between the basin and the bed rocks. However, the same average responses suggest a remarkable linear relationship with the wave incident angles. The average amplitude decreases as the incident angle increase and appears to be independent of frequency. We also found a strong frequency dependence on the basin responses as a function of basin depth and distance to the edge of the basin. At high frequency attenuation prevails amplification caused by the resonant effect and a decrease in velocity in the basin. At low frequency, amplification dominates over attenuation and the responses increase as the basin depth increases.

Depth Distribution and Source Mechanisms of the 1994 Northridge Earthquake Aftershocks

Lupei Zhu
University of Southern California

Regional broadband waveforms of 76 aftershocks of the 1994 Northridge earthquake were analyzed to determine their focal depths and source mechanisms, using the CAP source inversion technique. We improved the inversion technique by incorporating uncertainty analysis following the grid-search. This is done by computing the second derivatives of the misfit near the grid-search minimum which are then used to estimate the "true" minimum and the "flatness" of the misfit surface near the minimum. We also use ground velocity records instead of displacements for inversion to emphasize higher frequency signal (up to 1 Hz). This proved improving signal-to-noise ratio for small magnitude earthquakes (down to about 3.5 ML).

The focal depths from the waveform inversion were compared with the relocation depths using P and S travel times for a subset of 20 aftershocks that were recorded by the Southern California Short-period Seismic Network with at least one station within 10 km from the epicenter. Relocation was done using both a 3-D velocity model and a 1-D velocity model derived from the 3-D model for the Northridge region. The waveform depths agree with the relocation depths within 2 km when the latter are larger than 5 km. There are 3 aftershocks which are located at shallow depths (0 to 2 km) by the travel time relocation while the waveform inversion indicates that they are deeper (7 to 9 km). The discrepancy may be caused by inappropriate velocity model used by the waveform inversion for shallow earthquakes because of the complicated basin structure in the source region. Using the local 1-D model helps to reduce the difference to about 3 km. Our results show that there is a consistent spatial variation of aftershock source mechanisms. Most of the aftershocks are concentrated around the edge of the mainshock rupture plane with pure thrusting mechanisms. Aftershocks inside the mainshock area show dominant strike-slip mechanisms and occurred above the mainshock rupture plane. The source mechanisms of a cluster of aftershocks in the northwest of the main rupture plane indicate that the principal stress axis there is rotated due north, about 20 degrees anti-clockwise from the mainshock's principal stress direction. The depth distribution of these events shows a trend dipping to the north and suggests that these events may rupture on the north-dipping fault planes.